Distribution of this
document is unlimited

AD 641433

TECHNICAL REPORT
67-8-CM

RESPONSE OF NON-WOVEN SYNTHETIC FIBER TEXTILES TO BALLISTIC IMPACT

by

Thomas W. Ipson and Edward P. Wittrock

Denver Research Institute
University of Denver
Denver, Colorado

Contract No. DA19-129-AMC-157(N)

Project Reference:
1K024401A113

Series: TS-142

July 1966

Clothing and Organic Materials Division
U. S. ARMY NATICK LABORATORIES
Natick, Massachusetts 01760

FOREWORD

Needle-punched nylon felts have proved to offer superior ballistic resistance at low areal densities. Knowledge of the mechanism of felt deformation during ballistic impact could eventually lead to improved felts for armor application.

The work covered in this report was performed over a two-year period by Mr. Thomas W. Ipson and Mr. Edward Wittrock of Denver Research Institute, University of Denver, under Contract DA19-129-AMC-157(N). The theoretical approach led to an analytical model based upon momentum considerations.

Experimental results were obtained by a spark gap technique as a check on the analytical model. The model obtained analytically was mainly accurate in predicting experimental results at the lower range of impact velocities. One of the major gains from this work has been the intimate knowledge of the felt reaction to impact at different stations in the deformation cone.

The U. S. Army Natick Laboratories Project Officer was Mr. Roy C. Laible and the Alternate Project Officer was Mr. Anthony L. Alesi.

S. J. KENNEDY
Director
Clothing & Organic Materials Division

APPROVED:

DALE H. SIELING, Ph.D.
Scientific Director

W. M. MANTZ
Colonel, QMC
Commanding

TABLE OF CONTENTS

LIST OF FIGURES

LIST OF FIGURES (Cont.)

LIST OF FIGURES (Cont.)

LIST OF FIGURES (Cont.)

LIST OF FIGURES (Cont.)

LIST OF TABLES

NOMENCLATURE

Velocity

- V_o - initial impact velocity of the projectile at time zero (fps)
- V_p - projectile velocity at any time, t (fps)
- V_r - residual velocity of the projectile after complete perforation (fps)
- V_{zr} - transverse velocity of the felt material at a radius, r, and at any time, t (fps)
- C_L - radial longitudinal tensile wave velocity of the material (fps)
- u - radial velocity of the felt material that is imparted by the action of the longitudinal wave (fps)
- C_t - radial transverse wave velocity relative to the stationary felt material (fps)
- ω - radial transverse wave velocity relative to the r coordinate, $= C_t - u$ (fps)

Coordinant System

- r - radius measured from the axis of the projectile (inches and feet)
- z - transverse (axial) direction measured from the rear surface of the felt material (inches and feet)

Mass, Density, and Force

- m_p - projectile mass (slugs)
- ρ - mass density of felt material (lb - sec^2/ft^4)
- F - total force opposing projectile motion (lbs)

Time

- t - time after initial contact of projectile and felt material (seconds)

Dimensions

- R - radius of 0.22 cal. Fragment Simulating Projectile (.0183 ft)
- Δr - distance between axis of the impacting projectile and the center arc-gap station (inches)
- T - thickness of the felt material (inches)

ABSTRACT

When organic fiber felt materials are impacted by blunt fragments, stress waves propagating laterally into the material transfer projectile momentum to an increasing (roughly conical) volume of felt material. By applying a retarding force to the projectile, stresses in the felts can be maintained below rupture values, provided that the felts are free to move in the direction of the projectile. The objective of this program was to define the transient behavior of the felt and the force interaction between it and the projectile.

An experimental technique was developed whereby the position-time histories of eleven points (spark gaps) on the rear surface of a felt sample could be determined. The center spark station, being on the projectile trajectory, provides projectile displacement-time data. Other stations provide both radial and transverse displacements. The longitudinal radial wave gives material particles an initial radial velocity inward; later, the slower moving transverse wave imparts a transverse velocity to the felt, usually stopping or reversing radial motion. Measurement errors average less than two percent.

Six felt samples (nylon (3), orlon, dacron, polypropylene) were tested using the 17-grain fragment simulating projectile at various velocities up to and greater than the ballistic limit velocity. Graphical differentiation was used to obtain velocity-time, force-time, and force-distance relationships. Qualitative evaluations reveal that strength, elongation, and transverse wave velocity are the three predominant parameters in determining effectiveness. The energy absorbed by a felt is maximum at the ballistic limit velocity and decreases dramatically at higher (complete perforation) velocities. An analytical model based upon momentum considerations is compared to the experimental results.

RESPONSE OF NON-WOVEN SYNTHETIC FIBER TEXTILES TO BALLISTIC IMPACT

I. INTRODUCTION

Considerable interest has been generated in the possible utilization of inorganic fiber felts as materials for body armor. In the range of lower areal densities, these materials exhibit favorable resistance to ballistic perforation by fragment type projectiles. Previous investigations[1,2]* have been primarily of an empirical nature and have been directed toward establishing relationships between ballistic limit velocity and the various geometric and material parameters involved. These investigations have produced valuable information concerning the quantitative effect of such parameters upon the ballistic limit velocity. Consideration has been given to the physical properties of various fiber materials (tenacity, elongation at rupture, etc.), fiber length, denier, crimp, thickness, and variations in the needling process.

The objective of this research program was to more precisely define the transient process which occurs during the response of felt material to an impacting projectile and to analyze the force interaction between the felt and the projectile. Before felt materials can be designed to provide maximum ballistic protection, appropriate analytical models must be developed which will reveal influential parameters and the nature of their involvement in the penetration process. Precise, experimental data is required, not only to verify hypothetical models, but to provide the observational insight required for model development. The experimental approach taken was to accurately determine the position-time history of the projectile and of several points on the rear surface of felt samples during ballistic penetration. Such data provides the means for evaluating the prediction capability of a proposed model with a degree of precision exactly defined by the accuracy of the position-time data. While subject to the degeneration of accuracy associated with the graphical differentiation of experimental data, the data are also useful in revealing the characteristics of velocity-time, force-time, and force-distance relationships.

The development of analytical models logically proceeds through an iterative process during which hypothetical models are first proposed (based on observation) and then evaluated to determine their ability to predict position-time data. Subsequent refinements of

---

* Superscripts refer to the Bibliography, Section VI.

promising models are made until the required degrees of fundamental understanding and prediction precision are achieved.

Attempts to develop analytical models starting with the general theoretical equations associated with ballistic penetration often fail. The primary reason for this is that constituative relationships required to solve the equations are not available. Thus, the theorist must make assumptions or otherwise be faced with an auxiliary experimental program to determine constituative relationships. Such auxiliary experimental programs may bear little resemblance to the actual problem he is trying to solve and may lead him away from the central theme. Furthermore, such experiments do not furnish him with the means for verifying the validity of his model. Consequently, unless the state-of-the art is sufficiently well developed to sustain an approach based entirely on theory, it is more rewarding to recognize the importance of experiment for developing analytical models, as well as for verifying them, and to proceed accordingly. Pursued to its conclusion, the approach utilized during this program should ultimately result in a completely rational basis for the development of design criteria for felt materials to be utilized in ballistic protection applications.

A basic requirement of body armor is flexibility; immobility very quickly nullifies the advantages of ballistic protection. Felt materials and woven textiles meet related requirements since they exhibit very little resistance to bending or shearing deformations. As armoring materials, felts may be classified as non-rigid, ductile armors. As such, their behavior during impact departs radically from that of rigid materials such as the conventional metallic armors. Rigid armors respond to impacting blunt fragments primarily by developing inertial forces and highly localized shearing resistance. Figure 1 depicts the process which occurs during perforation of a rigid plate by a hard blunt fragment. This perforation process may be thought of in terms of a two-step concept, the first step being the inelastic collision of two masses, the fragment (m_p) and the plate plug (m_s). The second step involves shearing the plug from the plate. An analytical model based on this two-step process was successfully used to derive analytical expressions which accurately predict the post-perforation dynamics associated with hard blunt fragments and rigid plates.[3,4] If the plate defeats the fragment, displacements are small in comparison to the plate thickness. The time period during which the fragment is decelerated is extremely short. A projectile is stopped when the work, $\int F dx$ (retarding force through stopping distance) is equal to its

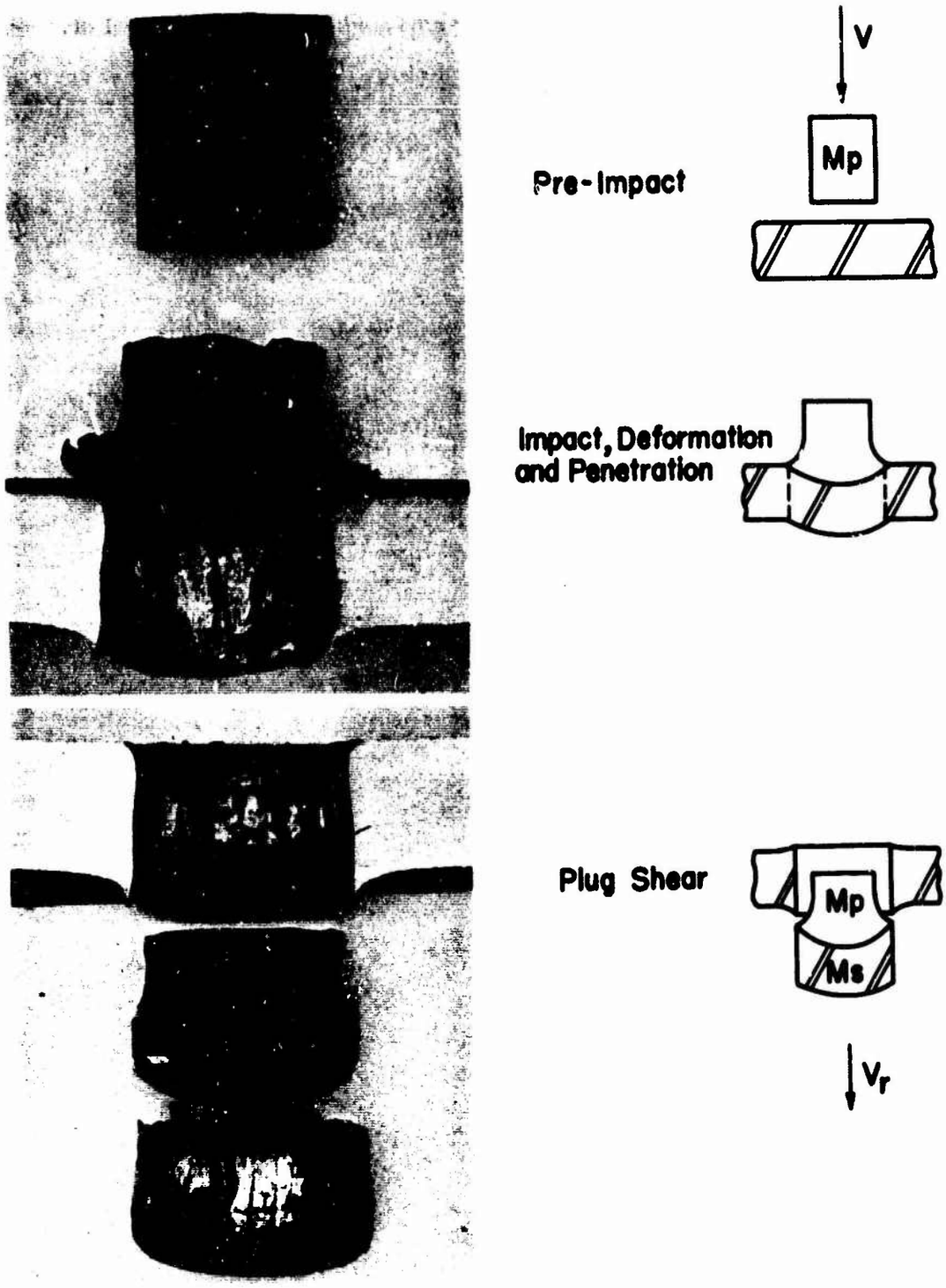

Figure 1. Rigid Plate Perforation by Blunt Fragments

initial kinetic energy or, in other terms, when an impulse, $\int F dt$, equal and opposite to its initial momentum is applied. Since extremely small quantities of time and displacement are characteristic of rigid plate impact, very large resistive forces must be developed so that the energy and momentum of the projectile can be absorbed. High strength, ductile, rigid materials such as steel can withstand very large stresses and thereby can develop significant ballistic resistance.

As previously stated, the behavior of felt materials during impact is quite different than that characteristic of rigid materials. The major difference is associated with the amount of displacement which occurs during the impact process. Figure 2 illustrates this gross deformation. It is an enlarged photograph of the rear side of a panel of nylon fiber felt, 0.40-inch thick, being impacted by a .22 cal., 17-grain, Watertown Arsenal Laboratories developed fragment simulating projectile (specifications are given in the Appendix). This photograph was taken with a one-microsecond duration light source at 230 microseconds after initial impact. The displacement along the line of flight is approximately three times the panel thickness. Also, as may be seen, the deformation is not localized to the area of impact but has spread out into the material. Felt materials fail at stress levels many magnitudes below those at which conventional armor materials fail. Although felts can support only relatively small forces, they develop ballistic resistance by applying these forces to the projectile over relatively large distances and through relatively long periods of time.

For clarity, discussions of the experimental program and the analytical investigations have been separated even though the respective efforts were performed concurrently. The Appendixes contain complete descriptions of the projectile and the six felts utilized during the experimental program (Table A-I). All valid position-time data are recorded in Table B-I and all residual velocity data are presented in Table C-I, in the Appendixes.

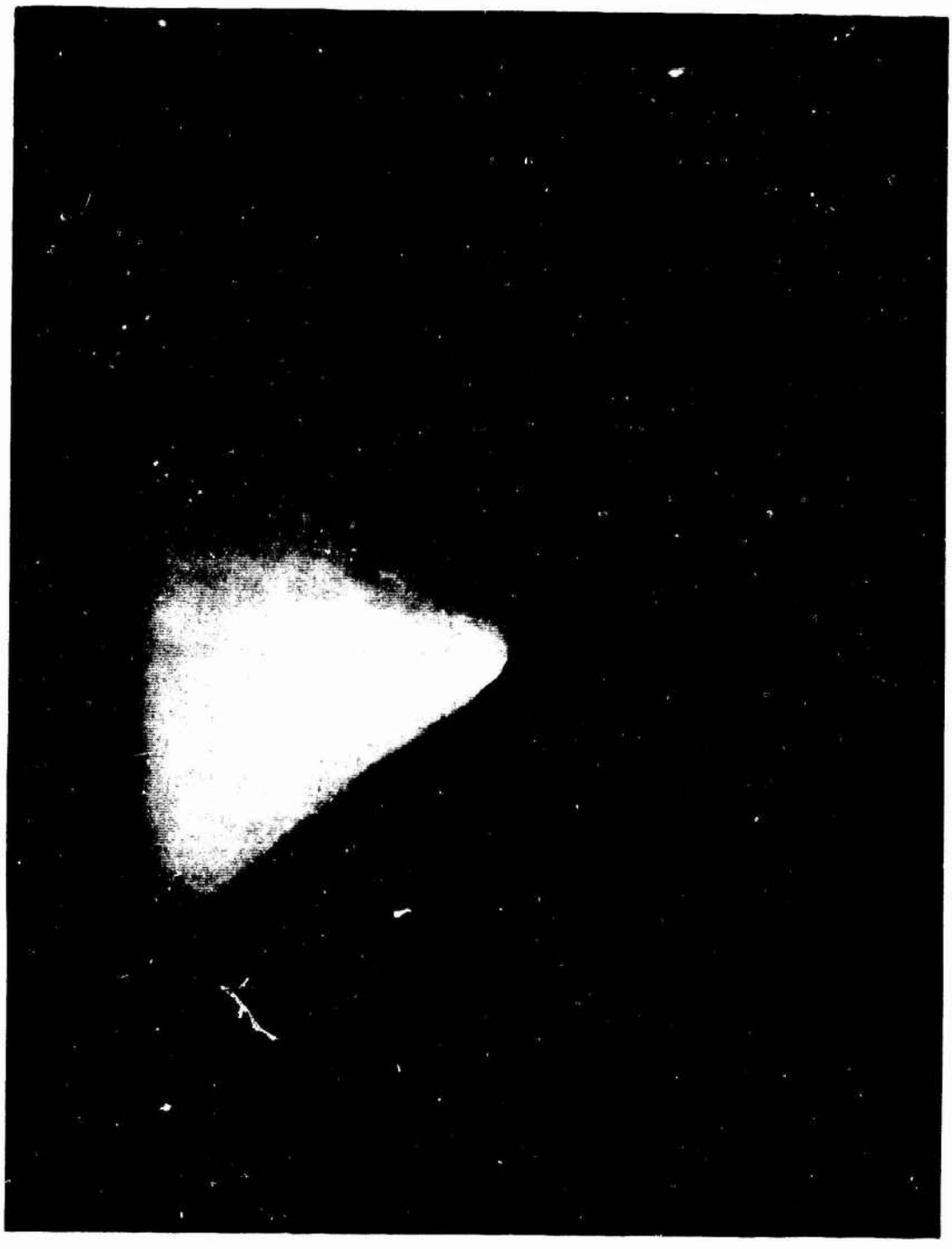

Figure 2. Response of Non-Woven Nylon Felt during Ballistic Impact. 230 Microseconds after Impact by 17-Grain Fragment Simulator. Initial Velocity - 650 feet per second. Felt - 43 ounces per square yard.

II. EXPERIMENTAL PROGRAM

The experimental program was directed toward obtaining a precise quantitative description of the behavior of felt materials during the impact process. The general behavior of a felt panel at a stage during impact is illustrated in Figure 3. The impacting projectile has accelerated felt material in the transverse direction. This transverse motion of the felt material has been propagated radially outward by means of a transverse wave, ω. Ahead of the transverse wave is a longitudinal tensile wave, C, propagating radially outward in the plane of the felt. This wave produces a radial velocity, u, directed inwardly toward the point of impact. To describe this behavior and the growth of the deformation profile depicted in Figure 3, it is necessary to obtain data concerning the transverse and radial motion of the felt material as a function time after initial contact of the projectile with the felt. Knowledge of the displacement of the felt material as a function of time and radius provides information related to strains, velocities, dispersion, etc. Wave propagation characteristics essential to the development and evaluation of analytical models are revealed by the position-time data. Since the motion of the felt material at zero radius can be assumed to be the same as that of the projectile (after initial compression of the material), data concerning this point will provide information about the motion of the projectile as it is decelerated. The velocity and deceleration history of the projectile are obtained by graphical differentiation of the displacement-time curve. The deceleration curve is used to obtain the total retarding force being developed by the felt.

A. Experimental Technique

To obtain the desired data, a unique technique was developed to measure the displacement of the felt during the impact event. This method consisted of defining and recording the position of various stations (spark gaps) on the rear surface of the felt panel at predetermined times during the impact. By defining the position-time function of these stations (initially located at various radial distances from the point of impact), the transient deformation of the material can be studied. Each station is represented by a small spark gap cut in a short segment of a fine wire. This wire is securely attached to the rear surface of the felt panel at each station; a loop is left in the unsecured wire between stations so that the motion of the felt at one station does not influence the motion of another by means of the interconnecting wire. Figure 4 is a photograph of the wire attached to a test panel of

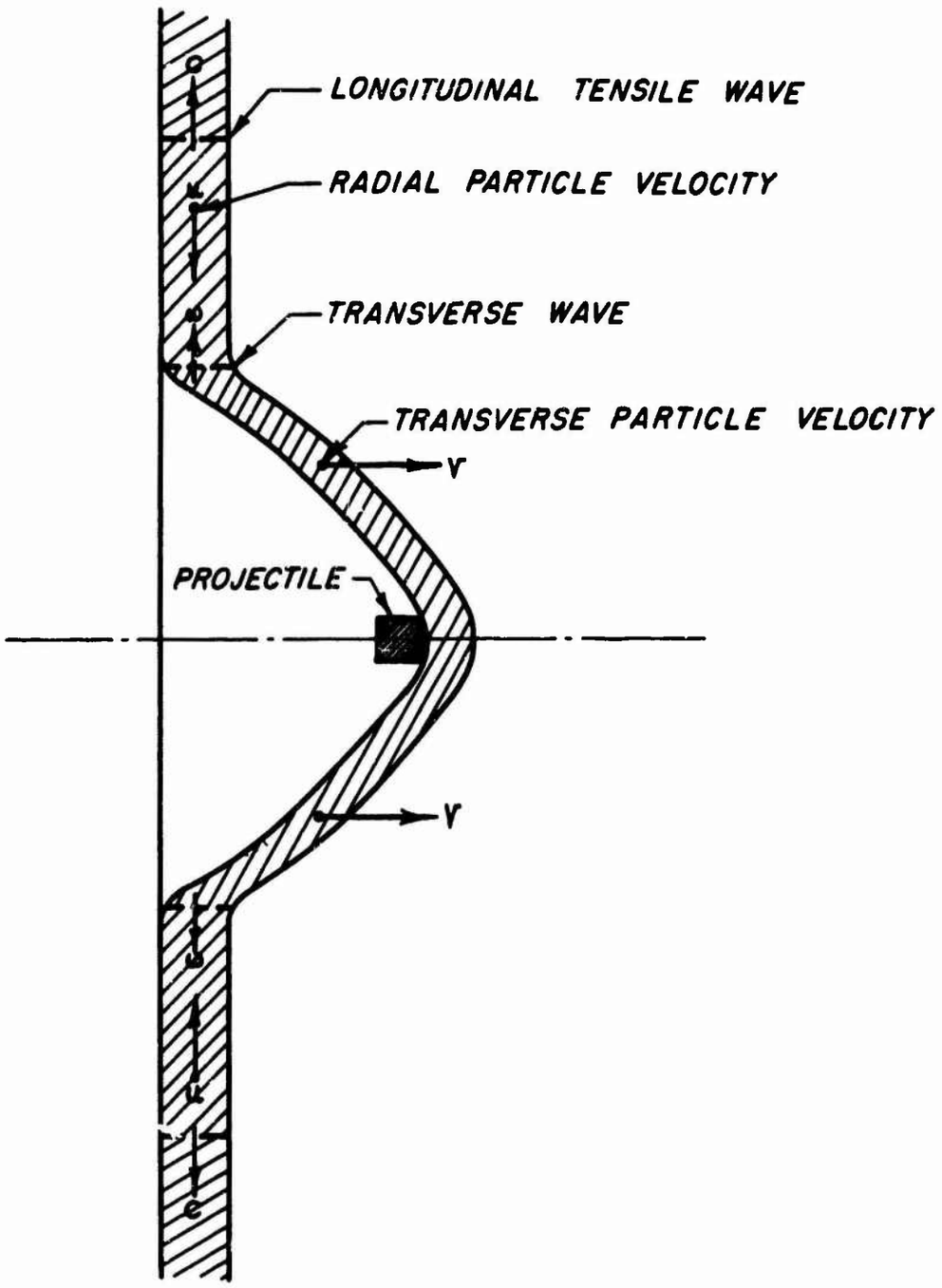

Figure 3. Illustration of the Wave and Material Behavior which Occurs during Ballistic Impact of Non-Rigid Felts

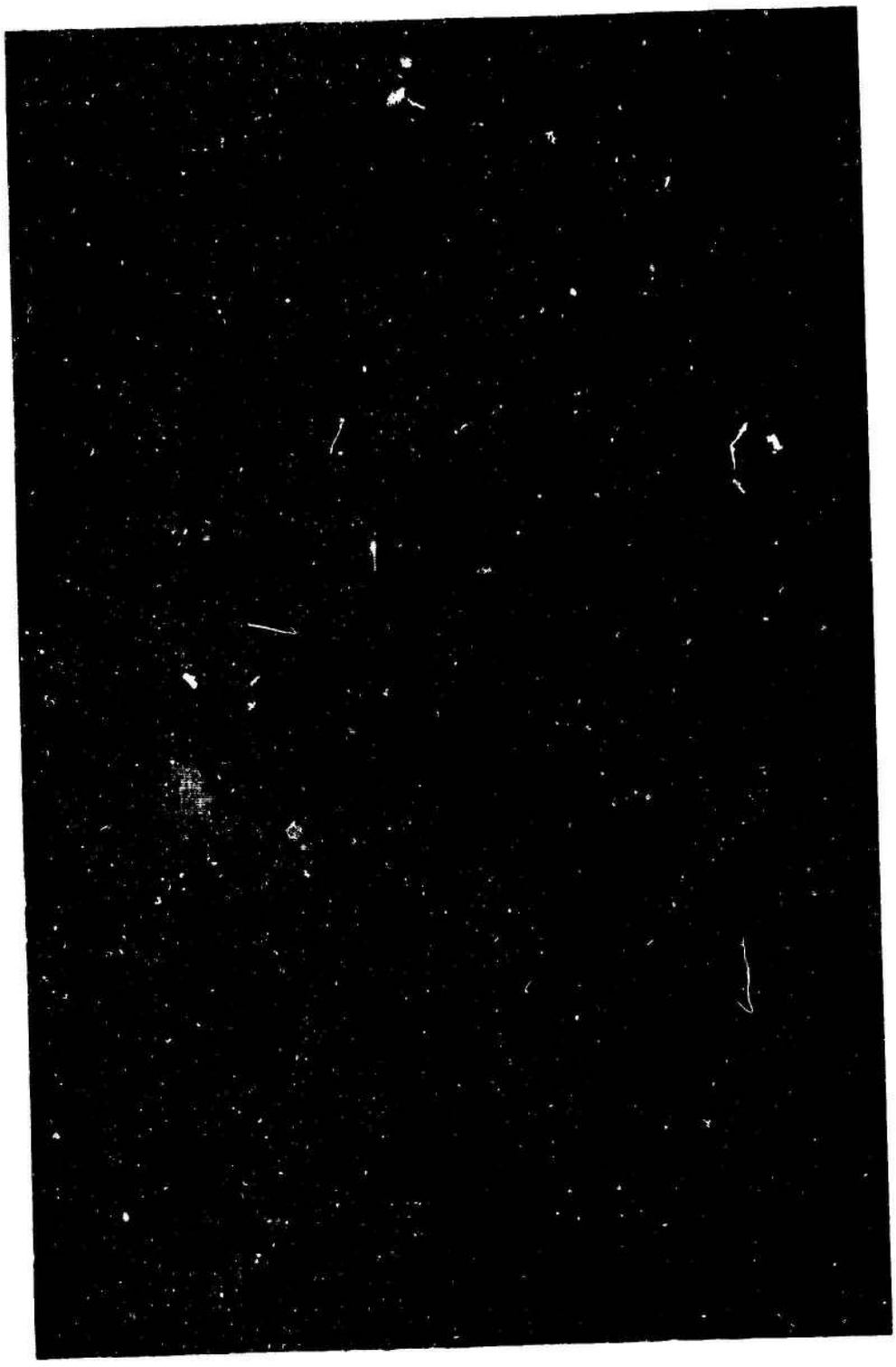

Figure 4. Attachment of Spark Gap Wire to Rear Surface of Nylon Felt Sample

felt. During the impact process, the position of each station and, thus, the position of the rear surface of the felt at this point, was defined by means of an intense arc created at each gap in the wire by a high frequency-high voltage pulse which was applied to the wire during the impact. These experiments were conducted in a dark room and the position of the stations (arcs) were recorded by an open shutter camera aimed perpendicular to the line of fire and focused on the profile of the felt panel.

The experimental technique is illustrated in Figure 5. All tests were conducted with a 17-grain fragment simulating projectile (T-37). These fragments were fired from a .22 cal. Hornet rifle and the impact velocity was controlled by varying the amount of propellant used. This impact velocity was measured by make switches which triggered a chronograph to determine the time of travel over the known distance separating the switches. The felt specimens were securely held in a rigid frame having a 4-inch diameter circular opening. This opening is sufficient in size to insure that no wave reflections will return from the frame to affect the behavior of the felt during the time of interest. At the point of impact, another make switch was attached to the front side of the felt panel. As the projectile contracted the felt, this switch provided a signal used to trigger the electrical pulses which were fed to the arc-gap wire attached to the rear surface of the felt. The electrical pulses consisted of 10,000-volt surges of 2-microsecond duration which occurred at a frequency of 11,600 cycles per second (86 microseconds between voltage spikes). The number of voltage pulses could be controlled and a pre-determined number was dialed into the equipment prior to firing. The first pulse occurred as the projectile encountered the felt and shorted the trigger switch; successive pulses occurred at intervals of 86 microseconds thereafter for the desired number of pulses (usually six to eight). The timing, and number of pulses, were checked by photographing the oscillographic display of the signal. As each voltage pulse occurred, an intense arc was created simultaneously at each of the arc-gaps thus providing a pinpoint of light which defined the location of each station every 86 microseconds during the impact event. This sequence was recorded on film by the open shutter camera. This record of the dots made by the electrical arcs shows the intermittent position of each station on the felt profile as it is deforming with time. Figure 6 is an example of the photographic record of the test data. The center horizontal series of dots represents the arc-gap station coincident with the projectile trajectory. This series shows the displacement-time history of the felt material immediately

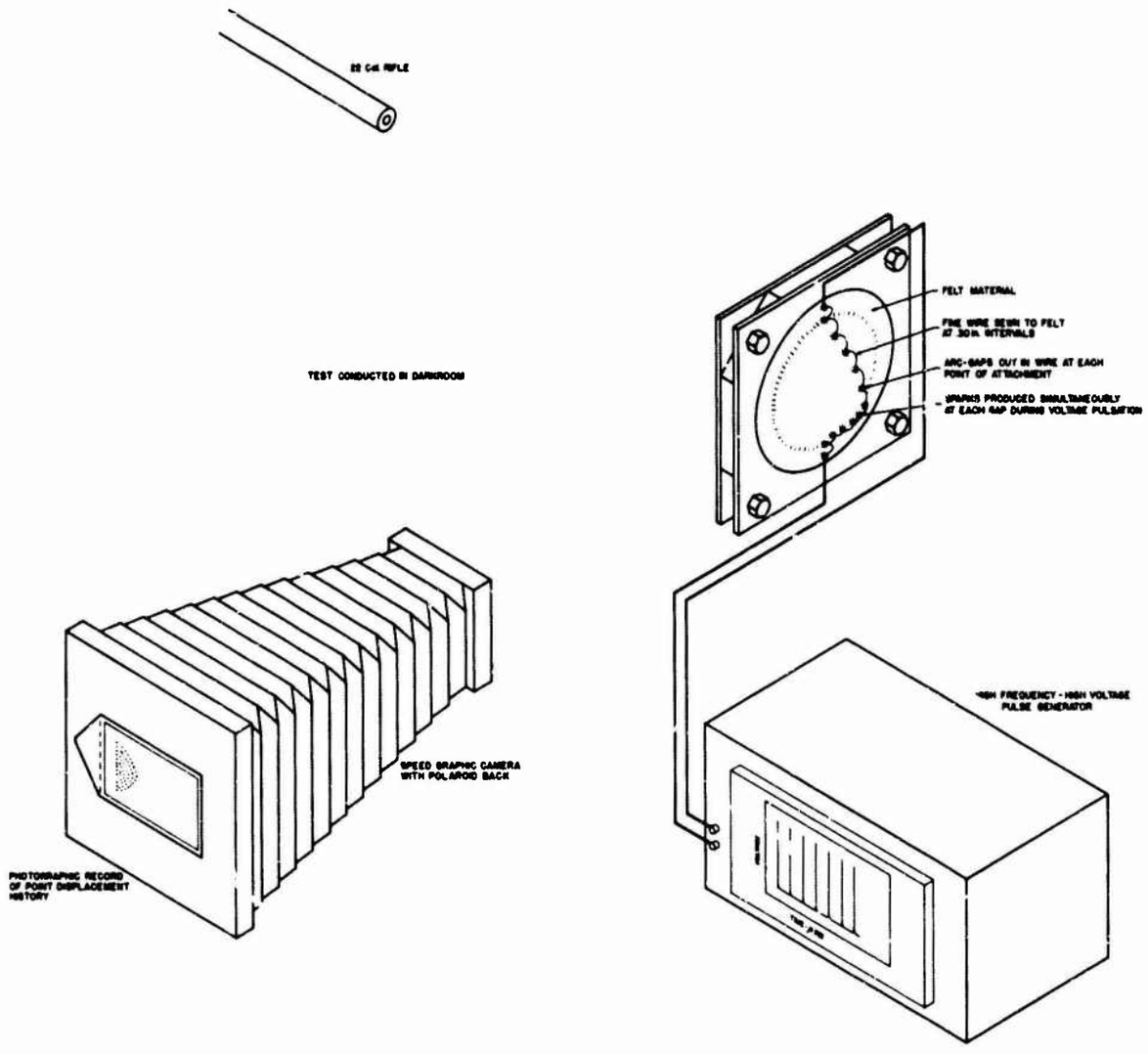

Figure 5. Schematic of the Spark-Gap Technique Used to Obtain Displacement-Time Data Regarding the Response of Felt Material to Impact

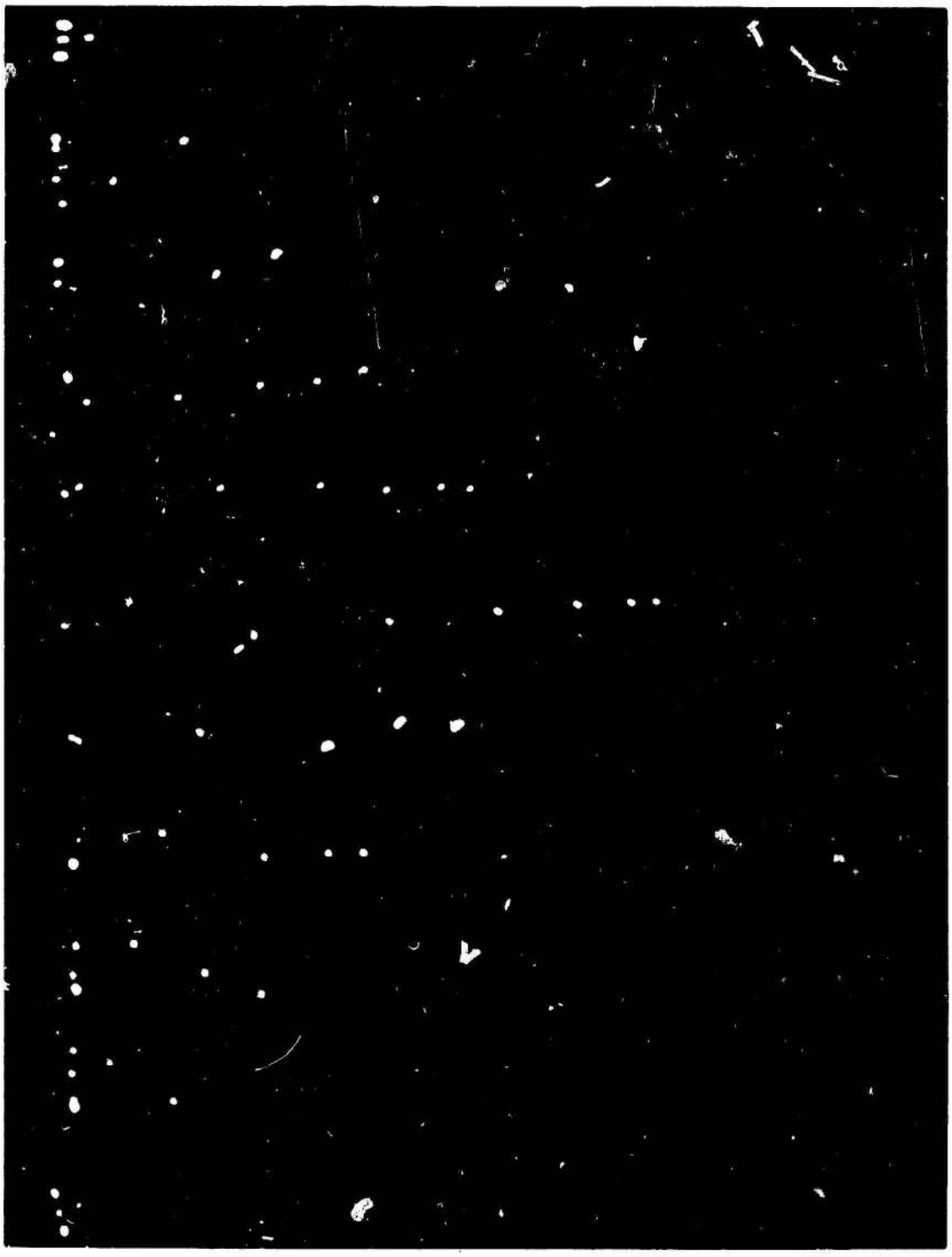

Figure 6. Enlarged (3X) Photograph of Typical Spark Display Showing Position-Time Relationship during the Impact Event for Eleven Stations on Rear Surface of Felt Material

in front of the projectile and, therefore, the displacement-time history of the projectile during the impact. The other series of dots show the displacement history of the felt at various radial distances from the point of impact. Figure 7 is a graphic reproduction of Figure 6. Dashed lines have been included to illustrate the deformation profile development and the path taken by each station. Note the radially inward movement of stations prior to the transverse movement. This is due to the inward radial velocity, u, that is imparted to the felt after the arrival of the longitudinal tensile wave, as depicted on Figure 3. The progress of the transverse wave is observed by noting the time interval during which transverse motion occurred at each radial station. The data illustrated by Figures 6 and 7 can be used to determine numerous relationships. These include transverse and longitudinal wave velocities, projectile kinematics, material motion as a function of time and radius, and the gross radial strain developed in the felt during the impact deformation. During the experimental program, a test series was conducted involving four different felt fiber materials selected to represent a wide variety of fiber characteristics.

B. Nature of the Required Data

Prior to planning the experimental program and developing the spark-gap technique, investigations were made to ascertain the type and nature of the experimental data required for this research. Studies were initiated and pertinent literature was reviewed concerning the ballistic impact of non-rigid materials to establish the general characteristics of the dynamic response of such materials (previously depicted in Figure 3). Initial deformation of the material results in a geometry roughly conical in nature, the position of the apex being controlled by the projectile movement and the diameter of the base by the progress of the stress waves. Stresses being applied to the felt material have a component in the transverse direction (perpendicular to the plane of the felt and in the direction of projectile motion) and a component in the radial direction (in the plane of the felt and directed inward toward the point of impact). These two components propagate with different velocities; the radial stress is propagated by means of a longitudinal tensile wave and the transverse stress (analogous to a shear stress) is propagated by means of a slower transverse wave. Material located at a given initial radius, r_o, from the point of impact is not affected by the impact of the projectile until the arrival at this point of the tensile wave, after which the material will have a radial velocity, u, toward the point of impact. The material continues to move toward the center until the transverse wave has propagated out to it (at a radius defined

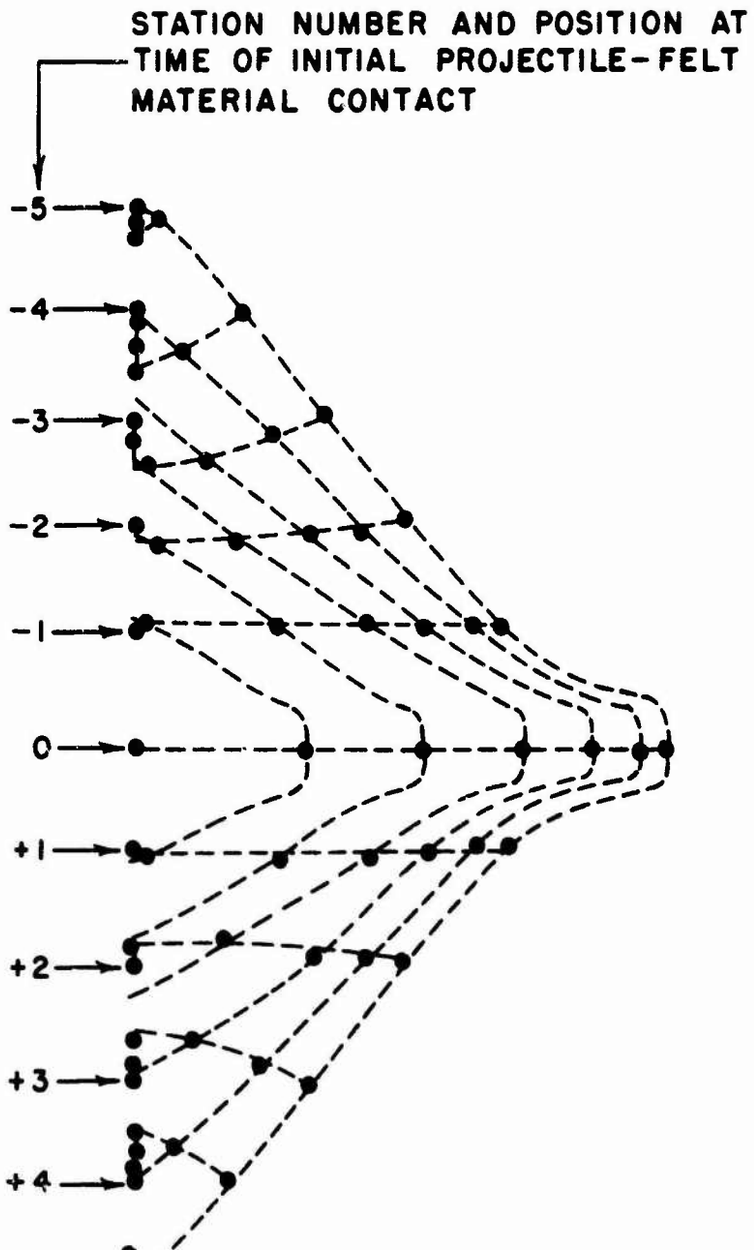

Figure 7. Graphic Reproduction of Spark-Gap Data Shown on Figure 6. Dashed Lines Illustrate Sequential Contours of the Deformation Profile and the Locus of Each Arc-Gap

as r in subsequent discussions) and imparts a transverse velocity to the material. Major displacement of the material is in the transverse direction, the direction of projectile motion. (Note that the transverse momentum of the material represents the total change in momentum of the projectile at any time.) The development of this deformation is controlled by the projectile motion and the stress wave action.

Numerous photographs of various stages of the impact phenomena (similar to that shown in Figure 2) were taken. These were used to determine the amount and rate of the displacements and the range of the material and stress wave velocities to be experimentally investigated. From this information, it was determined that the period during which the major projectile deceleration occurs is of the order of 500 microseconds and that the total displacements are large. The experimental technique and apparatus were designed accordingly. The frequency of the electrical equipment (11,600 cps) allows data measurement at 86 microsecond intervals during the impact event; six to eight sets of data points define the position-time history. The displacements are of such magnitude that they can be defined accurately by this method.

C. Data Analysis Procedure

The experimental data establish the position of points on the rear surface of the felt at successive instants of time during the impact event. Referring to Figure 7 as an example, these data define the position of eleven radial stations at seven times during the impact. The initial positions of the stations are recorded at a time coinciding with the initial encounter of the projectile with the front surface of the felt. Positions of the stations are recorded at 86 microsecond intervals; thereafter, until the final voltage pulse occurs at 516 microseconds. The stations or arc-gaps are designated numerically as shown on Figure 7. The arrows point to the position of these stations at zero time, the time of initial impact. No movement of the felt has occurred at this time and these points represent the original position of the radial stations with regard to the undisturbed felt. The center series of seven dots (station 0) represents the movement of the rear surface of the felt along a trajectory coinciding with that of the projectile. In this test, seven voltage pulses programmed into the electronic equipment occurred in proper sequence as confirmed by the oscillograph record of the voltage signal. Prior to firing, the distance separating the two end arc-gaps (stations -5 and +5, Figure 7) was accurately measured to obtain a reference dimension. The film negative is enlarged by means of projection techniques and measurements of the

displacements of the stations are made. The reference distance between end stations provides the required correlation between displacements measured from the enlarged image of the data film and true displacements. The displacement data for the other radial stations are somewhat more complicated than that for station 0 since both radial and transverse displacements occur. Radial motion at these stations is initiated by the radial longitudinal wave after a sufficient time has elapsed for wave propagation; transverse motion is initiated later when the transverse wave arrives. Consider station number +3, Figure 7, which was located prior to impact at a radius of 1.82 inches from the center station. It is observed that only six points are recorded for this station on the film. Since seven voltage pulses are definitely known to have been applied to the arc-gap wire and, consequently, seven arcs occurred at each arc-gap, the presence of only six points at station +3 implies the existence of two superimposed points. Thus, the point representing the original location of the station also represents the position of this station at the time of the second voltage pulse (86 microseconds after initial impact). The longitudinal wave had not propagated out to this radius during the first time interval. The third data point (the second dot in the series for station +3) is radially displaced. Thus, the longitudinal tensile wave arrived at this station during the time interval between the second and third voltage pulse. The fourth data point (third dot) also shows radial displacement due to the radial material velocity, u, created by the tensile stress being propagated by the longitudinal wave. The fifth point (fourth dot) shows displacement in the transverse direction; therefore, the transverse wave met the inward moving station +3 between the fourth and fifth voltage pulse (between 344 and 430 microseconds). The sixth and seventh data points show continued transverse and radial displacement.

Projectile motion is determined using the center gap (station 0) which lies on the projectile trajectory. While this point actually lies on the rear surface of the material, the motion of this point closely corresponds to the motion of the projectile after initial compression of the material at the point of impact. Displacement-time data obtained from Test No. 40-C are plotted on Figure 8 (experimental test data is compiled in Table B-1 in the Appendix). It should be remembered that this is the displacement of the station 0 arc-gap; consequently, the projectile displacement-time curve would be displaced downward by an amount representing the compressed thickness of the material. The projectile impact with the front surface represents zero time and station 0 on the rear surface does not move until the compressive wave is transmitted through the material. During this short period of time it will be

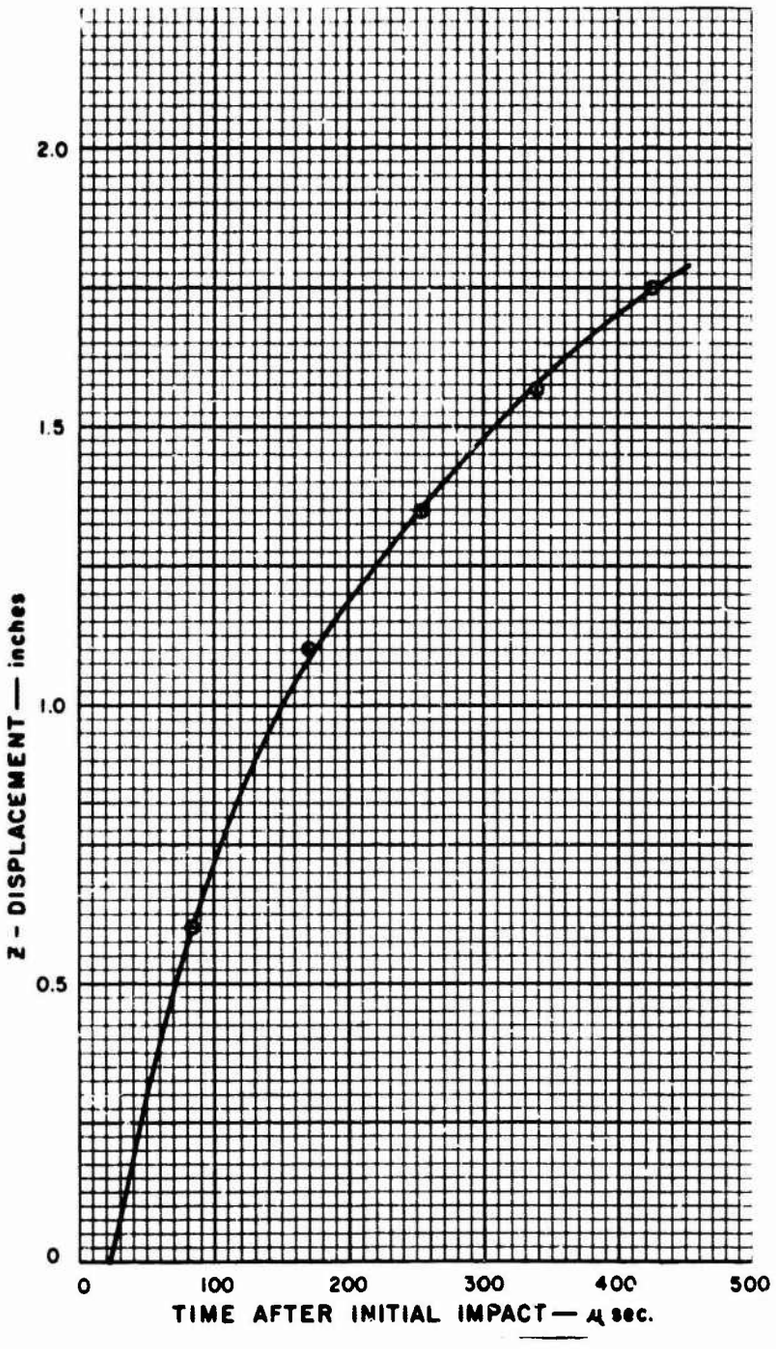

Figure 8. Axial Displacement of the Center Arc-Gap as a Function of Time after Initial Impact of the Projectile with the Front Surface of the Felt. Test No. 40-C, Impact Velocity - 900 feet per second. Material - 43 ounces per square yard Nylon Felt.

shown that the change in projectile velocity of station 0 is negligible as compared to the accuracy of the velocity measurement. This observation provides the condition that the displacement-time curve of this station must intersect the abscissa with a slope corresponding to the projectile impact velocity, V_o. A smooth curve is fitted to the data points such that it intersects the time axis with this slope. At 900 feet per second impact velocity, the interface impact pressure is only about 1500 psi, a small elastic stress in the projectile; elastic stress waves move through the projectile at about 18,000 feet per second. Consequently, the projectile behavior is accurately defined as that of a rigid body. Due to the grossly inelastic behavior of the felt it will be essentially compressed by the time that station 0 begins to move. Subsequent changes in thickness will be very small compared to measured displacements and will have very little effect on the position of data points. Impact impedance mismatch and the characteristic inelastic response of the felt material completely nullifies any compressive stress wave effects related to the primary impact. Consequently, it can be positively concluded that the displacement-time curve will be a continuous (smooth) function. Since some positive force-time function will be continually applied to the projectile, the slope of the displacement-time curve must continually decrease (there can be no reversals in slope). Thus, a smooth curve, meeting these conditions, is drawn to correspond as closely as possible to the data points; deviations between the data points and the curve are attributed to experimental variations.

The velocity-time curve shown on Figure 9 was obtained by graphical differentiation of the displacement-time curve, Figure 8. The displacement-time curve actually represents the motion of station 0; however, as explained above, it is valid to use this curve to obtain projectile velocity since (after initial compression of the felt) these velocities are identical. The initial rate of change of velocity is due to the impact interface pressure which is governed by impact impedance. The value of the interface pressure in this case is about 1500 psi (a force of about 60 pounds on the projectile) resulting in a change of velocity of approximately 20 feet per second during the first 25 microseconds. As the impacted felt material is displaced in the direction of projectile motion, relative motion occurs between this material and that material laterally adjacent. This relative motion creates two radial stress waves which propagate into the material inducing both radial and transverse motion to an increasing volume of the felt material. Resulting stresses increase the decelerating force acting on the projectile, causing a more rapid decrease in velocity (the region between 50 and 150 microseconds on Figure 9). As the projectile velocity

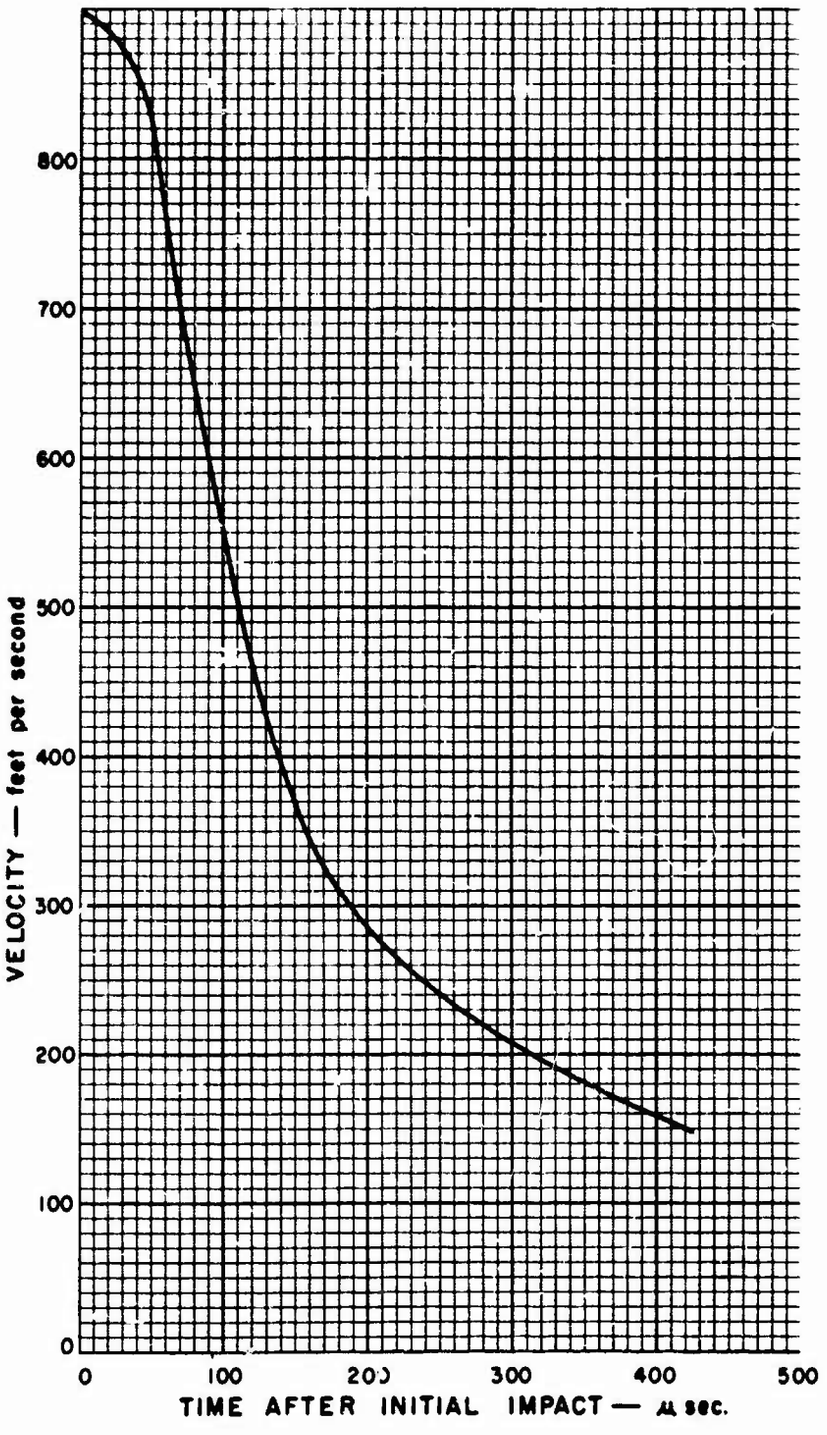

Figure 9. Projectile Velocity as a Function of Time after Initial Impact. Test No. 40-C, Impact Velocity - 900 feet per second. Material - 43 ounces per square yard Nylon Felt.

decreases, transverse particle velocities in the material at any radius decrease (as do the related stresses). In addition, the ratio of projectile velocity to wave velocity decreases, changing the angular relationship between the moving felt and the projectile axis; this reduces the tensile stress component applied to the projectile. This compound effect produces the drastic reduction in deceleration indicated above 200 microseconds in Figures 9 and 10.

Graphical differentiation of the velocity-time curve results in values for acceleration which can be used to develop the force-time relationship shown on Figure 10. This curve more clearly illustrates the effects discussed in the previous paragraph, a major portion of the retarding impulse being applied between 25 and 200 microseconds.

Figures 8 and 10 can be used to develop the relationship between force and displacement shown on Figure 11. This curve shows that the felt must be free to move at least 1.5 inches in order to absorb the major portion of the projectile s kinetic energy.

As illustrated above, the displacement-time data obtained at station 0 are used to determine the motion of the projectile as well as the motion of the material at that station. Due to symmetry, these motions have no radial components. At other stations, both radial and transverse displacements are observed as shown on Figure 7. Table B-I in the Appendix presents all valid data concerning the r (radial) and z (transverse) components of stations as functions of time obtained during the test program. Typically, the inward radial displacements due to the action of the longitudinal radial wave are relatively small and, to a large extent, are more than offset by outward radial displacements due to the subsequent action of the transverse radial wave. In contrast, the transverse displacements due to the action of the transverse wave are much larger. For these reasons, major attention is given to transverse motions of the felt material. Transverse displacement of the various radial stations can be analyzed in the same manner as that used to study transverse (axial) motion of the center station. This provides a means of describing the transverse motion behavior of the felt material as a function of time and radius.

It is important to remember that the transverse momentum of the felt material represents the total momentum transferred from the projectile at any time. Consequently, equations of motion derived from momentum considerations will involve only the transverse motion of the material. Motion equations derived from energy considerations

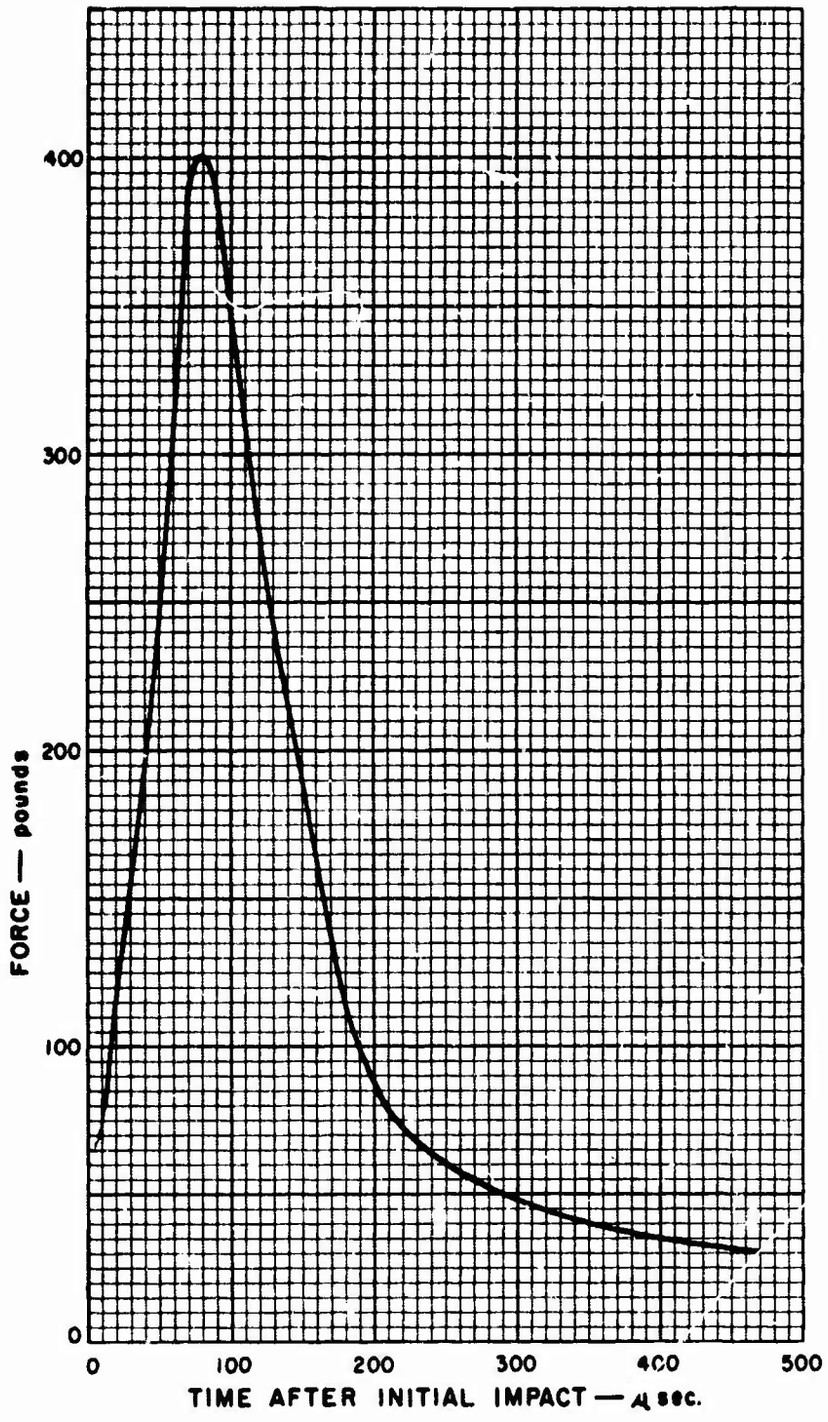

Figure 10. Force Opposing Projectile Motion as a Function of Time after Initial Impact. Test No. 40-C, Impact Velocity - 900 feet per second. Material - 43 ounces per square yard Nylon Felt.

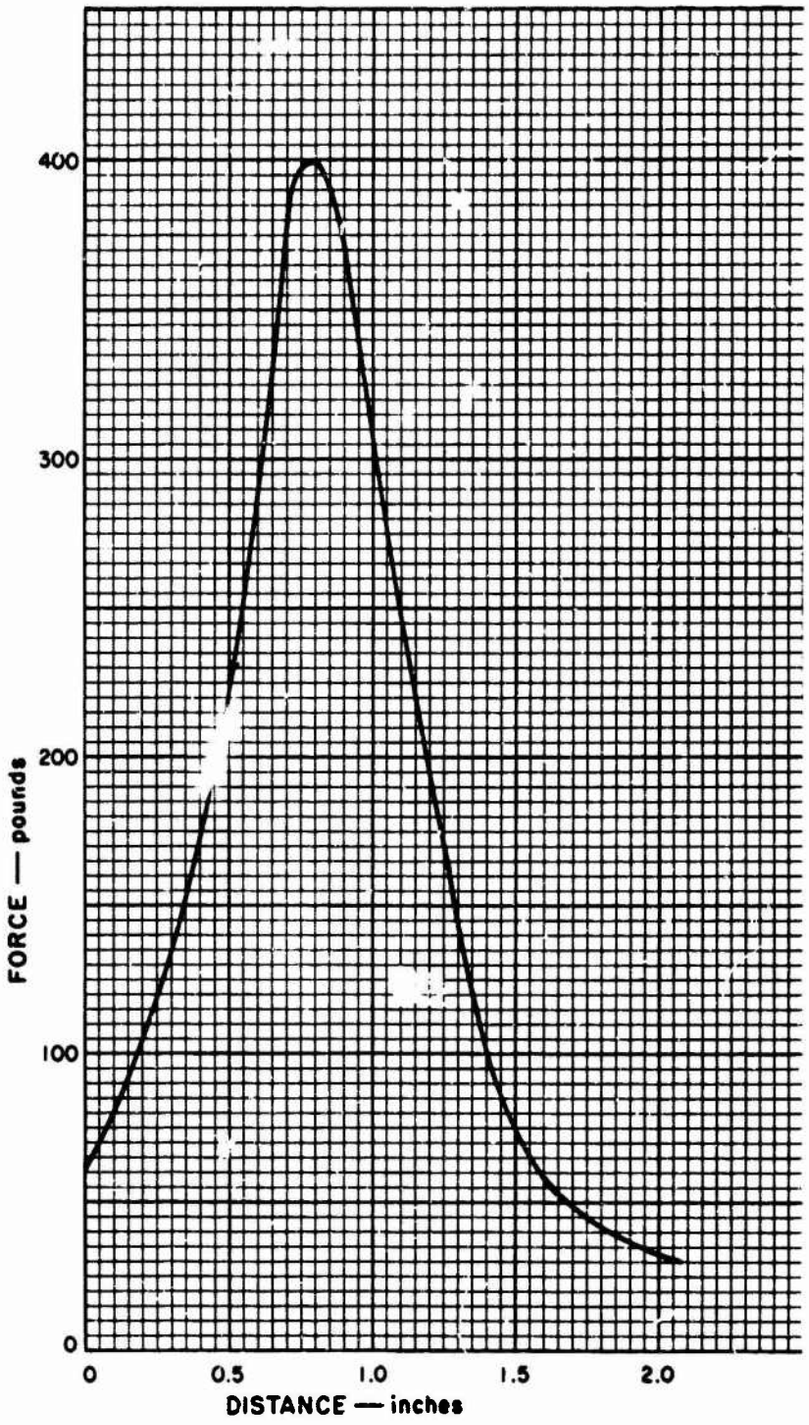

Figure 11. Force Opposing Projectile Motion as a Function of Distance Traveled. Test No. 40-C, Impact Velocity - 900 feet per second. Material - 43 ounces per square yard Nylon Felt.

will involve both transverse and radial motions; however, since radial kinetic energies are small compared to transverse kinetic energies, it may be reasonable to ignore radial motion of the material in energy equations as well.

Transverse displacements of the material at stations 0, -1, -2, -3, and -4, Test 40-C, are plotted on Figure 12. The curve drawn through the data points for station 0 is that previously presented on Figure 8. Radius, r_o, indicates the position of these stations at time = 0. Radius, r, indicates the position of these stations at the time of arrival of the transverse wave. The difference, $r_o - r$, represents radial displacement due to the action of the longitudinal radial wave prior to arrival of the transverse radial wave. Graphical differentiation of the curves shown on Figure 12 results in the velocity-time curves presented on Figure 13. Initial velocity of station 0 is obtained directly by measuring projectile velocity. (The curve for this station is reproduced from Figure 9.) Until the transverse wave reaches a station, the transverse velocity is zero. Upon arrival of this wave, the maximum transverse velocity is almost instantaneously achieved; its magnitude is determined by measuring the slope of the displacement-time curve at the intercept with the time axis. Velocity at each station subsequently decays. The maximum transverse velocity imparted to the material also rapidly decays with radius. Velocities are directly related to stresses. The decrease in velocity with both time and radius indicated on Figure 13 reveals the nature of the transverse wave. The decrease in maximum transverse velocity with radius reflects the decay of the intensity of the transverse wave due to dispersion. The decrease in velocity with time at any station illustrates the wave shape which is a function of projectile motion and material behavior.

The displacement-time data also provides information from which longitudinal and transverse wave velocity, C and ω, can be deduced. Radial displacement of any station will be initiated upon arrival of the longitudinal radial wave. While time of arrival is not measured directly, the time interval (86 microseconds) during which it arrives is provided by the time-displacement data. The bars on Figure 14 represent the time intervals associated with longitudinal wave arrival at each station located at some displacement, r_o. Initiated at the radius of the projectile (0.11 inch), the wave will propagate outward starting about 30 microseconds after initial impact of the projectile with the front surface of the material at time = 0. Using this point, and assuming a constant longitudinal wave velocity, the straight line shown indicates the position of the wave front with time. Note that the

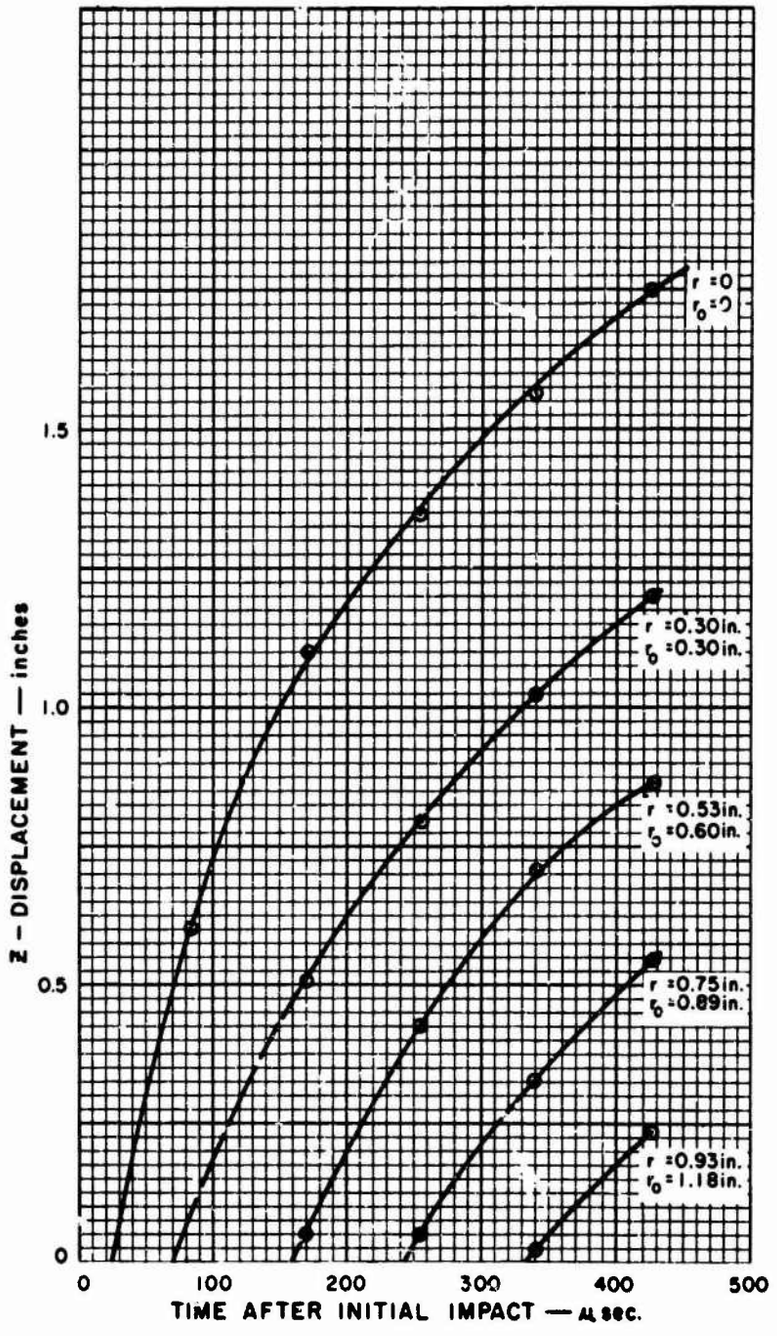

Figure 12. Transverse Displacement of Felt Material at Several Radii as a Function of Time after Initial Impact. Test No. 40-C, Impact Velocity - 900 feet per second. Material - 43 ounces per square yard Nylon Felt. (r_o - Initial Position of Station; r - Position of Station at Time of Arrival of Transverse Wave)

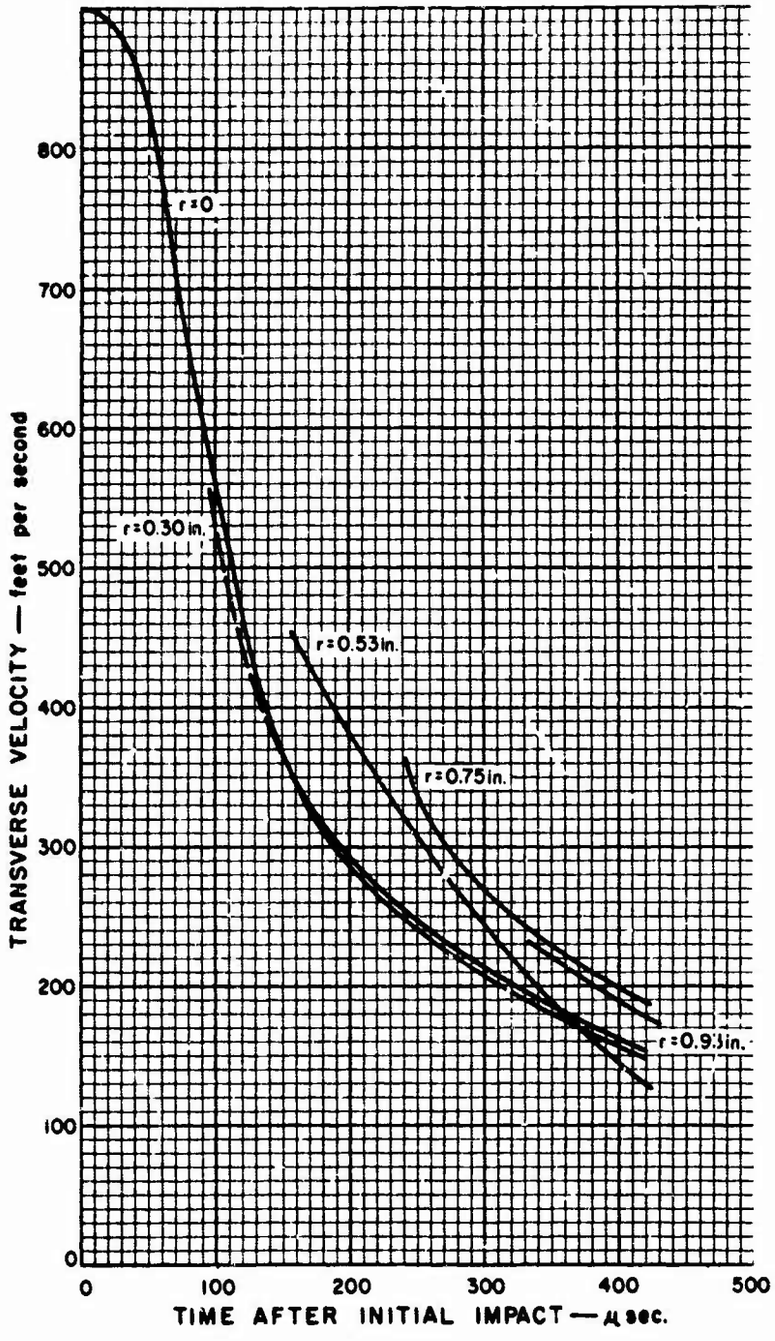

Figure 13. Transverse Velocity of Felt Material at Several Radii as a Function of Time after Initial Impact. Test No. 40-C, Impact Velocity - 900 feet per second. Material - 43 ounces per square yard Nylon Felt. (r - Position of Station at Time of Arrival of Transverse Wave)

data fix the position of this line within rather narrow limits. The slope of this line corresponds to the longitudinal wave velocity, C, assumed constant (about 650 feet per second).

Displacement-time data for test 40-C were used to develop time contours similar to those shown on Figure 7. From these, the radius representing the position of the transverse wave front can be determined at these specific points in time. These points are shown as circles on Figure 14. Triangular data points represent information obtained from Figure 12. The slope of the curve indicates absolute transverse wave velocity, ω, the wave velocity with respect to the material is greater by an amount equal to the radial particle velocity (i.e., $\omega + u$). Values of ω obtained by measuring the slope of the curve approach 300 feet per second, initially, decaying rapidly to an apparently constant velocity of 195 feet per second.

D. Accuracy of Experimental Data

Errors which can arise in the displacement-time data are related to (1) the transfer of the reference dimension from the experiment to the position-time plot (such as Figure 7), and (2) the measurement of individual displacements on the plot. Inherent errors related to the transfer of the reference dimension have been determined to be less than two percent. (Errors are related to spark gap dimensions and spark images on the photograph.) Maximum error in the measurement of individual relative displacements is equal to the maximum actual spark radius of 0.016 inch. Table I shows the total combined maximum errors as a function of the actual magnitude of the measured displacement. The actual value of displacement will fall within the range established by the measured value plus or minus the indicated error. It should be noted that these errors are maximum, excluding human errors in reading and recording. They are related to an extremely high confidence level; average error values are much lower.

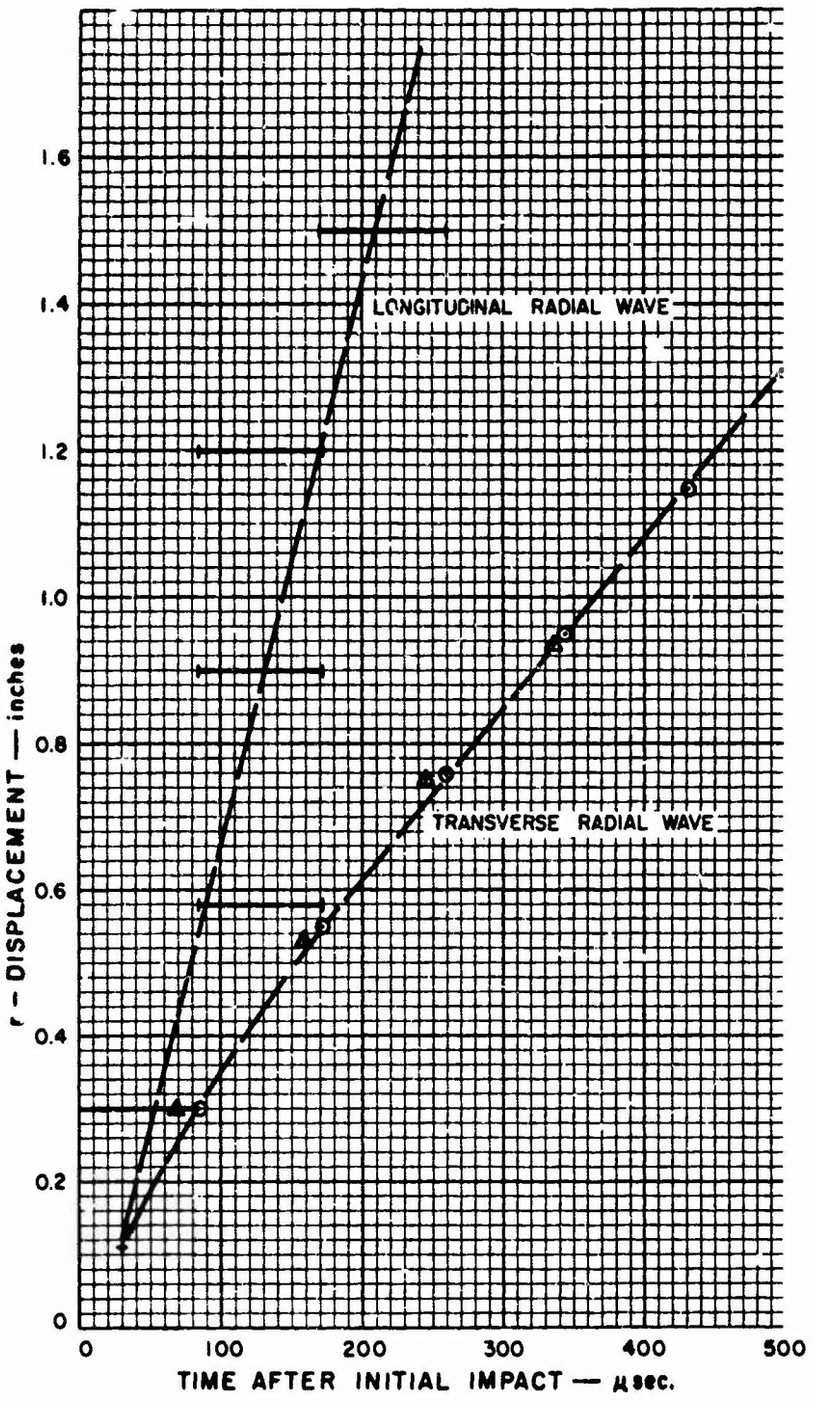

Figure 14. Relationship Between Radial Displacement and Time of Arrival for the Longitudinal and Transverse Radial Wave Fronts. Test No. 40-C, Impact Velocity - 900 feet per second. Material - 43 ounces per square yard Nylon Felt.

TABLE I

MAXIMUM MEASUREMENT ERRORS
IN DISPLACEMENT-TIME DATA

Displacement	Maximum Error	
Inches	Inches	Percent
0.01	0.014	140
.10	0.018	18
1.00	0.036	3.6
10.00	0.22	2.2

Figure 8, on which displacement data depicting projectiles motion are plotted, illustrates the typical range of displacement measurements. This range lies between 0.5 inch and 1.75 inches.

Again, emphasizing that the errors given in Table I are maximum, and considering the range within which measurements are being made, average errors in the displacement data obtained by the spark-gap technique are of a few (1 to 2) percent. The high precision of this displacement data provides an accurate means for establishing the validity of displacement-time relationships predicted by analytical models. Equations of motion derived from the models can be integrated, either exactly by mathematical means or precisely by numerical means, to yield such relationships. Thus, the displacement-time data obtained during the experimental program provide an invaluable data bank for establishing the validity of model predictions within a 1 to 2 percent accuracy range.

The displacement-time data have been used to develop velocity and force functions such as those discussed in connection with Figures 9, 10, 11, and 13. This development has involved the careful fitting of curves to the displacement data and subsequent, single and double, graphical differentiation. If a continuum of displacement-time data points were available, the fitting of a curve and its subsequent graphical differentiation would result in velocity values that would reflect, directly, the original accuracy of the displacement data. While the experimental data are very accurate at specific values of displacement and time, exact knowledge of values within the regions between data points is not available. Therefore, errors are introduced as a result of the interpretation of the data. Great care has been exercised in use of the graphical differentiation technique. The most critical step is in

fitting the curve to the displacement-time data, graphical differentiation of this curve introduces only small errors which result from the mechanical measurement of slopes. It is impossible to calculate values for the accuracy of resulting velocity and force relationships. However, the degree of observed consistency in the graphical results obtained from a large number of individual experiments indicates that these relationships are valid for describing the characteristics of ballistic interaction.

The method which is used to determine the longitudinal tensile wave velocity, C, involves 86 microsecond time periods rather than precise time of arrival values. Therefore, the resulting values for C are nominal values. The determination of the transverse wave velocity, ω, is more precise, involving the fitting of transverse deformation profile contours to the position-time data provided by the photograph of the spark-gap display. The accuracy of transverse wave velocity measurements is of the same order of magnitude as the accuracies related to projectile and material velocity measurements.

E. Presentation of Experimental Results

During the experimental program, tests were conducted involving four felt materials (polypropylene, dacron, orlon, nylon) and three areal densities (nominally, 40 ounces per square yard for each of the four materials and 53 and 19 ounces per square yard for nylon). The properties of these felt materials are described in Table A-1 in the Appendix. The test projectile was the 17-grain fragment simulator (T-37), also described in Table A-1. A test series for each material was conducted in which the impact velocity of the projectile was varied from approximately 400 feet per second up to a value near the ballistic limit. All tests were conducted at zero degrees obliquity. A complete tabulation of all valid displacement-time data gathered during this research effort is given in Table B-1 of the Appendix. In addition to the displacement-time data obtained by the spark-gap technique, residual velocity tests (velocity after complete perforation) were conducted for five of the six felt materials. The 19 ounce per square yard nylon felt was not available at the time these tests were performed. The complete results of the residual velocity tests are presented in Table C-1 in the Appendix.

In section C, Data Analysis Procedure, the method was explained by which the experimental displacement-time data for the center station is used to develop velocity-time, force-time, and force-distance relationships. This information pertains to the behavior

of the projectile during the impact event from the time of initial contact with the felt material until major deceleration has been accomplished. This data greatly aids in the definition of the response to impact of felt materials since the projectile behavior is a direct result of the material behavior. Typical results obtained for these relationships are presented on Figures 15 through 32. For each material, curves are presented for (1) projectile velocity as a function of time after initial impact, (2) total retardation force developed by the felt material as a function of time after initial impact, and (3) this same force as a function of distance traveled. It is important to note that the force-distance relationship does not include the preliminary force-distance increment associated with initial compression of the felt in front of the projectile; this pressure and its relatively small magnitude were discussed previously in section C, Data Analysis Procedure. This increment can be estimated by including the known calculated constant impact force (at time = 0) for an initial distance equal to approximately two-thirds the thickness of the felt (estimated from post-impact observations). This increment is of little consequence and has not been included in the curves since it represents behavior prior to development of the radial transverse deformation of the felt material which is the predominant behavior.

Measured values for the longitudinal and transverse wave velocities, C and ω, are listed in Table II. The longitudinal wave velocities were obtained by assuming constant slopes for the displacement-time relationships; transverse wave velocities represent the constant slope portion of displacement-time curves (see Figure 14).

Figures 33 through 36 are presented to illustrate the ability of the displacement-time data to provide information which defines the behavior of the felt material during impact. These curves show the transverse velocity of the felt material at several radii as a function of time after initial impact. Tests for relatively high and low impact velocities are presented for polypropylene and nylon. These four figures are typical and illustrate the significant characteristics of material behavior.

The results for three of the five test series involving the measurement of velocity after complete perforation are presented as Figures 37, 38, and 39. These plots allow comparisons to be made between polypropylene and nylon felts of the same areal density and between nylon felts of two different areal densities. The data plotted on these curves are the residual velocity, V_r, of the fragment

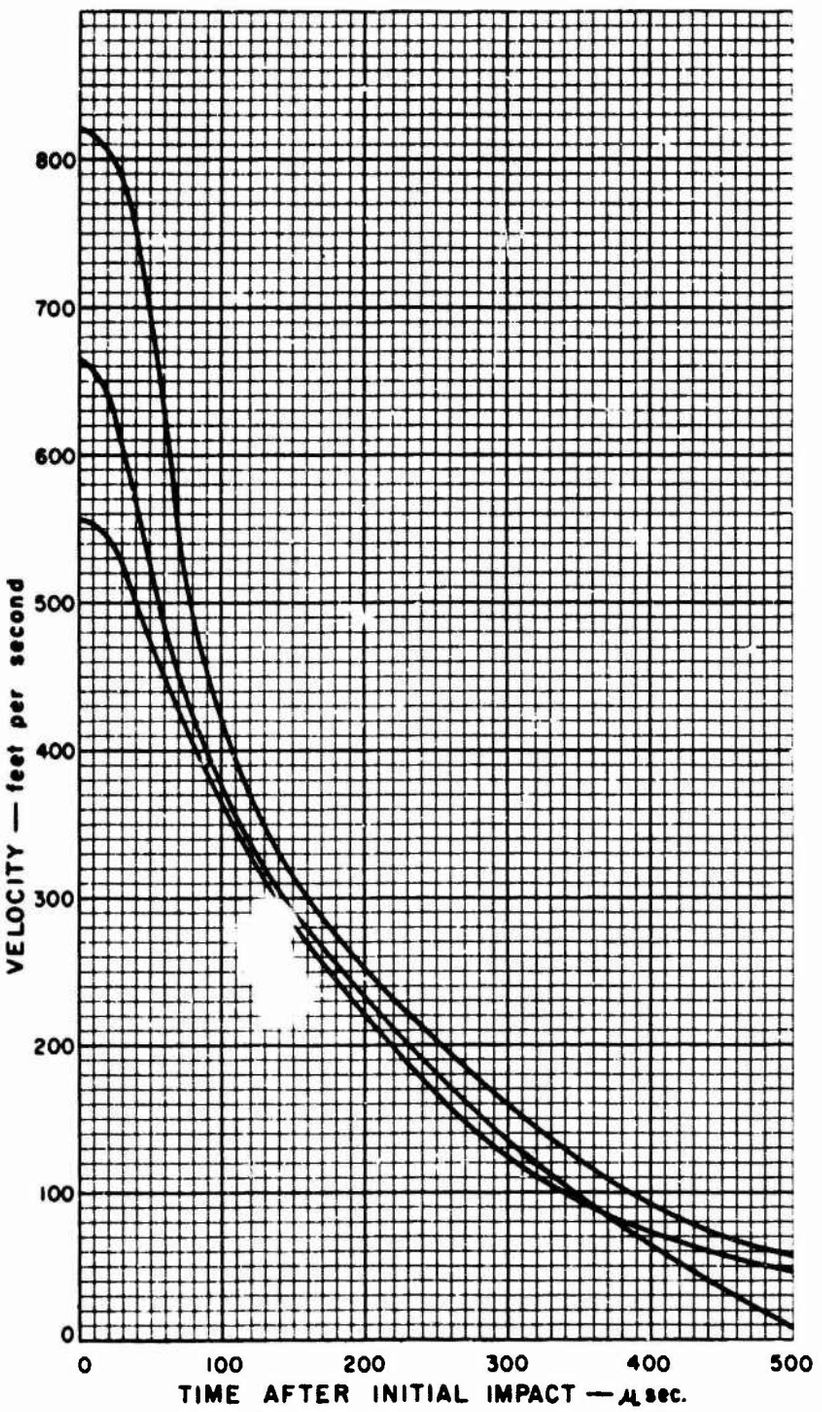

Figure 15. Projectile Velocity as a Function of Time after Initial Impact. Experimental Results for Tests 21-C, 24-C, and 25-C. Material - 40 ounces per square yard Polypropylene Felt.

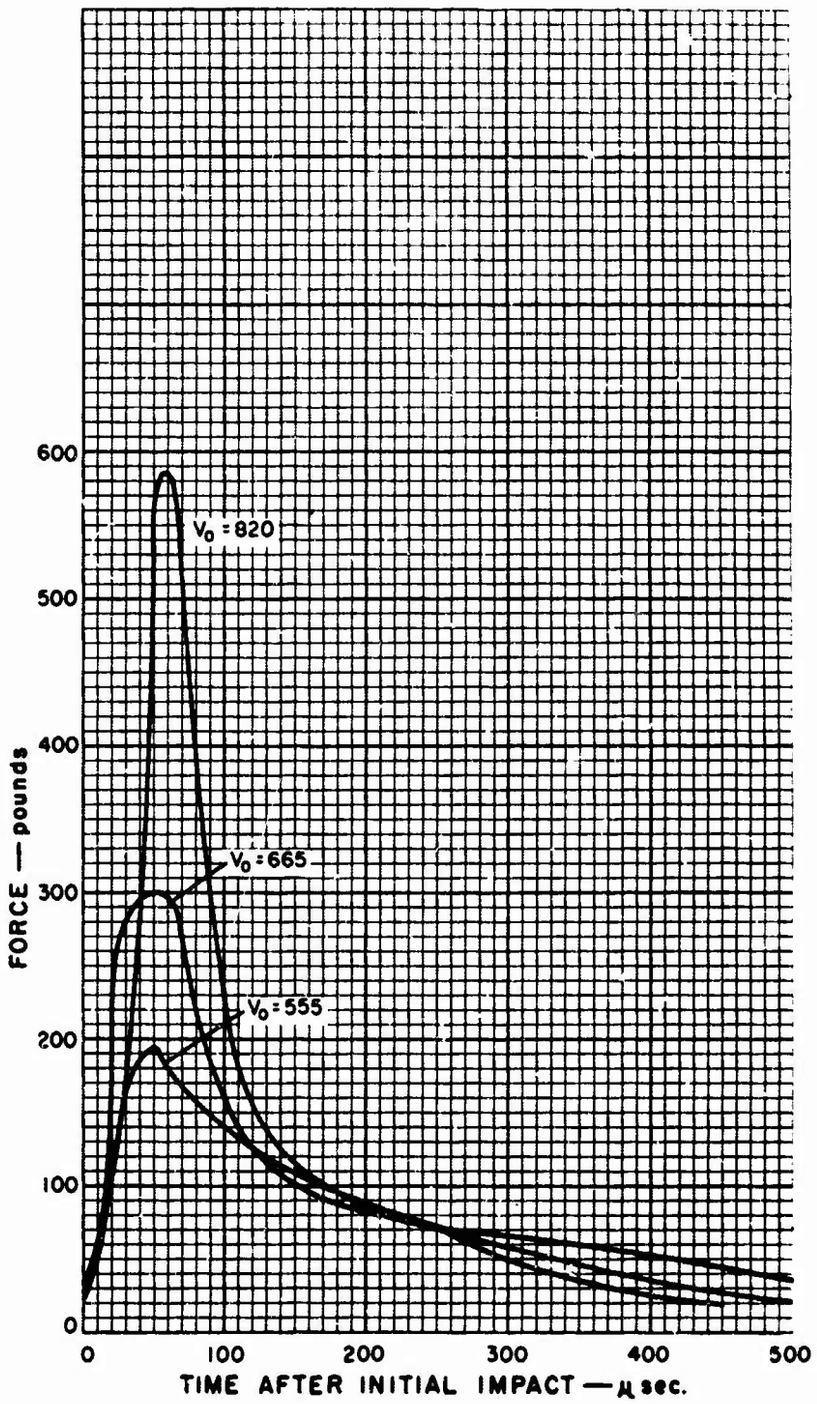

Figure 16. Force Opposing Projectile Motion as a Function of Time after Initial Impact. Experimental Results for Tests 21-C, 24-C, and 25-C. Material - 40 ounces per square yard Polypropylene Felt.

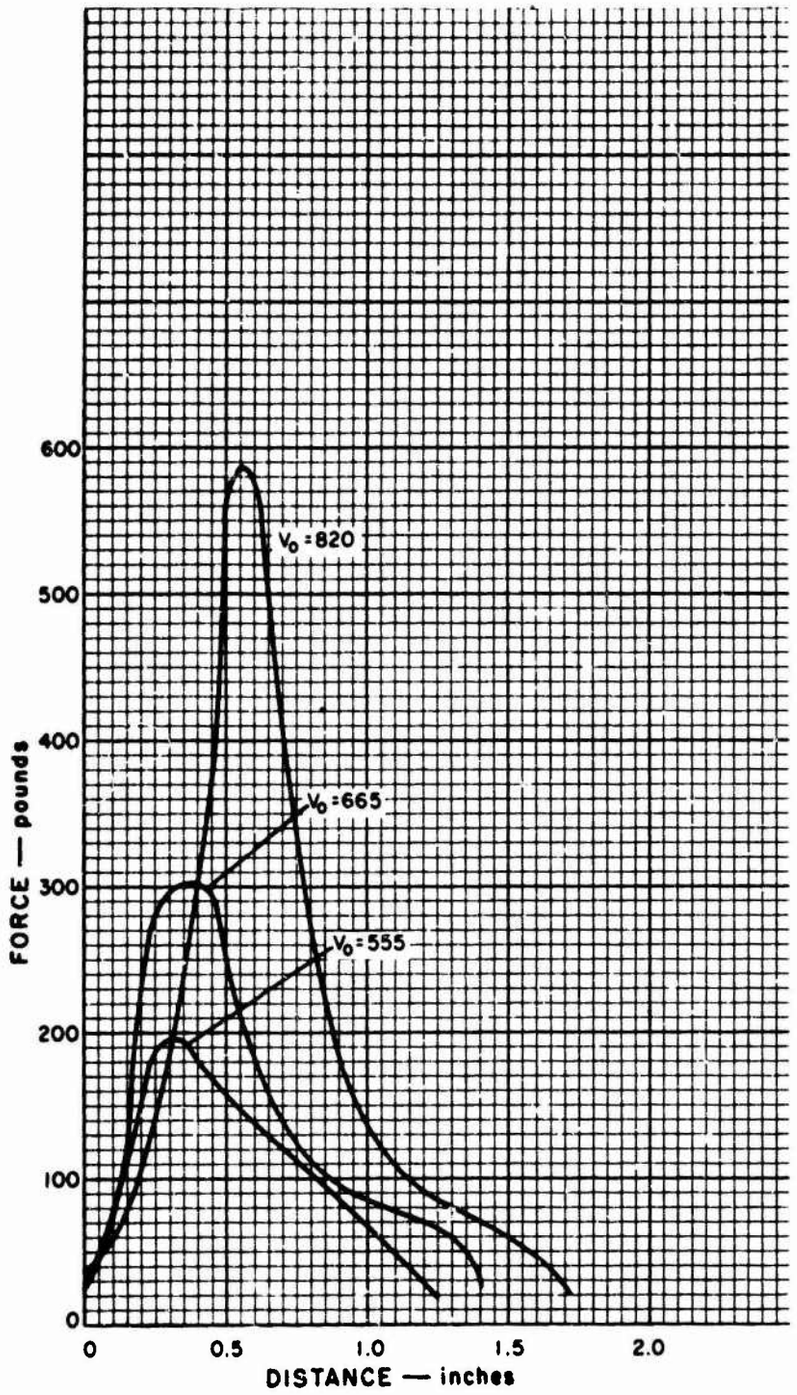

Figure 17. Force Opposing Projectile Motion as a Function of Distance Traveled. Experimental Results for Tests 21-C, 24-C, and 25-C. Material - Polypropylene Felt.

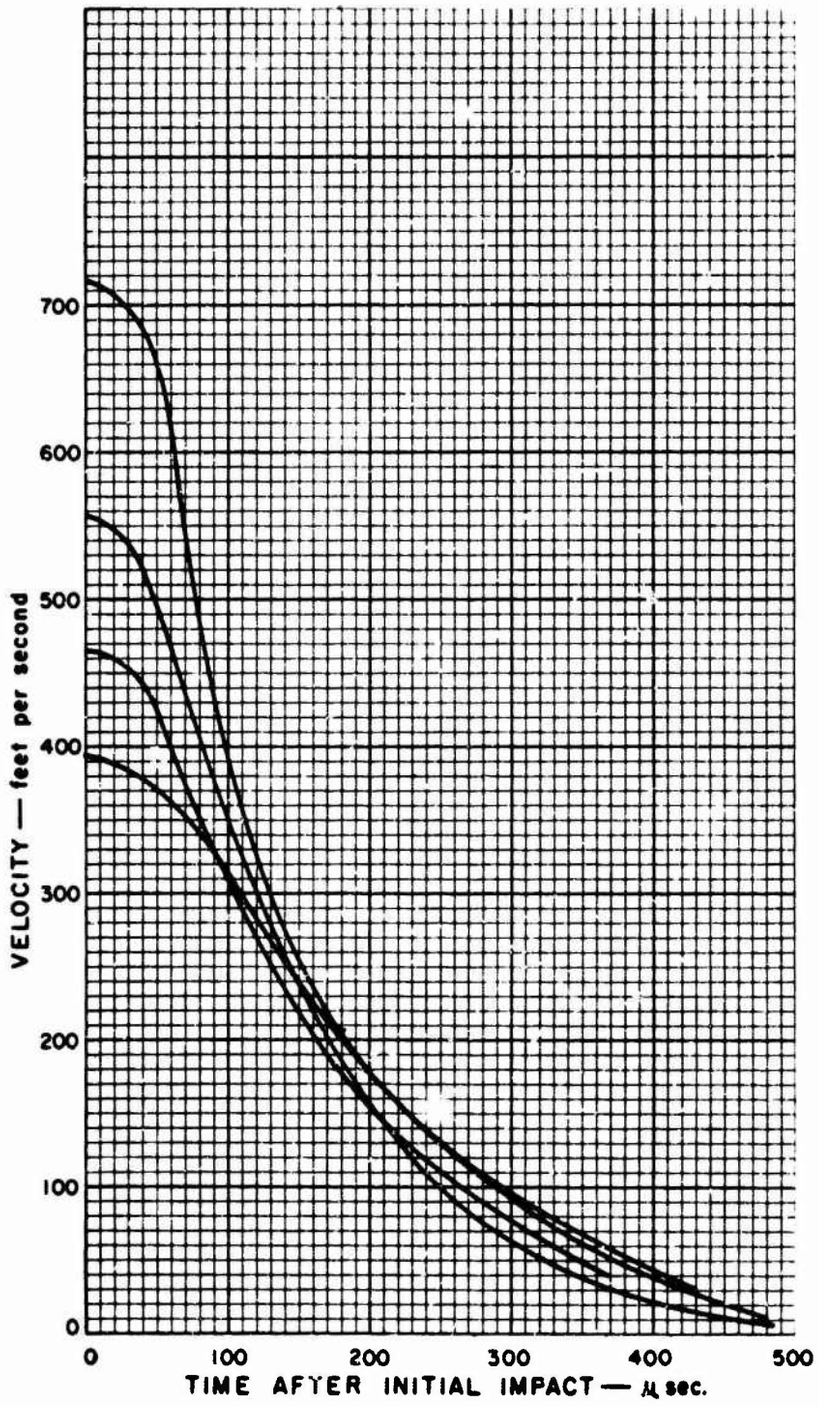

Figure 18. Projectile Velocity as a Function of Time after Initial Impact. Experimental Results for Tests 42-C, 43-C, 44-C, and 49-C. Material - 42 ounces per square yard Dacron Felt.

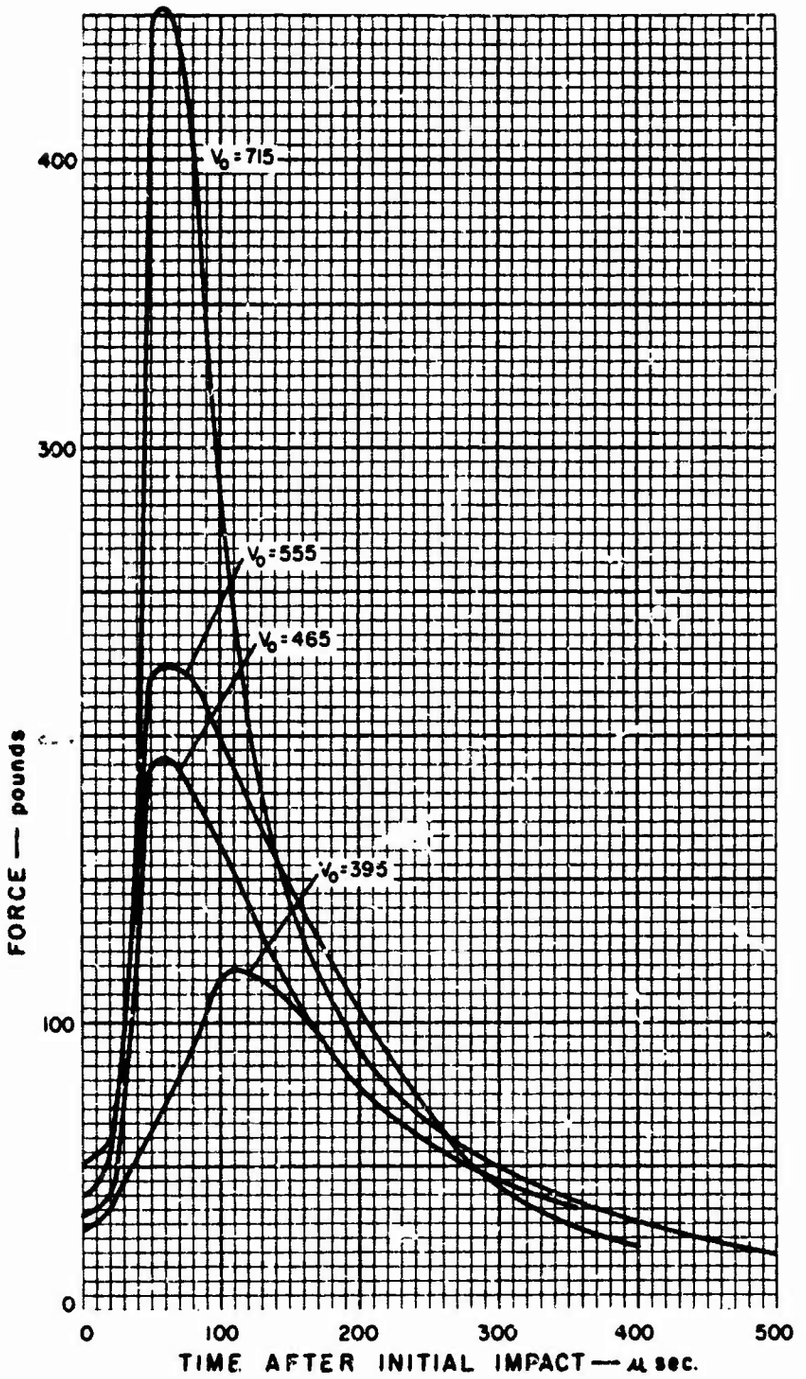

Figure 19. Force Opposing Projectile Motion as a Function of Time after Initial Impact. Experimental Results for Tests 42-C, 43-C, 44-C, and 49-C. Material - 42 ounces per square yard Dacron Felt.

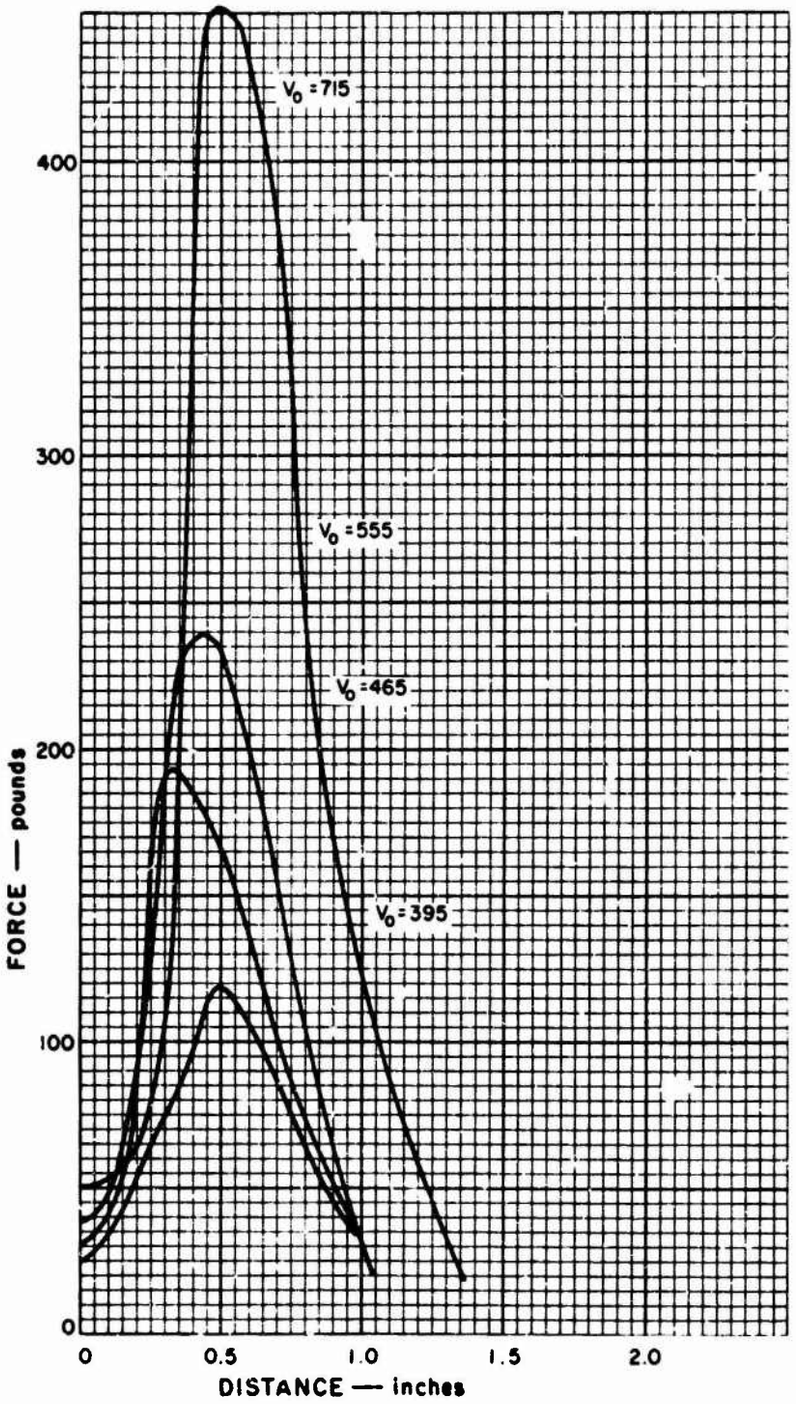

Figure 20. Force Opposing Projectile Motion as a Function of Distance Traveled. Experimental Results for Tests 42-C, 43-C, 44-C, and 49-C. Material - 42 ounces per square yard Dacron Felt.

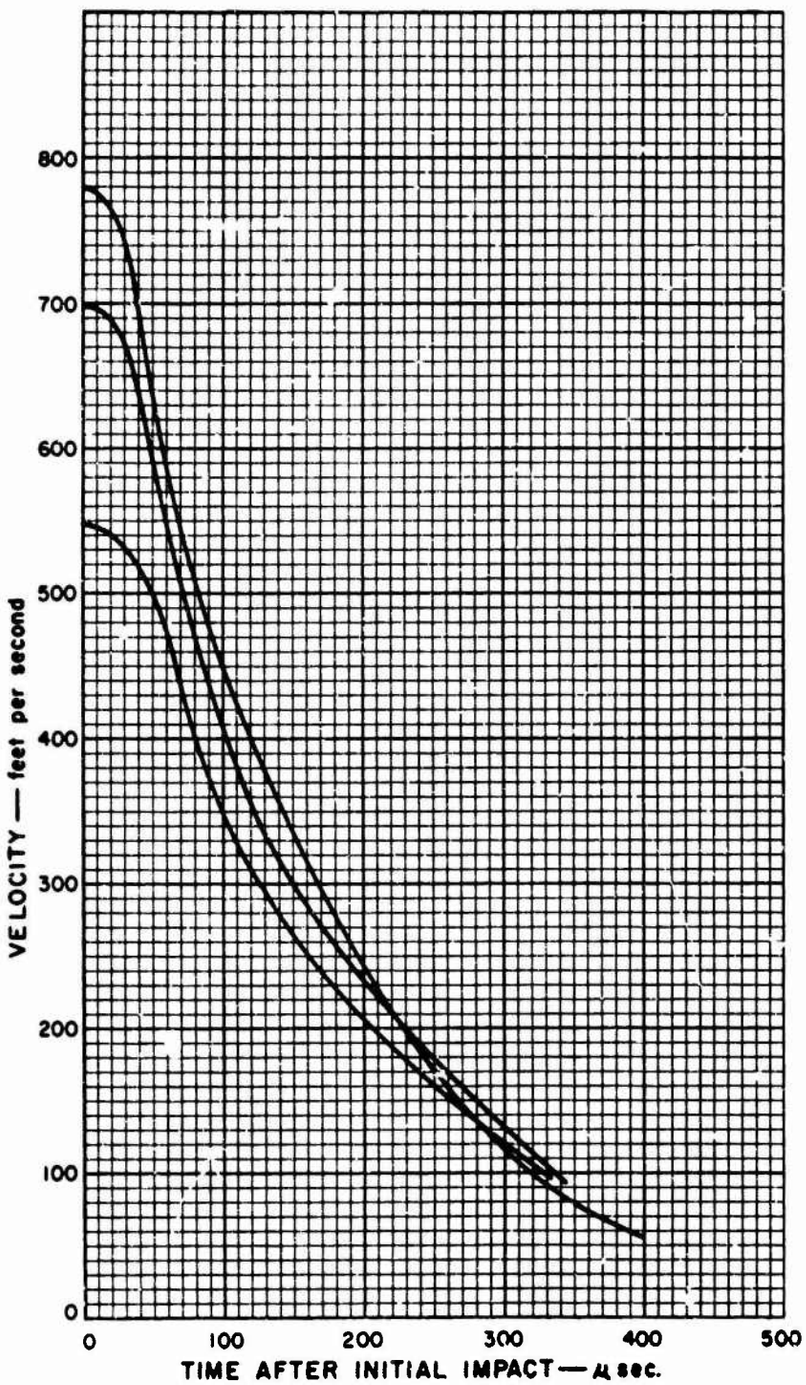

Figure 21. Projectile Velocity as a Function of Time after Initial Impact. Experimental Results for Tests 58-C, 59-C, and 62-C. Material - 43 ounces per square yard Orlon Felt.

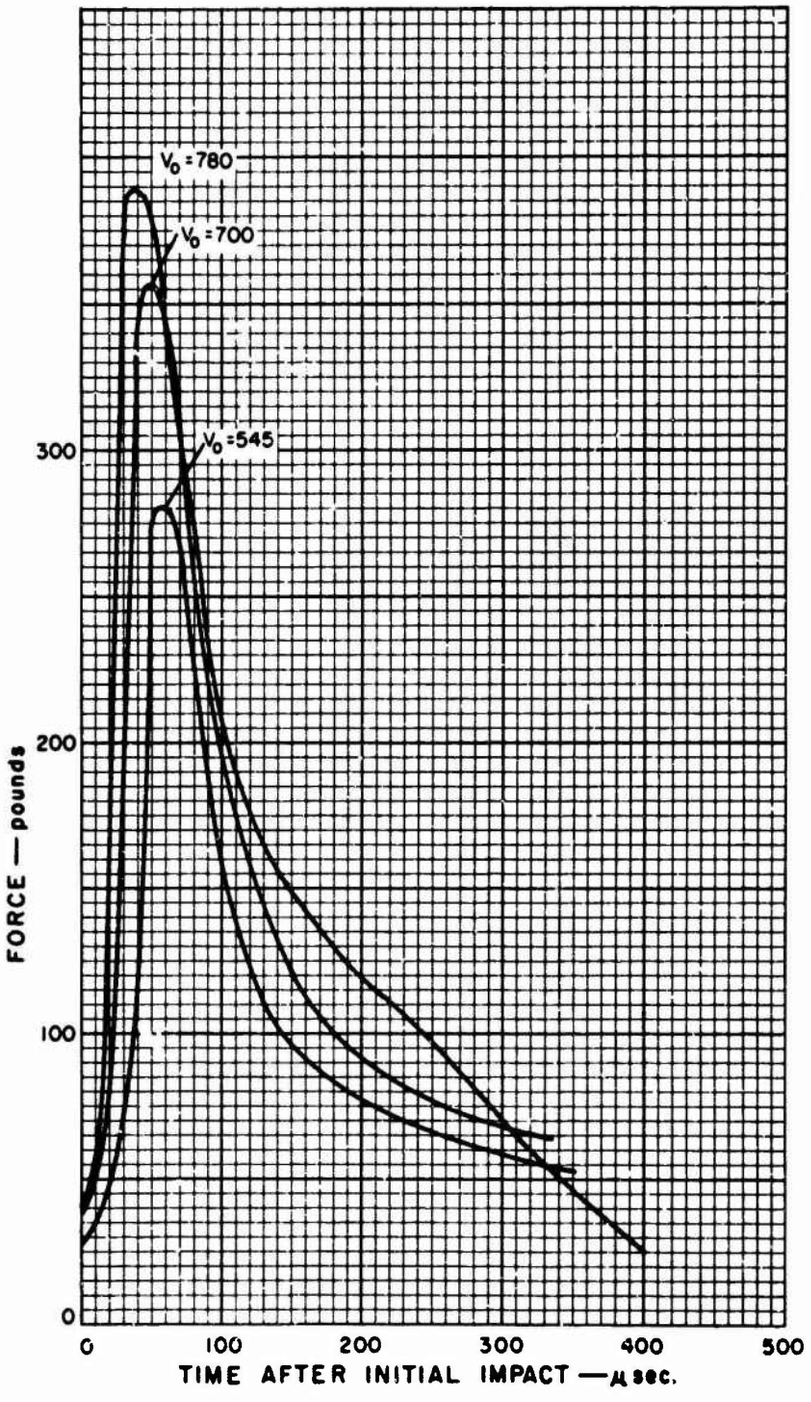

Figure 22. Force Opposing Projectile Motion as a Function of Time after Initial Impact. Experimental Results for Tests 58-C, 59-C, and 62-C. Material - 43 ounces per square yard Orlon Felt.

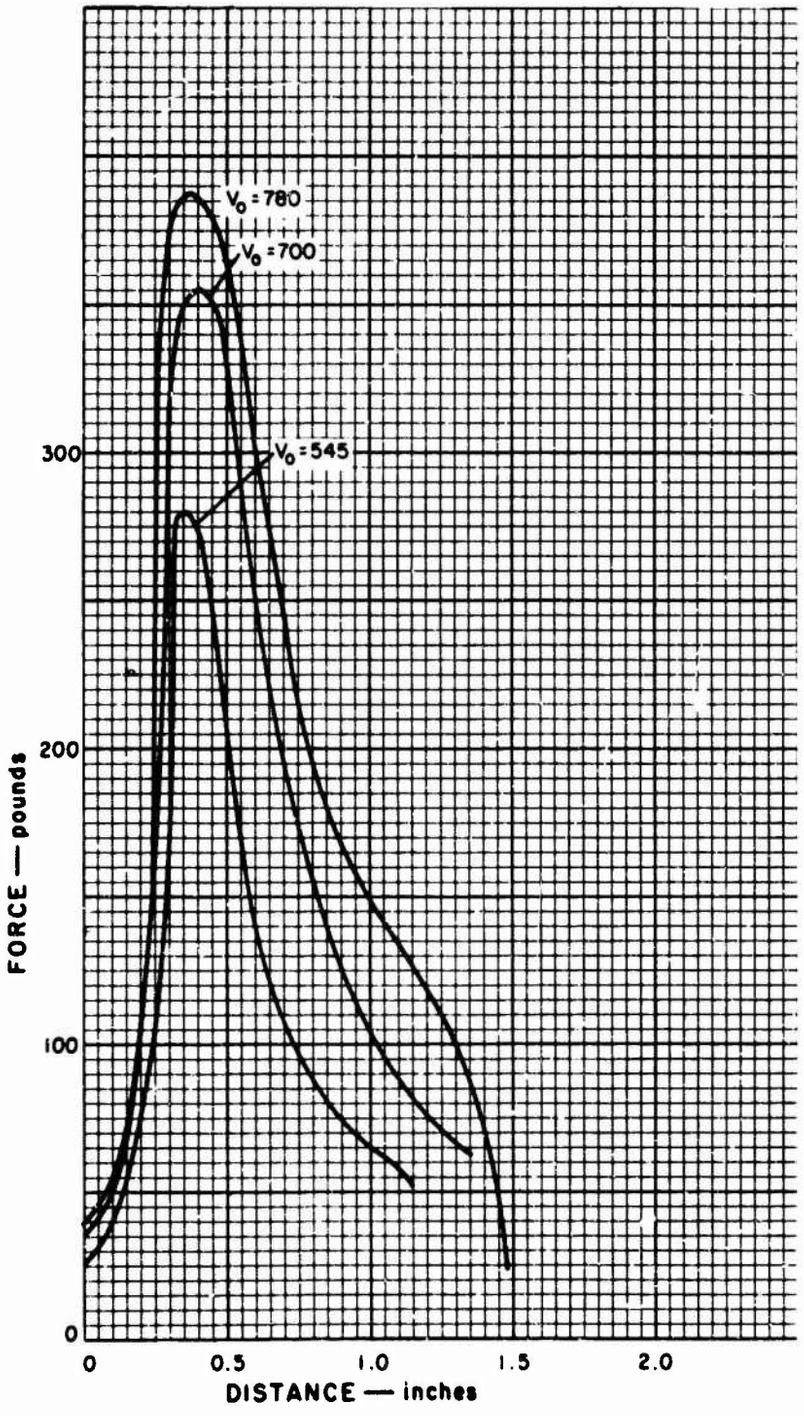

Figure 23. Force Opposing Projectile Motion as a Function of Distance Traveled. Experimental Results for Tests 58-C, 59-C, and 62-C. Material - 43 ounces per square yard Orlon Felt.

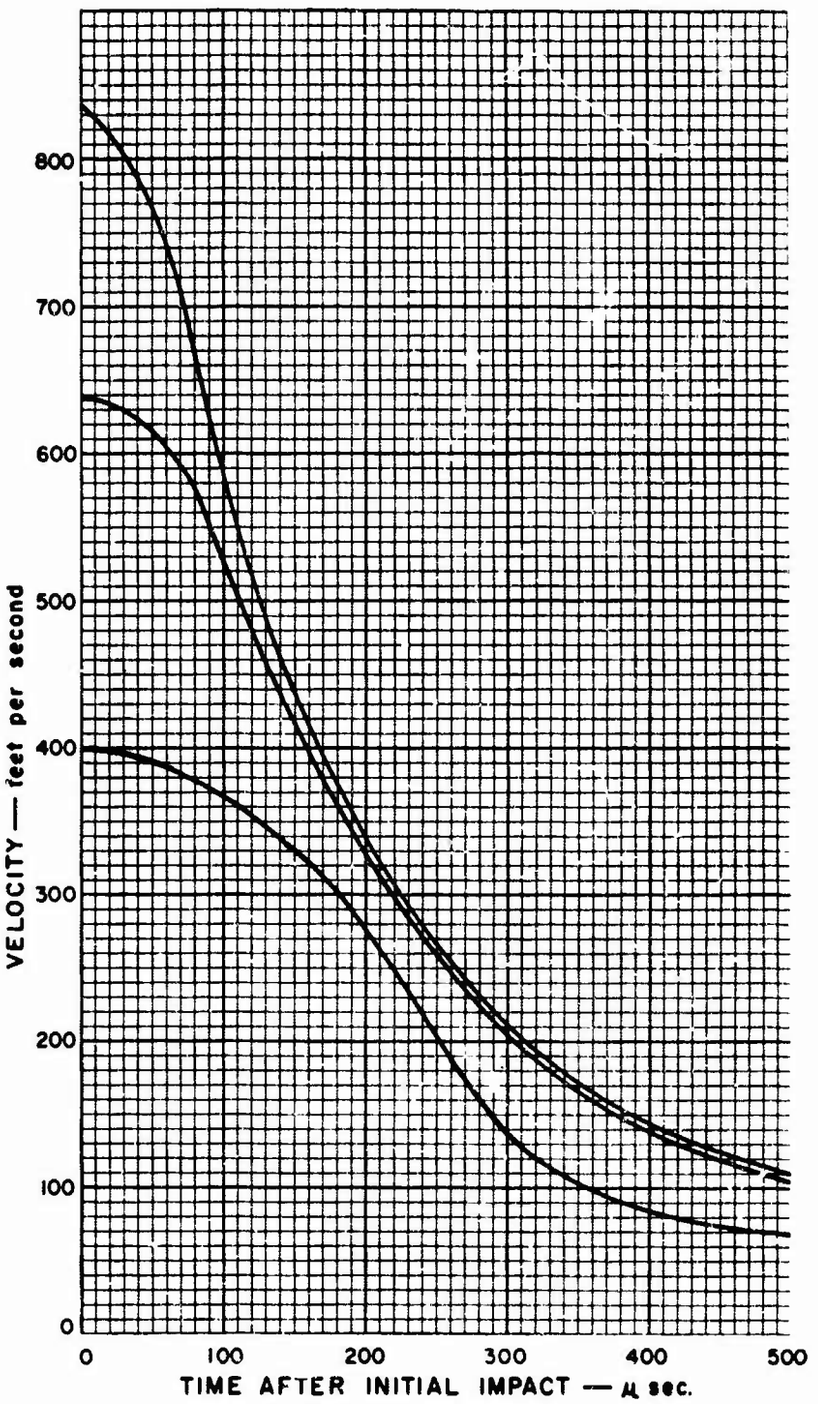

Figure 24. Projectile Velocity as a Function of Time after Initial Impact. Experimental Results for Tests 7-C, 15-C, and 19-C. Material - 53 ounces per square yard Nylon Felt.

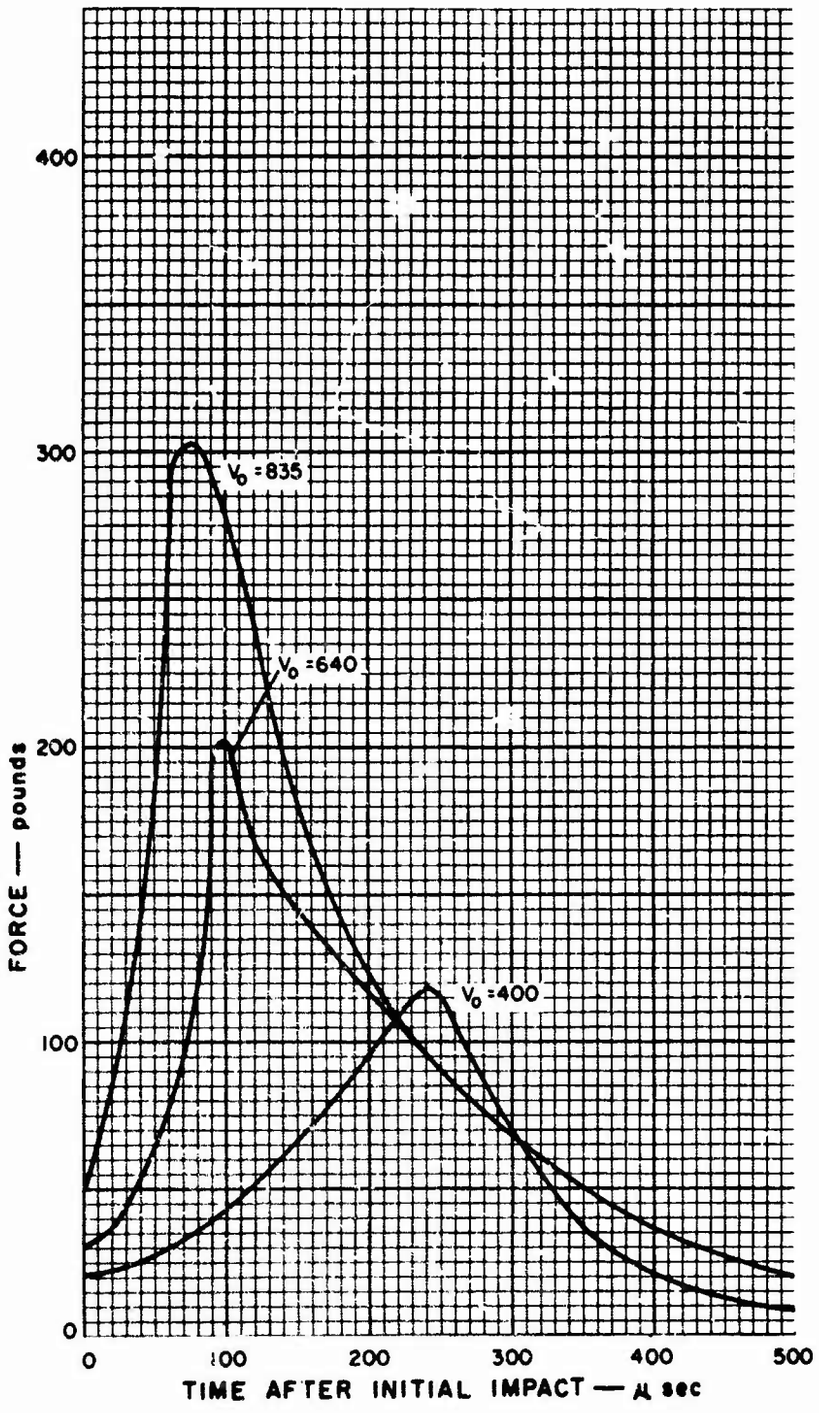

Figure 25. Force Opposing Projectile Motion as a Function of Time after Initial Impact. Experimental Results for Tests 7-C, 15-C, and 19-C. Material - 53 ounces per square yard Nylon Felt.

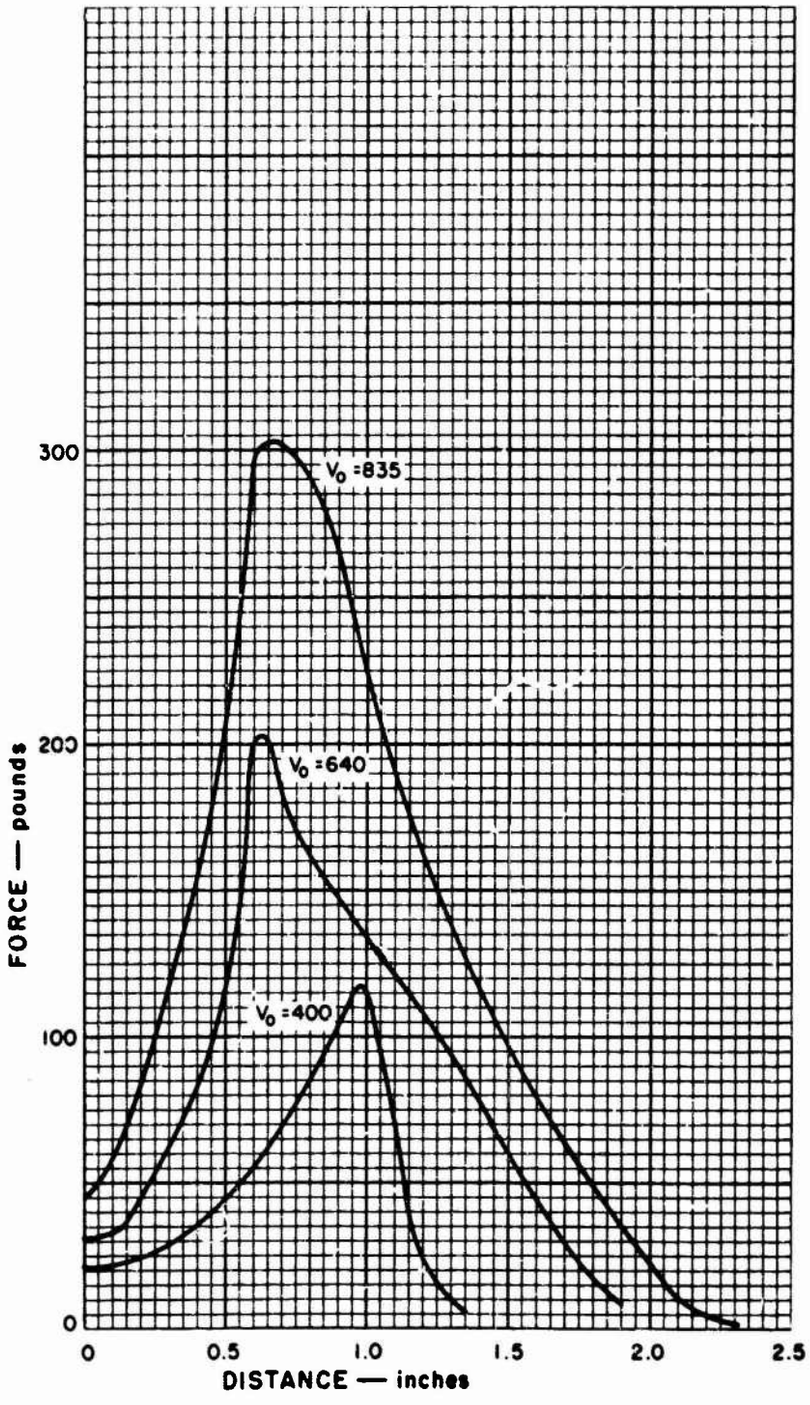

Figure 26. Force Opposing Projectile Motion as a Function of Distance Traveled. Experimental Results for Tests 7-C, 15-C, and 19-C. Material - 53 ounces per square yard Nylon Felt.

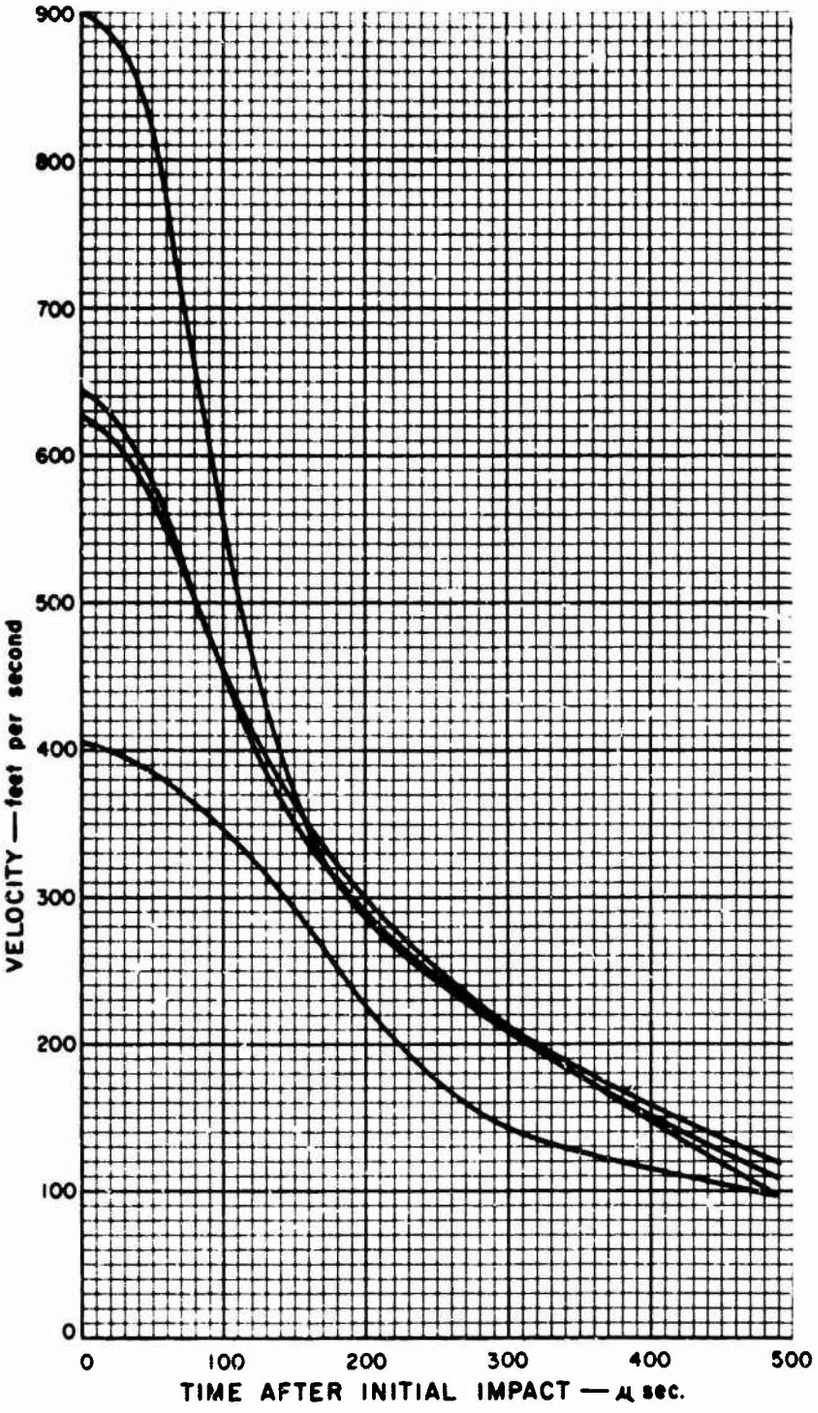

Figure 27. Projectile Velocity as a Function of Time after Initial Impact. Experimental Results for Tests 33-C, 36-C, 39-C, and 40-C. Material - 43 ounces per square yard Nylon Felt.

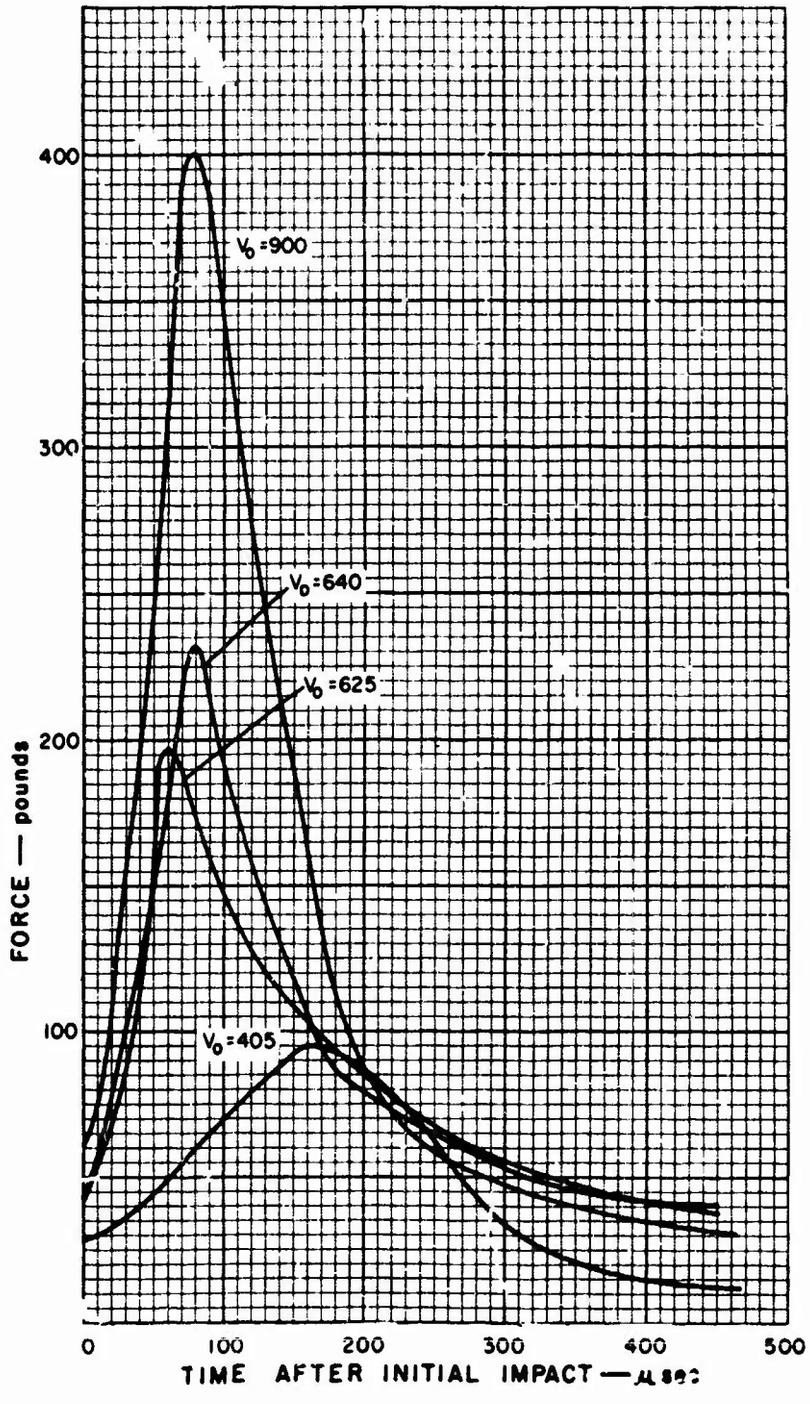

Figure 28. Force Opposing Projectile Motion as a Function of Time after Initial Impact. Experimental Results for Tests 33-C, 36-C, 39-C, and 40-C. Material - 43 ounces per square yard Nylon Felt.

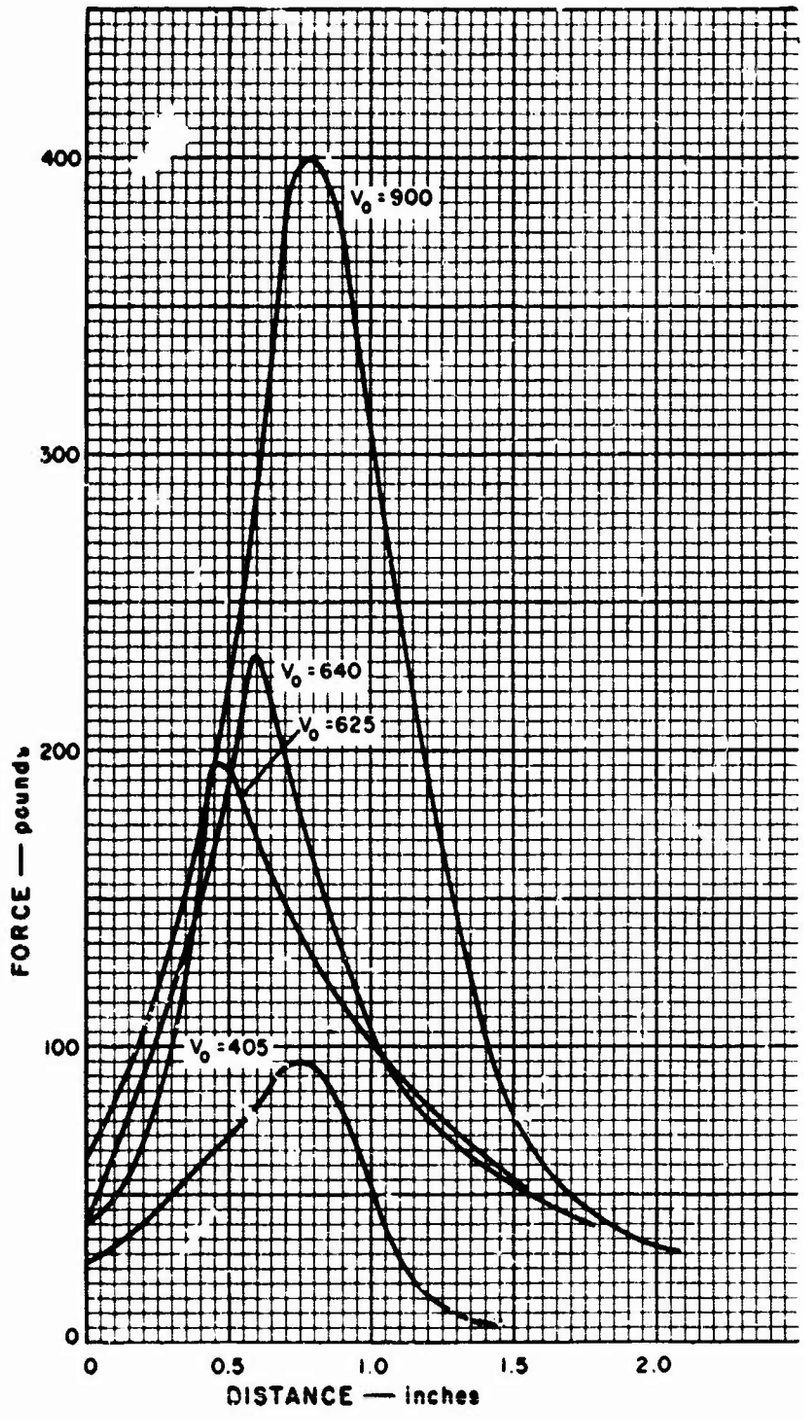

Figure 29. Force Opposing Projectile Motion as a Function of Distance Traveled. Experimental Results for Tests 33-C, 36-C, 39-C, and 40-C. Material - 43 ounces per square yard Nylon Felt.

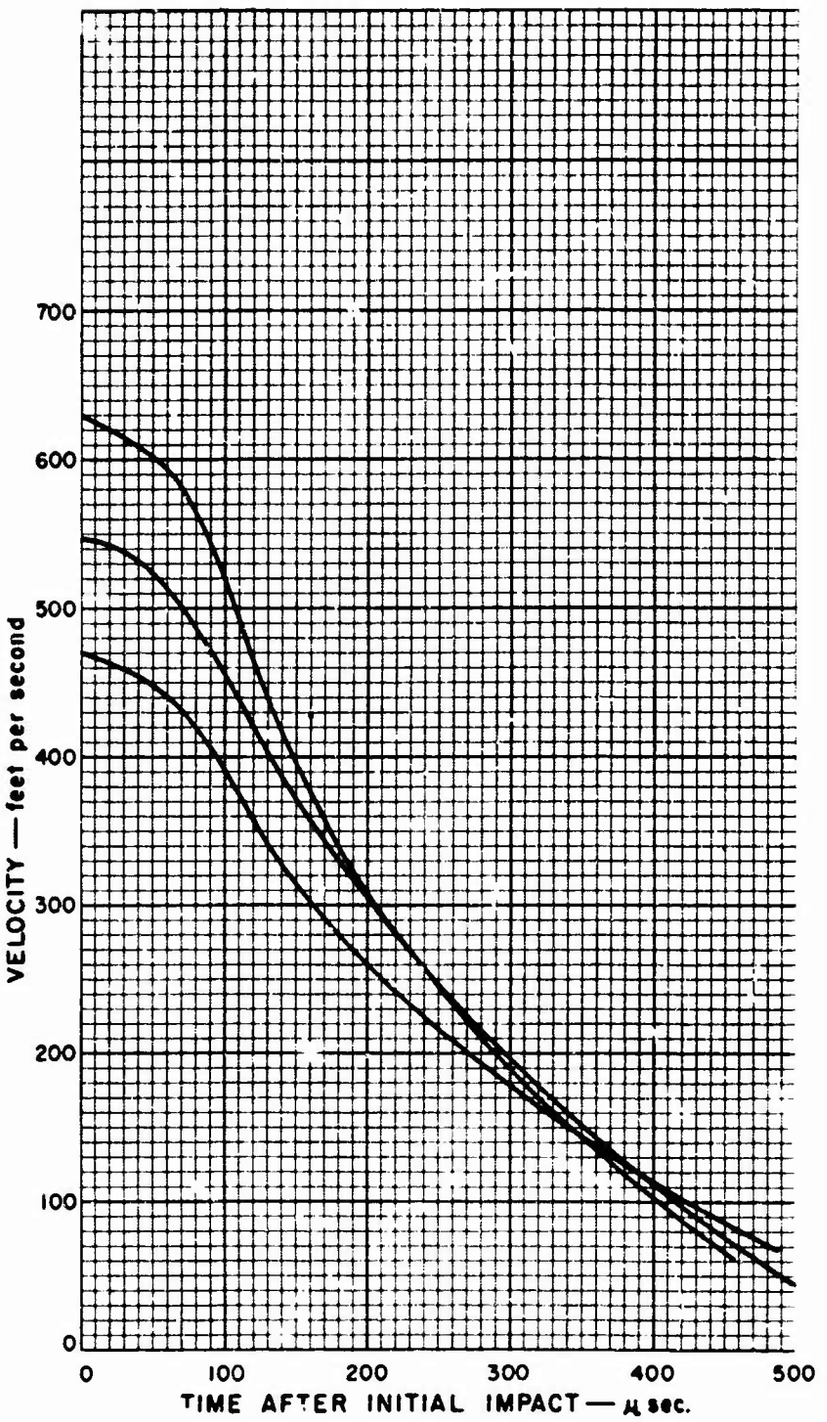

Figure 30. Projectile Velocity as a Function of Time after Initial Impact. Experimental Results for Tests 65-C, 66-C, and 68-C. Material - 19 ounces per square yard Nylon Felt.

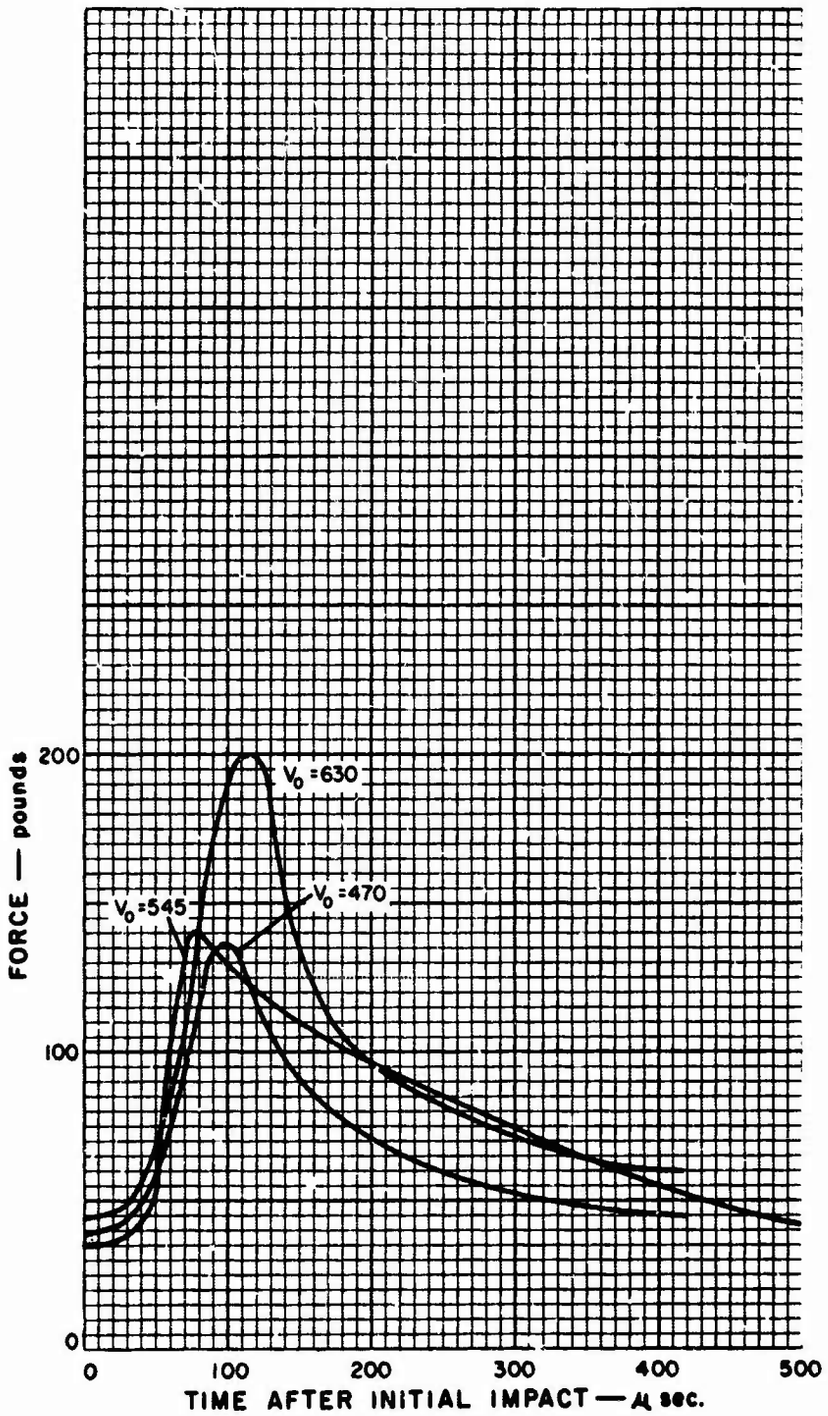

Figure 31. Force Opposing Projectile Motio : as a Function of Time after Initial Impact. Experimental Results for Tests 65-C, 66-C, and 68-C. Material - 19 ounces per square yard Nylon Felt.

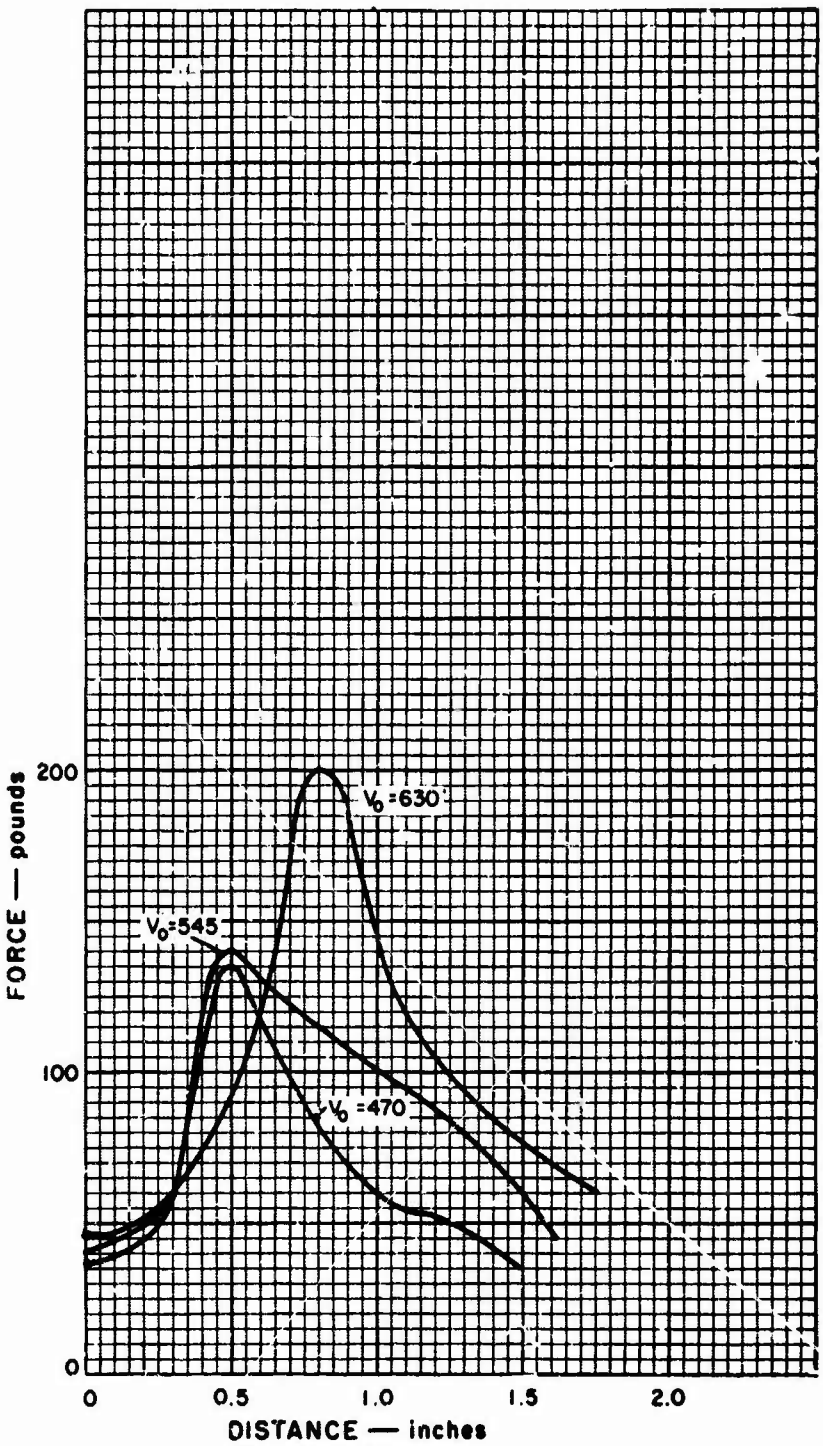

Figure 32. Force Opposing Projectile Motion as a Function of Distance Traveled. Experimental Results for Tests 65-C, 66-C, ard 68-C. Material - 19 ounces per square yard Nylon Felt.

TABLE II

LONGITUDINAL AND TRANSVERSE WAVE VELOCITY DATA

Material and Areal Density	Test No.	Impact Velocity V_o - fps	Longitudinal Wave Velocity C - fps	Transverse Wave Velocity ω - fps
Polypropylene 40 oz./yd^2	24-C	555	690	290
	21-C	665	695	275
	25-C	820	670	290
Dacron 42 oz./yd^2	44-C	390	480	240
	43-C	465	595	255
	49-C	555	690	295
	42-C	710	800	240
Orlon 43 oz./yd^2	58-C	545	585	280
	60-C	620	--	250
	59-C	700	750	270
	62-C	780	605	270
Nylon 43 oz./yd^2	39-C	405	545	180
	38-C	510	860	185
	36-C	630	580	155
	40-C	900	645	195
Nylon 53 oz./yd^2	7-C	400	415	145
	15-C	640	485	200
	12-C	730	485	190
	19-C	837	500	200
Nylon 19 oz./yd^2	65-C	465	680	225
	68-C	545	545	210
	66-C	630	--	255

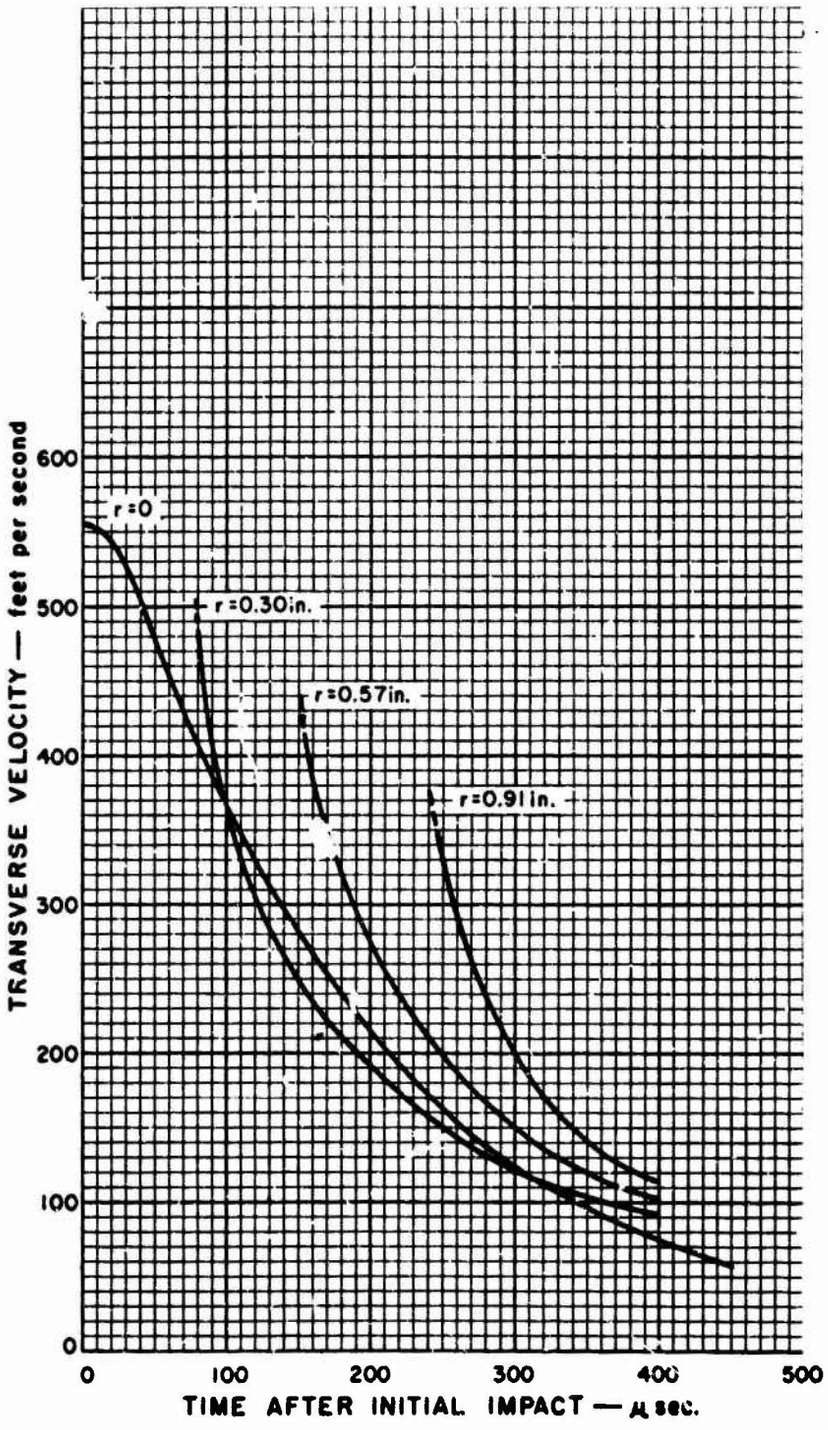

Figure 33. Transverse Velocity of Felt Material at Several Radii as a Function of Time after Initial Impact. Test No. 24-C. Material - 40 ounces per square yard Polypropylene Felt.

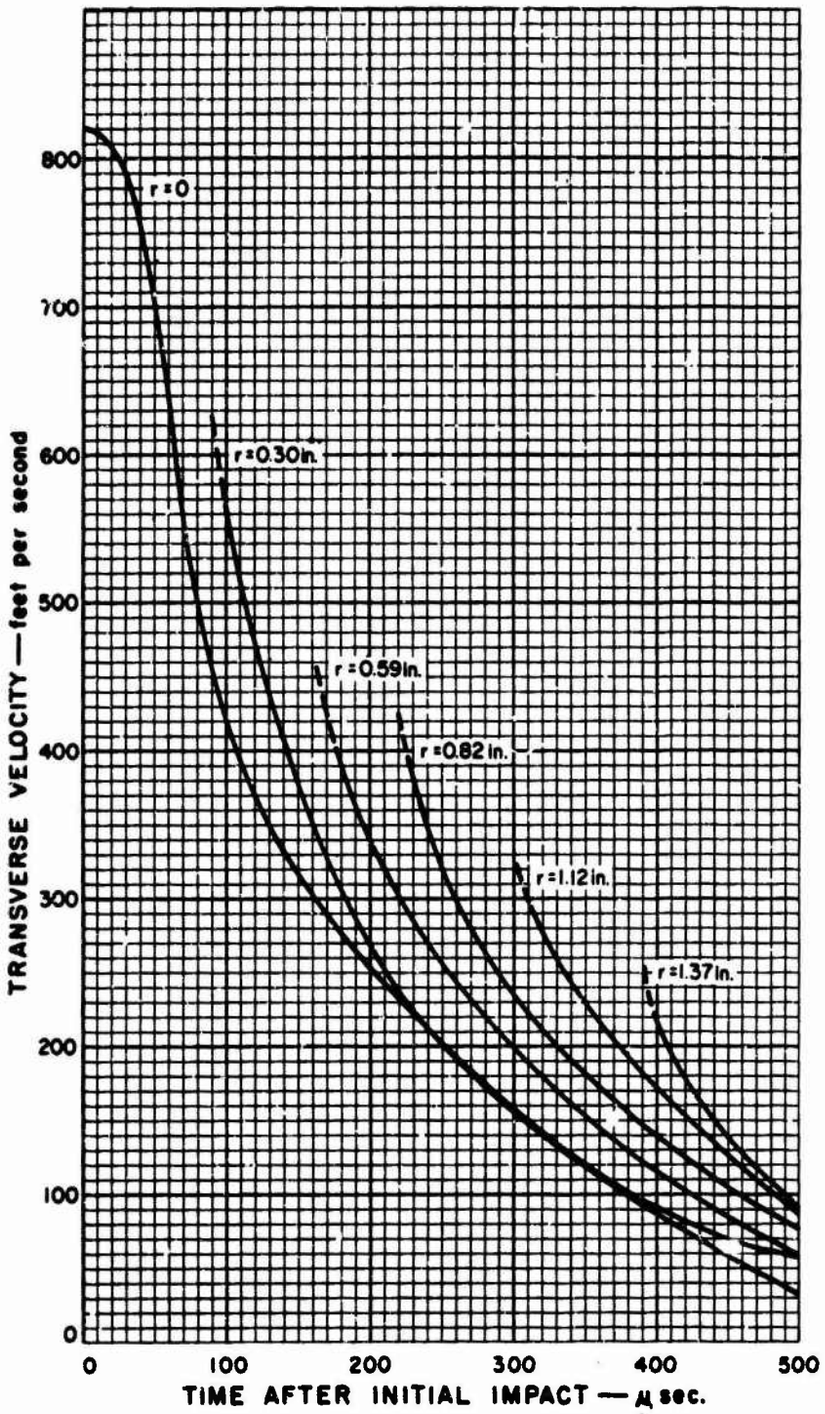

Figure 34. Transverse Velocity of Felt Material at Several Radii as a Function of Time after Initial Impact. Test No. 25-C. Material - 40 ounces per square yard Polypropylene Felt.

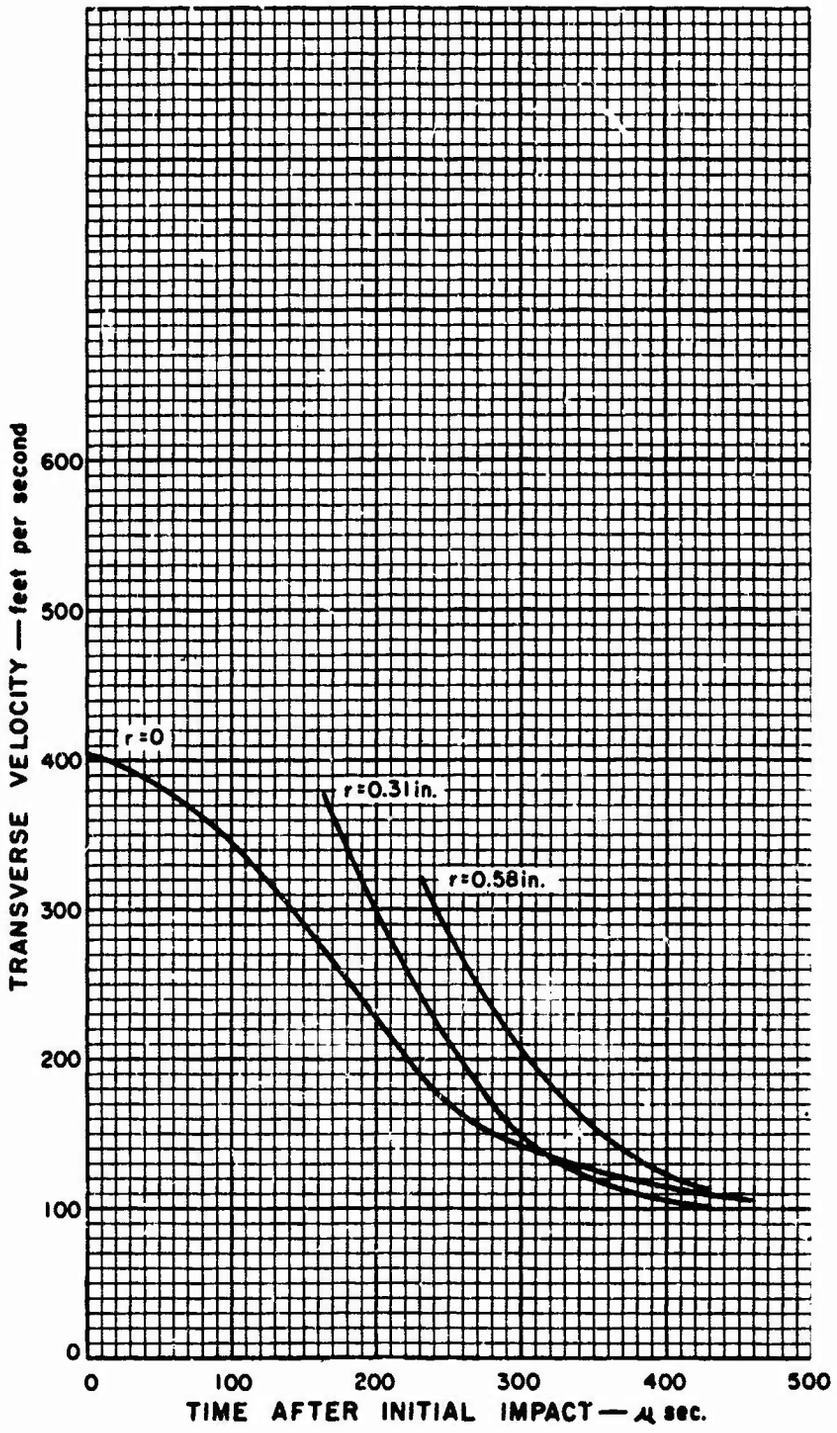

Figure 35. Transverse Velocity of Felt Material at Several Radii as a Function of Time after Initial Impact. Test No. 39-C. Material - 43 ounces per square yard Nylon Felt.

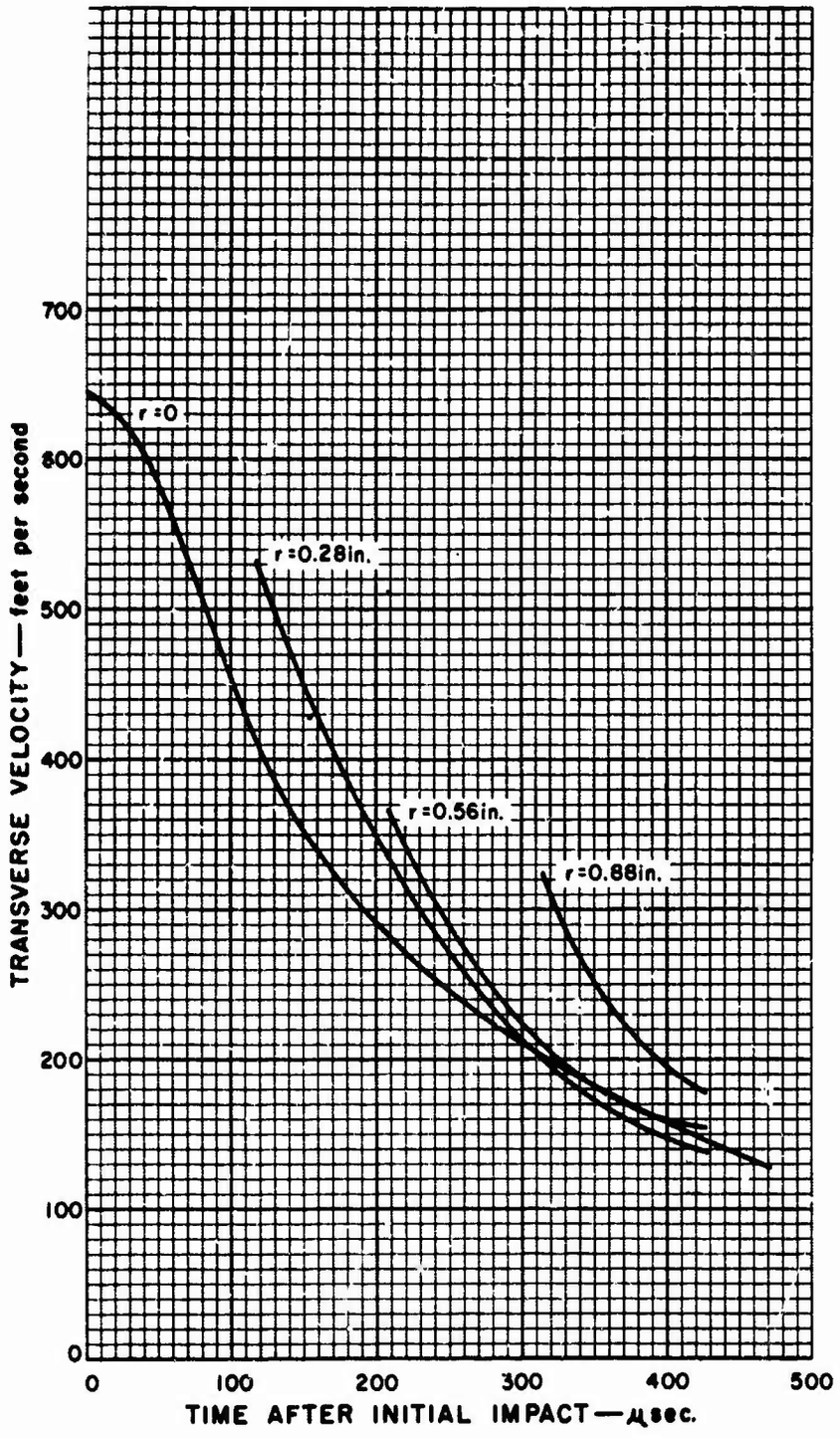

Figure 36. Transverse Velocity of Felt Material at Several Radii as a Function of Time after Initial Impact. Test No. 33-C. Material - 43 ounces per square yard Nylon Felt.

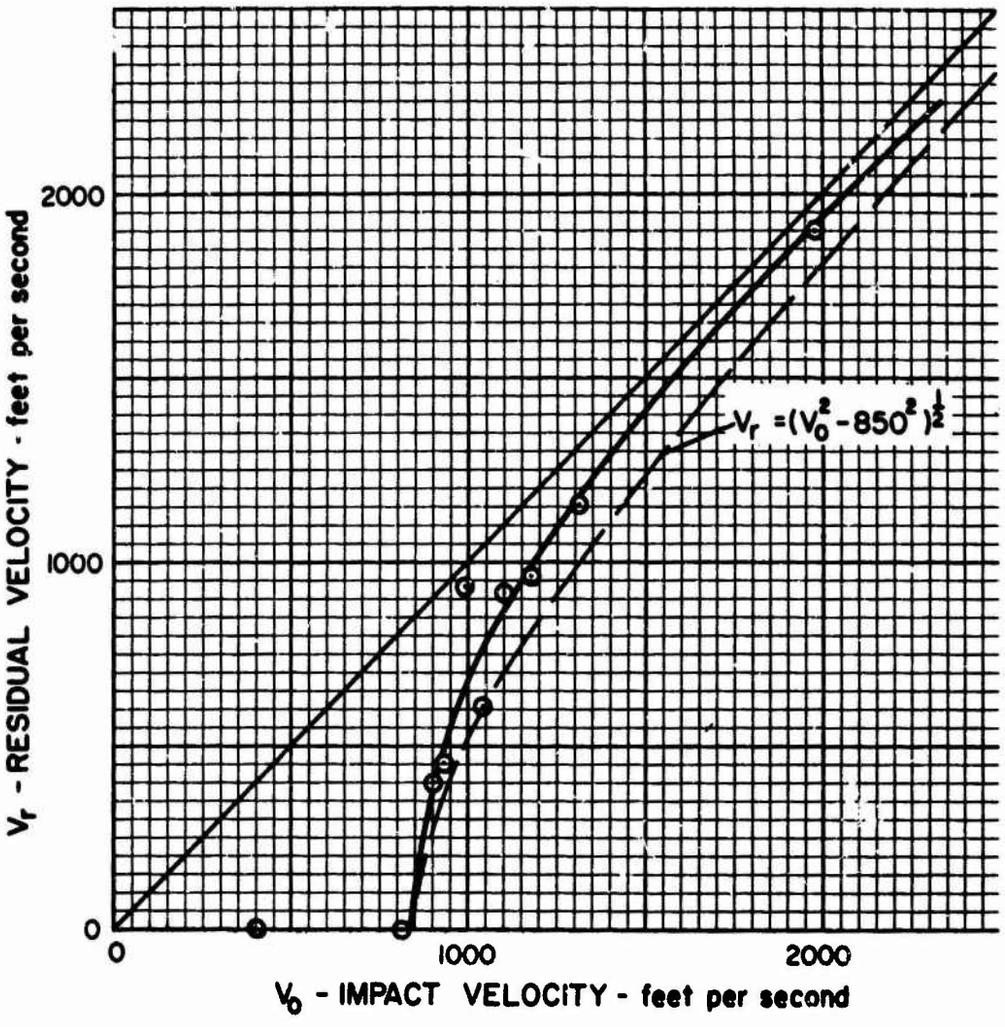

Figure 37. Residual Velocity after Complete Perforation. Material - 40 ounces per square yard Polypropylene Felt.

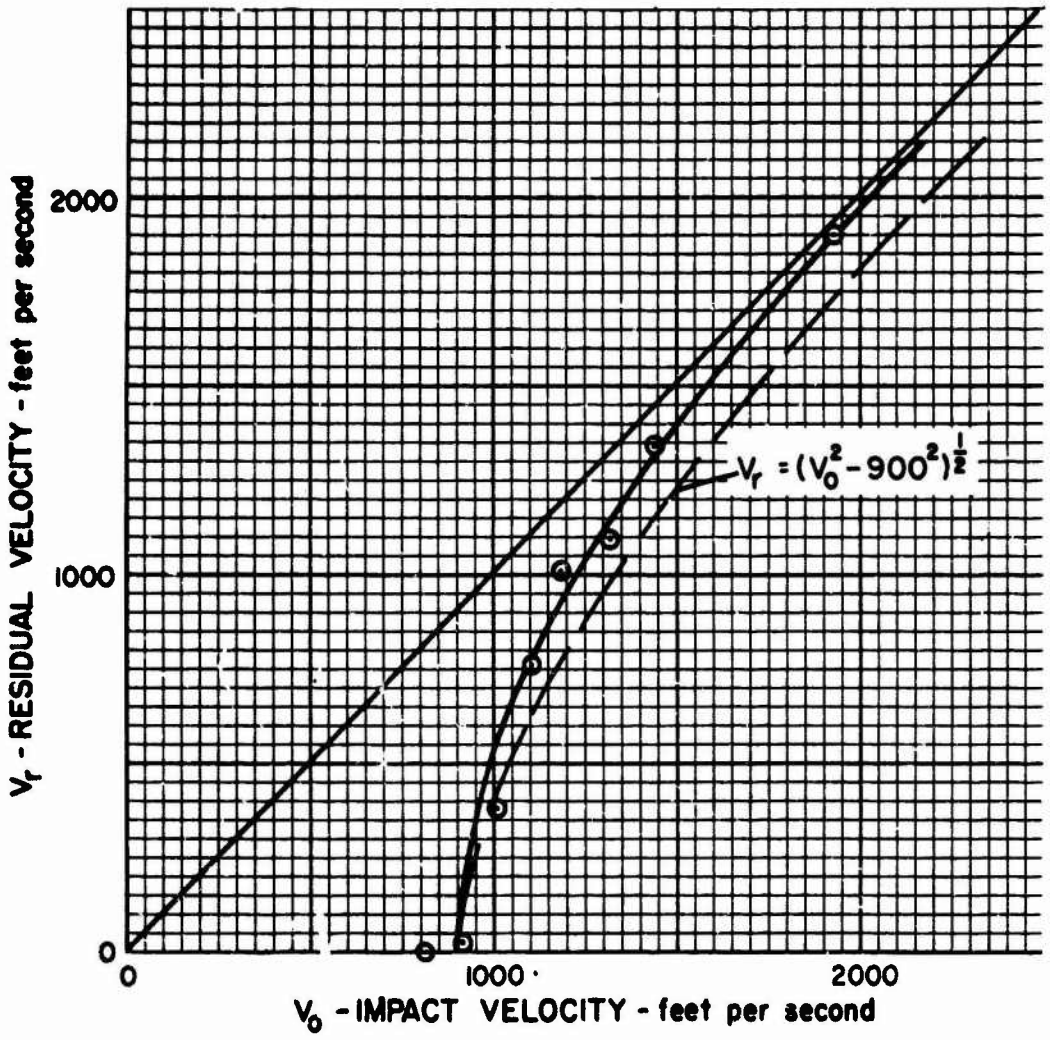

Figure 38. Residual Velocity after Complete Perforation. Material - 43 ounces per square yard Nylon Felt.

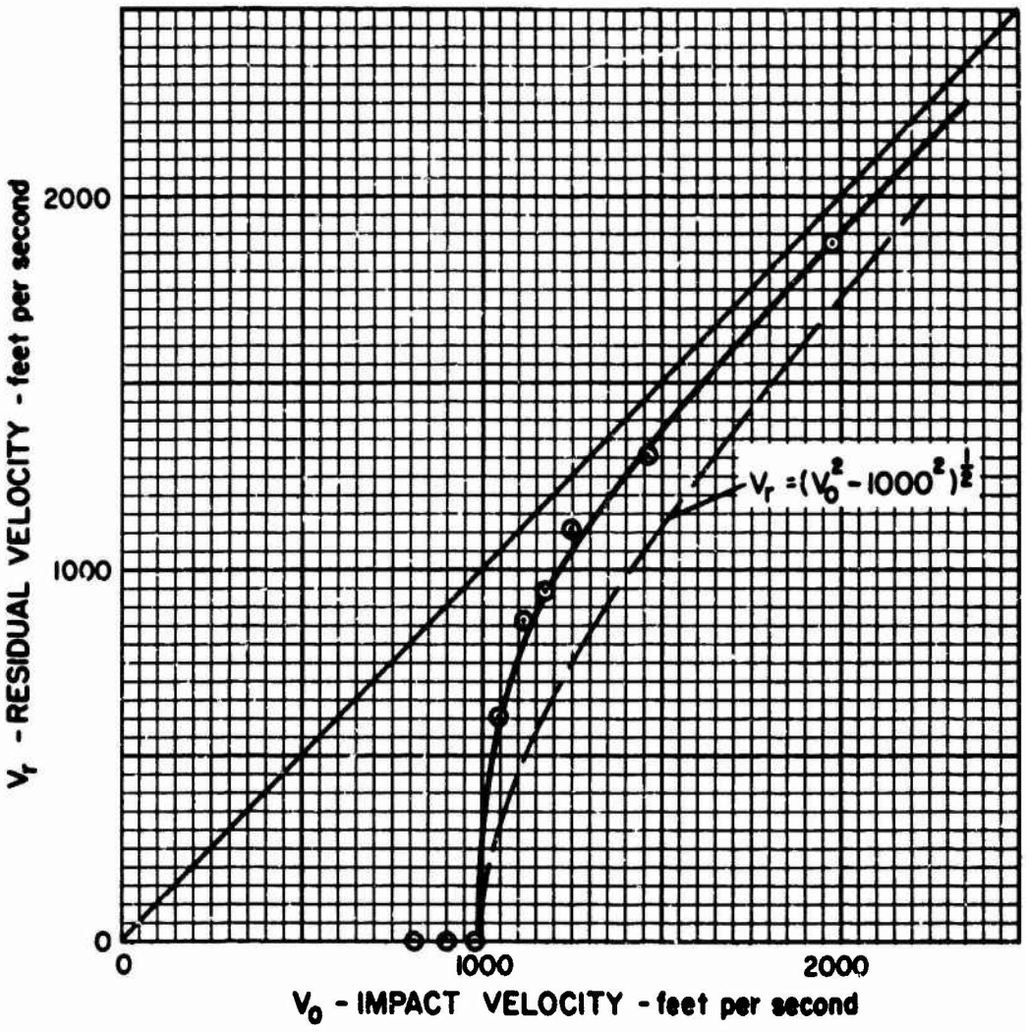

Figure 39. Residual Velocity after Complete Perforation. Material - 53 ounces per square yard Nylon Felt.

simulator measured after complete penetration as a function of impact velocity, V_O. The straight line through the origin represents the condition for no energy loss; i.e., $V_r = V_O$. The continuous smooth curve is fitted to the data and shows that the residual velocity rises rapidly after the minimum perforation velocity is exceeded (maximum impact velocity that results in zero residual velocity) and quickly approaches the initial velocity. The dashed curve represents a plot of the residual velocity equation shown on the figures: numerical values within the radical are experimental values for the minimum perforation velocity. This equation is the result of assuming that the energy lost by the projectile during perforation is a constant value and equal to the kinetic energy of the projectile traveling at the minimum perforation velocity.[3] The fact that the experimental curve rises more rapidly than the "constant energy loss" curve shows that the projectile energy loss during complete perforation of felt materials decreases sharply with increasing velocity. This dramatic decrease in energy transfer to the felt material with increasing velocity is readily explained by noting that, as perforating velocity rises, the ratio of projectile velocity to wave propagation velocity also rises so as to limit the amount of material available for sustaining the required strain; consequently, much less strain energy is involved in the failure of the material. Values for minimum perforation velocities determined for the five materials are listed in Table III.

TABLE III

MINIMUM PERFORATION VELOCITIES

Polypropylene 40 oz/yd^2	Orlon 43 oz/yd^2	Dacron 42 oz/yd^2	Nylon 43 oz/yd^2	Nylon 53 oz/yd^2
850 fps	800 fps	710 fps	900 fps	1,000 fps

These values of minimum perforation velocity can be considered as representative of protection ballistic limit velocities since an impact velocity only slightly above the minimum perforation velocity will result in a residual velocity capable of perforating the thin aluminum witness sheet.

III. CONCLUSIONS BASED UPON EXPERIMENTS

A. Displacement-Time Experimental Technique

1. The spark-gap technique which was developed and utilized for position-time measurements incorporates the unique capability of accurately determining both the radial, r, and transverse, z, displacements of numerous points on the rear surface of a felt material subjected to ballistic impact, at precise instants of time.

2. Displacement-time data generated during the test program represents a valuable and extensive source of precise information which can be used to examine the prediction capability of analytical models. Average error is typically less than two percent, depending upon the magnitude of the displacement measurement.

3. Displacement-time relationships can be differentiated to obtain velocity-time relationships pertaining to the motion of the projectile and the felt material. Projectile velocity relationships can be differentiated to obtain the force interaction between the projectile and the felt (i.e., force-time and force-distance). Graphical differentiation introduces inaccuracies; consequently, the velocity relationships are much less accurate than the displacement relationships, and the force relationships are more descriptive than definitive. Due to these inaccuracies, the prediction capability of analytical models should always be evaluated using the displacement-time data. However, the observational definition of dynamic behavior represented by the time-derivatives provides valuable insight useful in the development of models.

B. Residual Velocity Experimental Technique

The nature of steel projectile-felt material impact is such that projectile deformation energies are inconsequential. Residual velocity measurements provide a direct means for determining momentum and energy transfer to the felt during complete perforation by the projectile.

C. Characteristic Interaction Behavior

1. During the ballistic interaction between the projectile and the felt, momentum is transferred to the material by transverse stresses which produce particle velocities in the direction of projectile

motion. These rotational stresses give rise to two waves which move radially outward from the projectile axis. The longitudinal wave propagates radial tensile stresses and strains and imparts inward radial velocity to material particles. The transverse wave, propagating more slowly, induces transverse stresses, strains, and particle velocities; the transverse wave also changes the radial particle velocity, usually reversing the radial direction of particle motion. Wave velocity determines the amount of material involved in the absorption of momentum and energy at any time. At any projectile position, the unit strains in the material depend upon the amount of material involved. Consequently, higher wave velocities produce lower unit strains. Thus, it would appear that high wave velocities would be desirable; however, wave velocity is associated with the slope of the stress-strain relationship and a material exhibiting a high wave velocity would also experience higher stresses at a given value of unit strain. To defeat a projectile these stresses must not exceed the failure stress. The transverse momentum of the felt at any time is equal to the total change in momentum of the projectile and analytical models based upon momentum considerations will incorporate only transverse velocities. Energy considerations should also include radial components of velocity as well as the strain energy in the material; however, net radial velocities are usually quite small and probably can be neglected.

2. The initial negative slope of velocity-time curves reflects the interface pressure associated with primary impact. As the transverse stresses develop, the negative slope increases to a maximum. During the early portion of the ballistic interaction, the projectile possesses a high velocity. As the ratio of projectile velocity to stress wave velocity in the material drops, the unit strains decrease (for reasons explained in the previous paragraph) resulting in a reduction in stress. The conical half-angle which describes material deformation geometry is also a function of this ratio and increases as velocity decreases; this reduces the stress component acting to oppose projectile motion. Combined, these effects drastically reduce the retarding force acting upon the projectile and, subsequently, deceleration proceeds at a much lower rate. These general velocity-time characteristics were observed in every experiment.

3. The force interaction relationships obtained by graphical differentiation of the velocity curves indicate that peak forces occur somewhat later than might be expected. Peak forces would be anticipated shortly after the initial compression of the felt if the dynamic stress-strain relationships for these materials had a constant or

decreasing slope with strain; however, the initial slope of stress-strain relationships for felt is very low, increasing with strain until the failure strain is approached. Consequently, significant strains must exist before stresses in the material (and resulting force on the projectile) become maximum. In addition, impact compression waves will impart a component of transverse velocity to particles at radii somewhat larger than projectile radius which would introduce a delay time into the development of the maximum force. During the development of analytical models of the ballistic interaction, interaction force is often represented by a function which increases in magnitude with velocity. Functions which include a dependence upon displacement as well as velocity may have to be incorporated to properly define the early time behavior of the felt material.

4. The force interaction relationships expressed in terms of force and distance show that the projectile travels through significant distances (typically 1.0 to 1.5 inches at the higher impact velocities) before the major portion of the kinetic energy of the projectile has been absorbed. The material must be allowed to freely deform during the ballistic interaction if the material is to perform effectively.

5. The velocity-time curves for several stations plotted on the same graph define the felt material behavior at various radii from the axis of impact. These curves show that the transverse particle velocities (therefore, transverse stresses) being propagated by the transverse wave, decrease with increasing radius. This radial dispersion is a consequence of the two-dimensional geometry involved. However, these curves show that the rate of stress decay is highly influenced by the severity of the impact As the impact velocity increases, the rate at which the transverse stresses decrease with radius rises sharply. As noted previously, the unit strain in the material is a function of the ratio of projectile velocity to wave propagation velocity. Thus, the distribution of strain energy with radius in the material rises dramatically at low values of radius and decays rapidly as a function of radius. This influence of impact velocity upon the rate at which the stress levels (being propagated by the transverse wave) decrease with radius, reflects the predominance of plastic behavior at the higher velocities. Theories derived from analytical models based upon elastic behavior will be seriously compromised at higher impact velocities.

6. The results of the residual velocity tests have shown that the energy absorbed by the felt materials decreases rapidly once the ballistic limit has been exceeded. The kinetic energy absorbed at the ballistic limit velocity is the maximum that the material can absorb. These results confirm conclusions previously drawn regarding the influence of wave velocities, and their effect, upon the amount of material that is available to sustain strains. As the ratio of impact velocity to wave velocity increases, unit strains and stresses increase; the volume of material within which strain energies and kinetic energies are distributed (at any given projectile position) decreases. The residual velocity data at impact velocities just above the ballistic limit shows that significant energy is still being transferred before failure of the material. Therefore, the material does respond to the impact situation to some degree before failure occurs. Consequently, the ballistic limit velocity is not directly equivalent, in concept, to the critical transverse particle velocity; i.e., that velocity at which instantaneous rupture occurs because the strain related to this velocity equals the failure strain.

D. Comparisons of Material Behavior

1. The velocity-time relationships which define the motion of a projectile during ballistic interaction with each of the four felt materials are greatly affected by projectile velocity during the early stages of the deceleration process. This velocity dependent behavior reflects the influence of the high unit strains and stresses associated with high values of the ratio of projectile velocity to wave velocity in the materials. During this period, the plastic strain energy absorption rate is very high, being highly sensitive to projectile velocity. Consequently, the magnitude of the interaction impulse during this early time period is a sensitive function of initial impact velocity. The velocity history associated with the later stages of the deceleration process (after the major impulsive interaction has taken place) is, in general, insensitive to initial projectile velocity. The time associated with the major impulse is typically of the order of 100 microseconds for polypropylene, dacron, and orlon; for nylon, this time is characteristically 150 to 200 microseconds. The dynamic behavior of nylon is significantly different as compared to the behavior of the other materials. Static load elongation tests reveal that nylon felt is the most ductile material, exhibiting greater strain at a given value of stress. All of the felt materials exhibit unusual load-elongation curves which increase in slope with strain until the failure strain is approached. As expected, nylon propagates transverse waves at the lowest velocity (see Table II). The response

of nylon during ballistic interaction results in lower peak values of interaction force for any given impact velocity and the lowest rate of force buildup. The low values of wave velocity in nylon result in larger unit strains; however, its load-elongation properties prevent stress levels from rising as rapidly as they would in the other materials. The resulting relatively low value of interaction force must be applied for a longer period of time and through a greater distance to decelerate the projectile; consequently, the time associated with the major velocity dependent impulse is longer. The apparent disadvantages of low wave velocity and low ultimate strength exhibited by nylon felt are more than offset by its more ductile response at relatively low values of stress. Consequently, nylon possesses a relatively high ballistic limit capability. Polypropylene possesses about the same ballistic limit capability as a result of its higher ultimate strength and ability to propagate transverse waves at higher velocity. Thus, while the ballistic limit capabilities of nylon and polypropylene are similar, the manner in which they achieve this level of performance is not. The responses of orlon and dacron are very similar to that of polypropylene; however, their lower strengths result in inferior ballistic performance.

2. An important consideration in body armor applications is the amount of displacement of the felt material that occurs during the process of defeating the projectile. The force-distance relationships can be used to determine the space which must be maintained between the felt and the body. Ranking the four materials (40 ounce per square yard areal density) in order of increasing total deformation at the ballistic limit velocity, results in the following order: dacron, orlon, polypropylene, and nylon. However, dacron has the lowest ballistic limit velocity; nylon the highest. Polypropylene is nearly equivalent to dacron in terms of the distance required to stop the projectile and possesses a ballistic limit almost equivalent to nylon. Consequently, polypropylene is, in general, the best material for applications involving 40 ounce per square yard areal densities.

3. Three thicknesses of nylon felt were utilized during the test program, having areal densities of 19, 43, and 53 ounces per square yard. Ballistic limit velocities associated with these thicknesses are 750 (approximate), 900, and 1000 feet per second, respectively. To illustrate the superiority of the felt materials in this range of areal densities, corresponding values of areal density for 2024-T3 aluminum are 230, 300, and 340 ounces per square yard and for Hadfield steel are (unavailable), 170, and 180 ounces per square yard.[5]

The 43 and 53 ounce felts absorb almost identically the same specific kinetic energy (energy per unit weight) at their respective ballistic limit velocities. This ballistic energy absorbing superiority of felts depends upon keeping the stresses below failure level during the ballistic interaction process. Unit strains must be kept below failure strains. In the three felts studied, the principal reason for failure at and above the ballistic limit velocity is that the ratio of projectile velocity to wave velocity produces strains which cannot be propagated by stresses below failure level. This is dramatically illustrated by the residual velocity tests, which show that the kinetic energy absorbed at velocities above the ballistic limit velocity rapidly decreases to an insignificant proportion of that absorbed at the ballistic limit. All of the felts studied were thin enough to be able to freely respond; transverse momentum is imparted to the material readily by the transverse stress waves. Thicker materials are not free to respond (i.e., front "layers" are backed up by additional "layers") to the transverse wave. Consequently, failure stresses build up more rapidly causing the material to fail near the projectile radius without imparting significant momentum to the material. The combined effects of (1) the increased ratio of projectile velocity to wave velocity, and (2) the prevention of free response of the material to the transverse waves, drastically reduces the energy absorption capabilities of the felt materials. The ballistic advantages which they exhibit at low areal densities quickly vanish as thickness increases.

IV. ANALYTICAL INVESTIGATIONS

Observational insight gained from the experimental program, as well as the pertinent literature, suggests the characteristics which an analytical model should incorporate. The ability of the felt materials to absorb projectile momentum and kinetic energy depends upon the radial propagation of longitudinal and transverse stress waves having magnitudes below the rupture stress of the material. The velocities of the two radial waves, and the velocity history of the projectile, establish the unit strain which must be sustained at any projectile position. The dynamic strength and elongation characteristics of the felt material establish its capability to sustain these strains without rupture.

The pertinent three dimensional geometry with one axis of symmetry requires an analysis of waves diffusing within expanding cylindrical boundaries represented by the wave fronts. Wave analyses of this sort are badly behaved even when materials are linearly elastic and isotropic.[6] Felts are notoriously inelastic and non-linear in response, having stress-strain relationships which exhibit increasing slope with strain until failure strains are approached. Current theoretical developments fall far short of being able to cope with the one-dimensional, non-linear, visco-plastic problem which would define the strain-waves propagating in a "bar" of felt material, to say nothing of the three-dimensional (one symmetry) problem represented by the projectile-felt interaction. Consequently, the only logical approach is the development of analytical models based upon observation insight and experimental verification, using displacement-time data and empirical relationships such as those obtained during this effort.

A preliminary model based upon the appropriate momentum equation was hypothesized as a first step in the development of an analytical model relating material and geometrical parameters to observed ballistic interaction behavior. The model yields the appropriate general form of the velocity-time relationship and adequately describes behavior at the lower-projectile velocities. At higher projectile velocities, it predicts a velocity-time relationship which lies well above the experimental curves, indicating its inability to reflect the non-linear response of the felts. While the model falls far short of defining the influence of pertinent parameters, it does illustrate approach and provides additional insight valuable for further development.

Momentum Considerations

Consider the transverse ballistic impact of a felt material as shown in Figure 40. A cylindrical steel projectile of mass (m_p) traveling along the z axis impacts the felt at time zero. Due to the impulsive disturbance created by the impact, a transverse wave is created which travels radially outward at the assumed constant velocity, C_t. The presence of the longitudinal wave which preceeds the transverse wave is ignored. The radial material motion created by the longitudinal wave is symmetrical about and normal to the z axis; this radial motion does not contribute to transverse momentum. Let V_{zr} be the transverse velocity of the felt material at a radius, r, at any time, t. The steel projectile is assumed to behave as a rigid body.

Let the mass of the felt directly beneath the projectile assume the projectile velocity instantaneously; this mass is considered insignificant in comparison to projectile mass. Therefore, the area defined by $2\pi RT$ becomes the boundary at which the impulsive disturbance, due to the projectile motion, is applied to the felt. This disturbance (a discontinuity in transverse velocity) will propagate from this boundary at the velocity of the transverse wave. Writing the momentum balance for any time, t:

$$m_p V_o = m_p V_p + \int_R^{R + C_t t} V_{zr} dm \qquad (1)$$

where, dm, is the mass of a differential element of felt material at a radius, r, between the projectile radius, R, and the radius of the transverse wave front, $R + C_t t$. The quantity, dm, can be written as:

$$dm = 2\pi\rho T \, r \, dr$$

and equation (1) becomes:

$$m_p V_o = m_p V_p + 2\pi\rho T \int_R^{R + C_t t} V_{zr} r dr \qquad (2)$$

If V_{zr} could be expressed in terms of V_p, r, and t, equation (2) could be solved directly to obtain an equation of motion. An assumption is made as to the form of the projectile velocity-time relationship. The form of this relationship is empirically formulated using experimental velocity-time relationships.

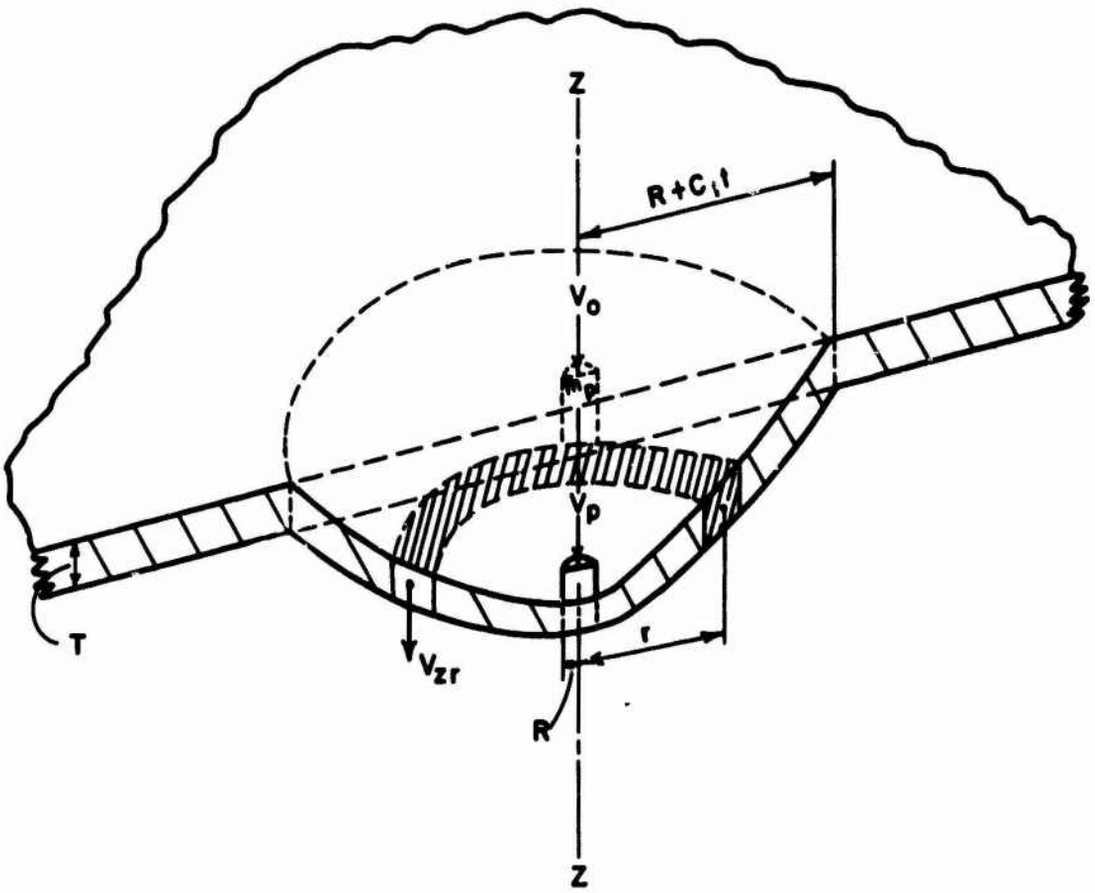

Figure 40. Transverse Impact of a Cylindrical Projectile and a Sheet of Felt Material

$$V_p = V_o e^{-Kt^{3/2}} \tag{3}$$

This empirical function for the equation of motion of the projectile is of little value unless the term K can be written as a function of the material properties. To do this, assumptions are made which establish a relationship between V_p and V_{zr}.

The relationship between the projectile velocity and the material velocity at any radius and time is established by the wave action. If this were a one-dimensional problem, the velocity of the material at a radius, r, and a time, t, would be equal to the projectile velocity at an earlier time $(t - \frac{r}{C_t})$. In the two-dimensional case, a simple relationship between the time and space variable does not exist. Also, the effect of radial dispersion will reduce the magnitude of the transverse wave. The effect of radial dispersion is assumed to be proportional to the square root of the ratio of the radius at which the disturbance is being applied, R, and the radius under consideration, r. An assumption is also made as to the relationship between the time and space variables associated with two-dimensional (cylindrical) wave propagations. If one-dimensional wave properties were assumed and the radial dispersion factor included, equation (3) could be used to express V_{zr} as follows:

$$V_{zr} = \sqrt{\frac{R}{r}}\, V_o e^{-K\left(t - \frac{r-R}{C_t}\right)^{3/2}} \tag{4}$$

However, a more convenient equation, and one which more closely approximates two-dimensional wave phenomena, is obtained by rewriting equation (4) as:

$$V_{zr} = \sqrt{\frac{R}{r}}\, V_o e^{-K\left[t^{3/2} - \left(\frac{r-R}{C_t}\right)^{3/2}\right]} \tag{5}$$

or, expressed in terms of equation (3):

$$V_{zr} = \sqrt{\frac{R}{r}}\, V_p e^{K\left(\frac{r-R}{C_t}\right)^{3/2}} \tag{6}$$

When r is equated to R, equation (6) produces the equation for the projectile velocity and, therefore, the correct equation of the material at a radius R. At the radius of the wave front, $R + C_t t$, the material velocity is the initial velocity, V_o, reduced by the radial dispersion factor, $\sqrt{\frac{R}{r}}$.

Equation (5) can be substituted into the momentum equation, equation (2), with the following results:

$$m_p V_o = m_p V_p + 2\pi\rho T \int_R^{R + C_t t} \sqrt{\frac{R}{r}}\, V_p e^{K\left(\frac{r - R}{C_t}\right)^{3/2}} \, r\, dr \tag{7}$$

The solution of this equation will produce the desired value for the term, K. This step is simplified with very slight effects upon the results if R is considered insignificant in comparison to $C_t t$. Making this simplifying assumption and integrating equation (7) produces:

$$V_o = \frac{4/3\pi\rho T\sqrt{R}}{m_p K} C_t^{3/2} \left[V_p e^{Kt^{3/2}} - V_p \right] \tag{8}$$

From equation (3), the term $V_p e^{Kt^{3/2}}$ is equal to V_o. Equation (8) becomes:

$$V_o - V_p = \frac{4/3\pi\rho T\sqrt{R}}{m_p K} C_t^{3/2} \left[V_o - V_p \right] \tag{9}$$

Rearranging equation (9):

$$K = \frac{4/3\pi\rho T\sqrt{R}}{m_p} C_t^{3/2} \tag{10}$$

Using this value of K, the equations of motion for the projectile and the felt material become, respectively:

$$V_p = V_o e^{-\frac{4/3\pi\rho T\sqrt{R}}{m_p} (C_t t)^{3/2}} \tag{11}$$

and:

$$V_{zr} = \sqrt{\frac{R}{r}}\, V_o e^{-\frac{4/3\pi\rho T\sqrt{R}}{m_p}\left[(C_t t)^{3/2} - r^{3/2}\right]} \tag{12}$$

In equations (11) and (12), C_t is the transverse wave velocity. However, in the derivation, the effect of the longitudinal wave has been ignored: the transverse wave has been considered as moving in an undisturbed material. In the actual case, a longitudinal tension wave precedes the transverse wave and creates a radial particle velocity, u, toward the center. Therefore, the wave which transmits transverse motion travels at an apparent velocity, ω, which is equal to C_t less u. In terms of the fixed r coordinate system, the radius which bounds the material possessing transverse motion, at any time, is equal to ωt. But, since material has flowed into this area, the mass determined by ρ, T, and the radius ωt does not define the total amount of mass involved. The correct mass involved is defined by ρ, T, and the radius $C_t t$. Equations (11) and (12) do recognize the presence of the longitudinal wave if the value of C_t is the velocity of the transverse wave relative to the fixed coordinate system. In order that equations (11) and (12) may be compared to the experimental data, C_t is determined using the experimental values of ω and approximating u based upon experimental observation. As a first approximation, it can be stated that the value of u is, in general, equal to 1/4 ω or:

$$C_t = 5/4\ \omega \tag{13}$$

Substituting this value for C_t into the equation of motion results in:

$$V_p = V_o e^{-\frac{1.86\pi\rho T\sqrt{R}}{m_p}(\omega t)^{3/2}} \tag{14}$$

and:

$$V = \sqrt{\frac{R}{r}}\, V_o e^{-\frac{4/3\pi\rho T\sqrt{R}}{m_p}\left[(5/4\,\omega t)^{3/2} - r^{3/2}\right]} \tag{15}$$

Equations (14) and (15) do a reasonable job of predicting the experimental results for impact velocities well below the ballistic limit velocities. However, as the impact velocity approaches the ballistic limit velocity, the discrepancy between the prediction of these equations and experiment

increases sharply. This is a result of the fact that K was assumed constant in order that it could be evaluated in terms of the material parameters. The fact that K includes the transverse wave velocity term, ω, could reflect the impact velocity dependency of K. ω is observed to be higher during the very early part of the impact, quickly assuming a relatively constant value. Also, this analysis does not attempt to do other than average the effects of the non-linear stress-strain behavior of the felt materials.

While these equations of motion do predict results at low impact velocities and indicate the possible role of density, thickness, projectile mass, radius, and wave velocities, they fail at the extremely important high range in velocity. Equations, valid near the ballistic limit velocity, are required to establish the relationships between material parameters and ballistic limit.

V. RECOMMENDATIONS

In view of the results of this research program, the following recommendations are made as to the direction of future efforts. The behavior of felt materials during their response to ballistic impact has been quantitatively defined by experiment. Before the required comprehensive relationships between material parameters and ballistic limit velocities can be determined, observed qualitative behavior will have to be incorporated more carefully into analytical models by means of comprehensive analytical investigations. Although initially complex, it is expected that these models will become more simple in form as physical understanding improves. The experimental data generated during this program should form an ample basis for model development involving iterative analytical derivation, evaluation, and modification. The complexity of general theoretical relationships and the state-of-the-art related to the phenomena of transverse ballistic impact and plastic wave propagation are such that the many possible simplifying assumptions must be examined in order to obtain valid and useful solutions in closed form. The experimental data provides insight as to possible simplifications and the required means for examining and validating assumptions. It provides a source of extensive information for the final evaluations of theoretical results.

VI. BIBLIOGRAPHY

References

1. Rusell W. Ehlers, Paul J. Angelo, Jr., "Determination of the Mechanics of Projectile Penetration of Non-Woven Structures," Lowell Technological Institute Research Foundation, Final Report, Contract No. DA19-129-QM-1935(01 6037-62), Project No. 7-80-05-001, January 1964.

2. J. G. Krizik, D. M. Mellen, S. Backer, "Dynamic Testing of Small Textile Structures and Assemblies," Textile Division, Mechanical Engineering Dept., Massachusetts Institute of Technology, Final Report, Contract No. DA19-129-QM-1308, Project No. 7-93-18-019, January 1961.

3. R. F. Recht, T. W. Ipson, "Ballistic Perforation Dynamics," Journal of Applied Mechanics, September 1963, Vol. 30, Series E, No. 3.

4. R. F. Recht, T. W. Ipson, "The Dynamics of Terminal Ballistics," Final Report, Contract No. DA-23-072-ORD-1302, Denver Research Institute, University of Denver, for Army Tank Automotive Center, 1 February 1962. ASTIA File Nos. AD 274 128 (Unclassified Report) and AD 328 796 (Confidential Appendix).

5. Aberdeen Proving Ground, Development and Proof Services, "Report on a Test of Personnel Armor Materials with Fragment Simulating Projectiles," D.A. Project No. 593-08-020. Armor Test Report No. AD-1190.

6. P. M. Morse, Herman Feshback, "Methods of Theoretical Physics," Parts I and II. McGraw Hill Book Co., Inc., New York, 1953.

Pertinent Literature

7. W. James Lyons, "Impact Phenomena in Textiles," The M.I.T. Press, Cambridge, Massachusetts, 1963.

8. Werner Goldsmith, "Impact". Edward Arnold Publishers, Ltd., London, England, 1960.

9. B. Karunes, E. T. Onat, "Plastic Wave Propagation Effects in Transverse Impact of Membranes," Journal of Applied Mechanics, March 1960.

10. Julius Miklowitz, "Flexural Stress Waves in an Infinite Elastic Plate Due to a Suddenly Applied Concentrated Transverse Load," Journal of Applied Mechanics, December 1960.

11. F. O. Ringleb, "Motion and Stress of an Elastic Cable Due to Impact," Journal of Applied Mechanics, September 1957.

12. G. E. Hudson, "Theory of Dynamic Plastic Deformation of a Thin Diaphragm," Journal of Applied Physics, Vol. 22, No. 1, 1951.

13. Mellon Institute, "Ballistic Protective Buoyant Mater[illegible]," Contract No. N140(138)72793B, Quarterly Report No. 12 (October 1962 - December 1962).

14. R. C. Liable, R. H. Supnik, "High Speed Testing as a Measure of the Resistance to Penetration of Needle-Punched Felts," Journal of Applied Polymer Science, Vol. 8, 1964.

15. Edward P. Wittrock, "An Investigation of Lateral Impact on Non-Rigid Felt Plates," A Masters Thesis, University of Denver, May 1965.

APPENDIX - A

PROJECTILE AND FELT MATERIAL PROPERTIES

TABLE A-I

PROJECTILE AND MATERIAL PROPERTIES

Fragment Simulating Projectile (T-37)

Weight - grains	Mass - slugs	Diameter - inches	Overall Length - inches	Material	Hardness
17.0 ± .5	7.55×10^{-5}	0.215	0.250	Steel SAE-1020	R_c 29-31

Felt Materials

Material	Areal Density - oz/yd^2	Nominal Thickness - inches	Mass Density - slugs/ ft^3	Staple Length - inches	Fiber Denier (a)
Polypropylene	40	0.45	0.230	2.5	3
Type 54 Dacron	42	0.40	0.272	4.5	4.5
Type 42 Orlon	43	0.50	0.223	4.5	4.5
Type 100 Nylon	43	0.40	0.279	4.5	15
Type 100 Nylon	53	0.50	0.263	4.5	15
C-500-58 Nylon	19	0.11	0.448	3	6

(a) Denier is the weight in grams of 9000 meters of the fiber.

APPENDIX - B

DISPLACEMENT-TIME DATA

DISPLACEMENT-TIME DATA

All of the valid displacement-time data that was obtained during the experimental program are presented in Table B-I. These data concerr. the position of various points on the rear surface of the felt material at successive instances in time during the impact event. The spark-gap technique that is described in section II. A. was used to obtain these data. The high degree of precision of these data is discussed in section II. C. The displacement-time data included herein provide a valid and extensive source of information with which to compare the results of analytic investigations.

As stated, only valid data are reported. Many of the tests produced questionable or invalid data due to several factors; among these were: electrical equipment malfunction or inaccurate timing, projectile tumble during the deceleration, complete perforation, spark-gaps opening up during test, and excessive discrepancy between the line of fire and the center arc-gap station. All of the felt materials are, to some degree, anisotropic due to the uni-directional combing of the fibers prior to needling. However, each felt was composed of several layers of combed matting needled together. Successive layers were overlayed with perpendicular combing directions, thus eliminating anisotropy to a great extent. An apparent "grain" is left on the felt materials due to the direction of the last needling process. Several tests were conducted in which the line of the spark-gap stations was varied with respect to the direction of this grain. No differences in results were noted. For consistency, all tests were conducted with the line of the spark-gaps being parallel to the direction of last needling.

In Table B-I, the displacement-time data are reported by individual tests. The test number, felt material, areal density, and impact velocity of the 17-grain fragment simulating projectile are shown. The displacement-time data are reported in terms of the r and z coordinants of each spark-gap station at various times after initial impact. Figure B-1 illustrates the coordinate system used.

The spark-gap stations are located on the rear surface of the felt material. Eleven stations were used and are referred to as shown on Figure B-1. The z axis is perpendicular to the plane of the felt and passes through the center station (Station 0). The r axis lies on the rear surface of the felt and contains each of the eleven stations. The stations are numbered positive to the right, negative to the left. The r and z coordinants of each station are given at time zero (initial impact)

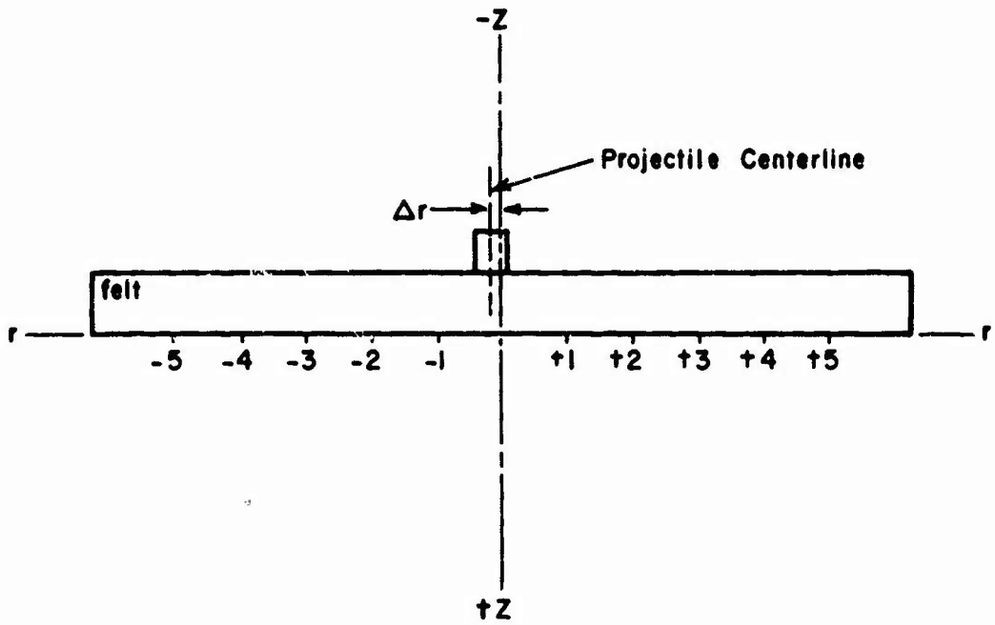

Figure B-1. Coordinate System Used to Define Displacement-Time Data

and at 86-microsecond intervals thereafter. At time zero, no motion has yet occurred and the corresponding coordinants refer to the original position of each station. Displacements in the positive z direction refer to displacements in the direction of impact. Except for Station 0, all radial displacements are positive since they refer to the radial distance from the original position of Station 0 (the z axis). During motion, Station 0 will not, necessarily, follow the z axis exactly. Positive r values for this station refer to radial displacements toward the right or positively numbered stations; negative values refer to displacements to the left. All positions are reported in terms of inches. The value of Δr, reported for each test, refers to the amount of deviation between the axis of the projectile and the z axis. It is important to note that the impact will be symmetrical about the axis of the projectile, and not about the z axis.

TABLE B-I

DISPLACEMENT-TIME DATA

TEST NUMBER - 7-C

IMPACT VELOCITY - fps - 400

FELT MATERIAL - NYLON

Δr - in. - -0.04

AREAL DENSITY - oz./yd^2 - 53

TIME AFTER IMPACT	STATION																					
	0		+1		−1		+2		−2		+3		−3		+4		−4		+5		−5	
μsec	r	z	r	z	r	z	r	z	r	z	r	z	r	z	r	z	r	z	r	z	r	z
0	.00	.00	.33	.00	.26	.00	.63	.00	.57	.00	.92	.00	.88	.00	1.19	.00	1.14	.00	1.56	.00	1.44	.00
86	+.10	.35	.33	.00	.32	.07	.60	.00	.54	-.02	.92	.00	.88	.00	1.19	.00	1.14	.00	1.56	.00	1.44	.00
172	+.13	.55	.36	.23	.38	.43	.60	.05	.55	.04	.92	.00	.84	-.01	1.19	.00	1.14	.00	1.56	.00	1.44	.00
258	+.08	.67	.40	.39	.34	.59	.60	.14	.57	.22	.88	-.01	.79	-.01	1.19	.00	1.10	.00	1.53	-.01	1.40	.00
344	+.11	.78	.38	.51	.34	.68	.64	.27	.60	.37	.86	-.04	.82	.04	1.16	-.01	1.06	-.01	1.50	-.02	1.35	-.01
430	+.08	.86	.40	.60	.33	.78	.65	.37	.62	.46	.88	.09	.84	.19	1.11	-.03	1.04	-.02	1.48	-.04	1.31	-.02
516	+.10	.92	.41	.67	.33	.86	.65	.44	.60	.57	.90	.17	.89	.30	1.12	.02	1.06	.05	1.47	-.08	1.28	-.06
602																						
688																						

TABLE B-I

DISPLACEMENT-TIME DATA

TEST NUMBER - 9-C

IMPACT VELOCITY - fps - 730

FELT MATERIAL - NYLON

Δr - in. - +0.06

AREAL DENSITY - oz./yd^2 - 5.3

TIME AFTER IMPACT	STATION																					
	0		+1		−1		+2		−2		+3		−3		+4		−4		+5		−5	
μsec	r	z	r	z	r	z	r	z	r	z	r	z	r	z	r	z	r	z	r	z	r	z
0	.00	.00	.32	.00	.29	.00	.58	.00	.59	.00	.90	.00	.86	.00	1.17	.00	1.19	.00	1.51	.00	1.48	.00
86	.00	.21	.32	.00	.29	.00	.58	.00	.59	.00	.90	.00	.86	.00	1.17	.00	1.19	.00	1.51	.00	1.48	.00
172	-.06	.71	.35	.23	.31	.24	.58	.00	.59	.00	.86	.00	.86	.00	1.17	.00	1.19	.00	1.51	.00	1.48	.00
258	-.03	.93	.38	.54	.35	.53	.54	.26	.51	.17	.82	-.03	.83	-.02	1.11	.00	1.19	.00	1.48	.00	1.48	.00
344	-.01	1.13	.37	.72	.31	.71	.62	.58	.57	.45	.81	.09	.76	-.06	1.05	-.09	1.16	-.01	1.42	-.02	1.43	-.02
430	.00	1.30	.38	.89	.31	.88	.62	.72	.58	.62	.88	.27	.73	.?.	1.02	.00	1.09	-.03	1.35	-.06	1.27	-.04
516	.00	1.40	.38	1.03	.30	1.02	.59	.80	.55	.75	.94	.43	.80	.40	1.08	.16	1.03	-.05	1.33	-.11	1.34	-.05
602	.00	1.49	.40	1.12	.30	1.12	.63	.89	.56	.84	.95	.54	.84	.54	1.22	.32	1.08	.17	1.40	.01	1.33	-.07
688																						

TABLE B-I

DISPLACEMENT-TIME DATA

TEST NUMBER - 11-C

IMPACT VELOCITY - fps - 700

FELT MATERIAL - NYLON

Δr - in. - +0.02

AREAL DENSITY - oz./yd^2 - 53

TIME AFTER IMPACT μsec	STATION																					
	0		+1		−1		+2		−2		+3		−3		+4		−4		+5		−5	
	r	z	r	z	r	z	r	z	r	z	r	z	r	z	r	z	r	z	r	z	r	z
0	.00	.00	.27	.00	.32	.00	.60	.00	.60	.00	.88	.00	—	—	1.18	.00	1.18	.00	1.50	.00	1.50	.00
86	-.02	.24	.27	.00	.32	.07	.60	.00	.60	.00	.88	.00	—	—	1.18	.00	1.18	.00	1.50	.00	1.50	.00
172	+.01	.59	.26	.18	.33	.09	.60	.00	.60	.00	.88	.00	—	—	1.18	.00	1.18	.00	1.50	.00	1.50	.00
258	+.01	.82	.31	.48	.37	.41	.52	.04	.53	.03	.88	.00	—	—	1.18	.00	1.18	.00	1.50	.00	1.50	.00
344	+.02	.99	.31	.66	.36	.66	.56	.29	.58	.30	.84	-.01	—	—	1.18	.00	1.18	.00	1.50	.00	1.50	.00
430	+.02	1.16	.30	.80	.33	.81	.62	.46	.64	.47	.78	-.03	—	—	1.16	-.02	1.12	-.01	1.47	-.02	1.45	-.02
516	+.03	1.28	.31	.92	.31	.92	.63	.59	.63	.61	.83	.22	—	—	1.12	-.03	1.05	-.03	1.42	-.03	1.41	-.03
602	+.03	1.37	.32	1.03	.33	1.02	.60	.69	.63	.71	.90	.39	—	—	1.06	-.04	1.07	.08	1.39	-.04	1.37	-.07
688	+.03	1.47	.32	1.09	.37	1.11	.53	.77	.64	.79	.99	.51	—	—	1.19	.15	1.17	.22	1.37	-.07	1.36	-.10

TABLE B-1

DISPLACEMENT-TIME DATA

TEST NUMBER - 12-C

IMPACT VELOCITY - fps - 730

FELT MATERIAL - NYLON

Δr - in. - +0.06

AREAL DENSITY - oz./yd^2 - 53

TIME AFTER IMPACT	STATION																					
	0		+1		−1		+2		−2		+3		−3		+4		−4		+5		−5	
μsec	r	z	r	z	r	z	r	z	r	z	r	z	r	z	r	z	r	z	r	z	r	z
0	.00	.00	.30	.00	.31	.00	.57	.00	.61	.00	.86	.00	.78	.00	1.18	.00	1.22	.00	1.50	.00	1.49	.00
86	+.02	.28	.30	.00	.31	.00	.57	.00	.61	.00	.86	.00	.78	.00	1.18	.00	1.22	.00	1.50	.00	1.49	.00
172	+.04	.72	.36	.25	.31	.19	.57	.00	.61	.00	.86	.00	.78	.00	1.18	.00	1.22	.00	1.50	.00	1.49	.00
258	+.01	1.05	.39	.46	.36	.52	.55	.21	.54	.12	.83	.00	.78	.00	1.12	-.02	1.16	.00	1.47	.00	1.49	.00
344	.00	1.25	.37	.75	.33	.70	.62	.50	.61	.36	.76	.06	.74	.07	1.06	-.03	1.10	-.02	1.40	-.01	1.49	.00
430	.00	1.41	.37	.93	.33	.85	.61	.65	.63	.53	.85	.28	.80	.26	1.02	.00	1.06	-.01	1.33	-.03	1.46	.00
516	.00	1.53	.38	1.06	.34	.99	.59	.74	.62	.64	.89	.44	.83	.38	1.05	.14	1.07	.07	1.30	-.03	1.41	.00
602	+.01	1.63	.38	1.16	.34	1.08	.60	.84	.64	.74	.87	.51	.84	.49	1.14	.28	1.13	.19	1.36	.04	1.35	-.02
688	+.02	1.70	.39	1.24	.33	1.15	.60	.93	.66	.83	.91	.60	.89	.60	1.20	.40	1.20	.30	1.44	.18	1.41	.09

TABLE B-I

DISPLACEMENT-TIME DATA

TEST NUMBER - 15-C

IMPACT VELOCITY - fps - 640

FELT MATERIAL - NYLON

Δr - in. - +0.03

AREAL DENSITY - oz./yd^2 - 53

TIME AFTER IMPACT	STATION																					
	0		+1		−1		+2		−2		+3		−3		+4		−4		+5		−5	
μsec	r	z	r	z	r	z	r	z	r	z	r	z	r	z	r	z	r	z	r	z	r	z
0	.00	.00	.30	.00	.31	.00	.58	.00	.61	.00	.87	.00	—	—	1.17	.00	1.21	.00	1.47	.00	1.52	.00
86	.00	.18	.30	.00	.31	.00	.58	.00	.61	.00	.87	.00	—	—	1.17	.00	1.21	.00	1.47	.00	1.52	.00
172	-.08	.66	.33	.27	.37	.16	.58	.00	.61	.00	.84	.00	—	—	1.17	.00	1.21	.00	1.47	.00	1.52	.00
258	-.06	.97	.41	.65	.46	.46	.53	.21	.57	.22	.77	.01	.78	.00	1.13	.00	1.17	-.01	1.47	.00	1.52	.00
344	-.05	1.17	.36	.82	.42	.69	.63	.47	.65	.57	.74	.00	.75	.13	1.05	-.02	1.12	-.03	1.42	.00	1.48	.00
430	-.03	1.33	.33	.93	.42	.82	.64	.63	.64	.62	.81	.12	.80	.33	1.00	.00	1.09	.00	1.36	-.01	1.44	-.01
516	-.03	1.45	.35	1.06	.44	.97	.62	.74	.64	.75	.87	.33	.85	.50	1.03	.16	1.12	.13	1.27	-.01	1.41	-.02
602	-.02	1.54	.34	1.14	.43	1.05	.69	.84	.66	.87	.89	.50	.86	.63	1.18	.34	1.20	.29	1.37	.11	1.45	.05
688																						

TABLE B-I

DISPLACEMENT-TIME DATA

TEST NUMBER - 19-C

IMPACT VELOCITY - fps - 840

FELT MATERIAL - NYLON

Δr - in. - +0.05

AREAL DENSITY - oz./yd^2 - 53

TIME AFTER IMPACT	STATION																					
	0		+1		−1		+2		−2		+3		−3		+4		−4		+5		−5	
μsec	r	z	r	z	r	z	r	z	r	z	r	z	r	z	r	z	r	z	r	z	r	z
0	.00	.00	.32	.00	.35	.00	.54	.00	.63	.00	.88	.00	.94	.00	1.19	.00	1.21	.00	1.50	.00	1.50	.00
86	-.08	.47	.32	.00	.35	.00	.54	.00	.63	.00	.88	.00	.94	.00	1.19	.00	1.21	.00	1.50	.00	1.50	.00
172	-.08	.96	.44	.31	.46	.16	.54	.00	.57	-.02	.85	-.02	.94	.00	1.19	.00	1.21	.00	1.50	.00	1.50	.00
258	-.09	1.31	.43	.81	.52	.56	.58	.34	.62	.18	.80	.00	.91	-.01	1.13	-.02	1.17	-.02	1.50	.00	1.50	.00
344	-.08	1.53	.40	1.07	.50	.80	.62	.64	.68	.48	.80	.19	.84	-.04	1.08	-.03	1.09	-.03	1.46	-.01	1.44	-.03
430	-.07	1.67	.40	1.20	.51	.96	.60	.80	.70	.68	.89	.39	.87	.27	1.07	.06	1.04	-.02	1.39	-.02	1.38	-.05
516	-.06	1.78	.42	1.27	.51	1.11	.61	.94	.70	.80	.91	.55	.94	.45	1.15	.24	1.08	.15	1.36	-.04	1.34	-.04
602	-.07	1.91	.42	1.39	.51	1.23	.63	1.05	.70	.92	.93	.66	.96	.58	1.24	.41	1.18	.32	1.45	.10	1.40	.06
688																						

TABLE B-I

DISPLACEMENT-TIME DATA

TEST NUMBER - 21-C

IMPACT VELOCITY - fps - 665

FELT MATERIAL - Polypropylene

Δr - in. - +0.02

AREAL DENSITY - oz./yd^2 - 40

TIME AFTER IMPACT	STATION																					
	0		+1		−1		+2		−2		+3		−3		+4		−4		+5		−5	
μsec	r	z	r	z	r	z	r	z	r	z	r	z	r	z	r	z	r	z	r	z	r	z
0	.00	.00	.29	.00	.03	.00	.58	.00	.58	.00	.88	.00	.89	.00	1.19	.00	1.18	.00	1.45	.00	1.49	.00
86	.00	.41	.31	.04	.34	.03	.58	.00	.58	.00	.88	.00	.89	.00	1.19	.00	1.18	.00	1.45	.00	1.49	.00
172	.00	.74	.38	.44	.04	.05	.57	.11	.58	.09	.78	-.03	.84	-.03	1.15	-.01	1.15	.00	1.45	.00	1.49	.00
258	.00	.97	.35	.66	.38	.65	.65	.42	.69	.44	.79	.13	.81	.08	1.07	-.02	1.05	-.02	1.45	.00	1.41	-.02
344	.00	1.12	.36	.83	.38	.87	.62	.59	.65	.61	.88	.37	.89	.33	1.12	.09	1.06	.06	1.43	-.02	1.37	.00
430	.00	1.18	.37	.94	.39	.99	.68	.73	.64	.73	.93	.52	.96	.05	1.25	.32	1.20	.03	1.49	.08	1.44	.07
516	.00	1.2.	.38	1.01	.37	1.05	.72	.84	.07	.85	.98	.64	1.00	.64	1.30	.42	1.30	.46	1.58	.21	1.54	.23
602	.00	1.23	.04	1.05	.37	1.08	.74	.92	.72	.93	1.02	.72	1.04	.74	1.35	.49	1.33	.54	1.66	.27	1.63	.36
688																						

TABLE B-I

DISPLACEMENT-TIME DATA

TEST NUMBER - 24-C

IMPACT VELOCITY - fps - 555

FELT MATERIAL - Polypropylene

Δr - in. - 0.00

AREAL DENSITY - oz./yd^2 - 40

TIME AFTER IMPACT	STATION																					
	0		+1		−1		+2		−2		+3		−3		+4		−4		+5		−5	
μsec	r	z	r	z	r	z	r	z	r	z	r	z	r	z	r	z	r	z	r	z	r	z
0	.00	.00	.31	.00	.28	.00	.61	.00	.59	.00	.91	.00	.89	.00	.120	.00	1.20	.00	1.50	1.50	1.50	.00
86	.01	.30	.31	.00	.28	.00	.61	.00	.59	.00	.91	.00	.89	.00	.120	.00	1.20	.00	1.50	1.50	1.50	.00
172	.00	.59	.39	.34	.36	.41	.59	.03	.55	.06	.85	-.02	.83	-.02	.120	.00	1.20	.00	1.50	1.50	1.50	.00
258	.00	.81	.38	.56	.32	.61	.64	.33	.63	.38	.81	.03	.81	.09	.112	-.01	1.10	-.02	1.45	1.43	1.44	.00
344	.02	.96	.38	.79	.34	.76	.65	.50	.62	.53	.89	.26	.88	.35	.110	.02	1.10	.05	1.40	1.40	1.40	.00
430	.00	1.04	.38	.80	.34	.84	.67	.62	.64	.64	.96	.50	.96	.53	.120	.23	1.23	.26	1.44	1.45	1.45	.07
516																						
602																						
688																						

TABLE B-I

DISPLACEMENT-TIME DATA

TEST NUMBER - 25-C

IMPACT VELOCITY - fps - 820

FELT MATERIAL - Polypropylene

Δr - in. - −0.06

AREAL DENSITY - oz./yd^2 - 40

TIME AFTER IMPACT μsec	STATION																					
	0		+1		−1		+2		−2		+3		−3		+4		−4		+5		−5	
	r	z	r	z	r	z	r	z	r	z	r	z	r	z	r	ii	r	z	r	z	r	z
0	.00	.00	—	—	.31	.00	.58	.00	.61	.00	.88	.00	.90	.00	1.19	.00	1.21	.00	1.50	.00	1.50	.00
86	-.06	.45	—	—	.34	.08	.58	.00	.61	.00	.88	.00	.90	.00	1.19	.00	1.21	.00	1.50	.00	1.50	.00
172	-.06	.82	—	—	.42	.61	.58	.23	.62	.20	.78	.00	.81	.00	1.10	-.01	1.15	-.01	1.50	.00	1.50	.00
258	-.07	1.17	—	—	.40	.84	.63	.56	.70	.52	.82	.31	.86	.24	1.02	.00	1.06	.00	1.45	-.02	1.42	.00
344	-.06	1.23	—	—	.42	1.01	.62	.71	.69	.69	.88	.51	.97	.39	1.16	.27	1.18	.22	1.40	.01	1.28	.00
430	-.03	1.33	—	—	.41	1.11	.67	.85	.75	.83	.96	.68	1.03	.63	1.27	.48	1.29	.42	1.52	.24	1.48	.17
516	-.05	1.40	—	—	.43	1.17	.70	.98	.78	.94	1.00	.81	1.08	.76	1.31	.59	1.34	.52	1.59	.27	1.60	.28
602	-.05	1.41	—	—	.43	1.18	.73	1.01	.82	.97	1.04	.88	1.14	.81	1.38	.67	1.43	.59	1.67	.44	1.69	.33
688																						

TABLE B-I

DISPLACEMENT-TIME DATA

TEST NUMBER - 28-C

IMPACT VELOCITY - fps - 815

FELT MATERIAL - Polypropylene

Δr - in. - -0.06

AREAL DENSITY - oz./yd^2 - 40

TIME AFTER IMPACT	STATION																					
	0		+1		−1		+2		−2		+3		−3		+4		−4		+5		−5	
μsec	r	z	r	z	r	z	r	z	r	z	r	z	r	z	r	z	r	z	r	z	r	z
0	.00	.00	.00	.00	.31	.00	.58	.00	.50	.00	.88	.00	.90	.00	1.18	.00	1.19	.00	1.49	.00	1.51	.00
86	.00	.50	.32	.00	.35	.11	.58	.00	.46	-.02	.88	.00	.90	.00	1.18	.00	1.19	.00	1.49	.00	1.51	.00
172	-.02	.87	.30	.51	.40	.67	.53	.30	.59	.32	.79	-.02	.80	-.01	1.11	-.01	1.10	.00	1.49	.00	1.51	.00
258	-.02	1.14	.29	.85	.36	.98	.59	.51	.62	.67	.78	.15	.87	.33	1.01	.00	1.03	.04	1.37	.00	1.34	.00
344	-.03	1.31	.28	1.00	.39	1.10	.59	.66	.63	.84	.88	.46	.92	.56	1.09	.20	1.15	.29	1.36	.02	1.37	.07
430	-.03	1.39	.28	1.10	.38	1.22	.62	.81	.66	.96	.97	.64	1.00	.72	1.24	.43	1.23	.48	1.47	.18	1.49	.27
516	-.05	1.42	.29	1.17	.39	1.22	.68	.94	.68	1.03	1.02	.77	1.05	.85	1.28	.56	1.31	.60	1.59	.35	1.60	.38
602	-.05	1.43	.29	1.18	.41	1.25	.71	1.01	.75	1.07	1.07	.84	1.11	.89	1.35	.65	1.40	.67	1.64	.42	1.69	.45
688	-.05	1.43	.29	1.18	.42	1.28	.71	1.01	.76	1.07	1.10	.83	1.15	.90	1.40	.69	1.44	.69	1.72	.43	1.69	.45

TABLE B-I

DISPLACEMENT-TIME DATA

TEST NUMBER - 32-C

IMPACT VELOCITY - fps - 790

FELT MATERIAL - Nylon

Δr - in. - −0.02

AREAL DENSITY - oz./yd^2 - 43

TIME AFTER IMPACT	STATION																					
	0		+1		−1		+2		−2		+3		−3		+4		−4		+5		−5	
μsec	r	z	r	z	r	z	r	z	r	z	r	z	r	z	r	z	r	z	r	z	r	z
0	.00	.00	.32	.00	.30	.00	.61	.00	.59	.00	.93	.00	.90	.00	1.23	.00	1.18	.00	1.55	.00	1.45	.00
86	.04	.52	.32	.00	.24	-.02	.61	.00	.59	.00	.93	.00	.90	.00	1.23	.00	1.18	.00	1.55	.00	1.45	.00
172	.07	1.04	.38	.41	.30	.42	.55	.00	.54	.04	.88	-.01	.84	.00	1.21	.00	1.18	.00	1.55	.00	1.45	.00
258	.07	1.36	.35	.75	.30	.87	.58	.37	.60	.48	.79	.00	.74	-.05	1.12	.00	1.08	.00	1.51	.00	1.39	.00
344	.05	1.56	.33	.98	.30	1.16	.58	.63	.60	.78	.79	.26	.78	.34	1.08	.00	.96	.00	1.42	.00	1.26	.00
430	+.04	1.75	.32	1.19	.31	1.35	.57	.81	.58	.95	.82	.47	.83	.54	1.03	.16	.99	.22	1.35	.00	1.21	.00
516																						
602																						
688																						

TABLE B-I

DISPLACEMENT-TIME DATA

TEST NUMBER - 36-C

IMPACT VELOCITY - fps - 630

FELT MATERIAL - Nylon

Δr - in. - 0.00

AREAL DENSITY - oz./yd^2 - 43

TIME AFTER IMPACT	STATION																					
	0		+1		−1		+2		−2		+3		−3		+4		−4		+5		−5	
μsec	r	z	r	z	r	z	r	z	r	z	r	z	r	z	r	z	r	z	r	z	r	z
0	.00	.00	.30	.00	.33	.00	.58	.00	.62	.00	.88	.00	.89	.00	1.21	.00	1.20	.00	1.51	.00	1.50	.00
86	.00	.39	.30	.00	.33	.00	.58	.00	.62	.00	.88	.00	.89	.00	1.21	.00	1.20	.00	1.51	.00	1.50	.00
172	.00	.71	.40	.36	.37	.24	.54	.00	.58	.00	.88	.00	.89	.00	1.21	.00	1.20	.00	1.51	.00	1.50	.00
258	.03	1.04	.40	.63	.39	.65	.55	.23	.57	.16	.88	.00	.81	.00	1.17	.00	1.20	.00	1.51	.00	1.50	.00
344	.03	1.27	.37	.82	.38	.90	.59	.46	.61	.42	.80	.00	.65	.07	1.11	.00	1.12	.00	1.47	.00	1.45	.00
430	.03	1.42	.37	1.00	.38	1.02	.59	.63	.61	.60	.80	.26	.76	.26	1.06	.00	1.04	.00	1.42	.00	1.38	.00
516																						
602																						
688																						

TABLE B-I

DISPLACEMENT-TIME DATA

TEST NUMBER - 38-C

IMPACT VELOCITY - fps - 510

FELT MATERIAL - Nylon

Δr - in. - +0.03

AREAL DENSITY - oz./yd^2 - 43

TIME AFTER IMPACT	STATION																					
	0		+1		−1		+2		−2		+3		−3		+4		−4		+5		−5	
μsec	r	z	r	z	r	z	r	z	r	z	r	z	r	z	r	z	r	z	r	z	r	z
0	.00	.00	.33	.00	.30	.00	.60	.00	.60	.00	.88	.00	.92	.00	1.18	.00	1.22	.00	1.49	.00	1.50	.00
86	-.06	.49	.38	.03	.30	.00	.60	.00	.60	.00	.88	.00	.92	.00	1.18	.00	1.22	.00	1.49	.00	1.50	.00
172	-.06	.86	.40	.48	.32	.35	.57	.07	.54	.00	.88	.00	.88	.00	1.16	-.01	1.22	.00	1.47	.00	1.47	.00
258	-.06	1.14	.40	.77	.32	.65	.60	.44	.56	.24	.85	-.03	.79	.00	1.09	-.02	1.14	-.01	1.40	.00	1.43	-.03
344	-.05	1.39	.41	.96	.30	.90	.61	.64	.58	.46	.82	.25	.80	.14	1.08	.00	1.09	-.01	1.39	.00	1.4	-.03
430	-.05	1.51	.39	1.10	.31	1.0	.61	.79	.58	.63	.88	.45	.85	.24	1.05	.15	1.05	.04	1.35	.00	1.38	-.03
516																						
602																						
688																						

TABLE B-I

DISPLACEMENT-TIME DATA

TEST NUMBER - 39-C

IMPACT VELOCITY - fps - 405

FELT MATERIAL - Nylon

Δr - in. - 0.00

AREAL DENSITY - oz./yd^2 - 43

TIME AFTER IMPACT	STATION																					
	0		+1		−1		+2		−2		+3		−3		+4		−4		+5		−5	
μsec	r	z	r	z	r	z	r	z	r	z	r	z	r	z	r	z	r	z	r	z	r	z
0	.00	.00	.32	.00	.30	.00	.60	.00	.62	.00	.90	.00	.91	.00	1.19	.00	1.23	.00	1.50	.00	1.50	.00
86	.00	.19	.32	.00	.30	.00	.60	.00	.62	.00	.90	.00	.91	.00	1.19	.00	1.23	.00	1.50	.00	1.50	.00
172	.00	.45	.35	.11	.35	.20	.56	.00	.57	.00	.90	.00	.91	.00	1.19	.00	1.23	.00	1.50	.00	1.50	.00
258	.00	.75	.40	.42	.38	.48	.56	.10	.56	.10	.85	.00	.87	.00	1.16	.00	1.19	.00	1.47	.00	1.47	.00
344	.00	.91	.38	.55	.36	.62	.59	.30	.60	.25	.80	.03	.84	.02	1.13	.00	1.15	.00	1.45	.00	1.45	.00
430	.00	1.02	.38	.67	.35	.75	.61	.43	.62	.44	.84	.15	.87	.15	1.09	.00	1.12	.00	1.42	.00	1.42	.00
516																						
602																						
688																						

TABLE B-I

DISPLACEMENT-TIME DATA

TEST NUMBER - 40-C

IMPACT VELOCITY - fps - 900

FELT MATERIAL - Nylon

Δr - in. - 0.00

AREAL DENSITY - oz./yd^2 - 43

TIME AFTER IMPACT	STATION																					
	0		+1		−1		+2		−2		+3		−3		+4		−4		+5		−5	
μsec	r	z	r	z	r	z	r	z	r	z	r	z	r	z	r	z	r	z	r	z	r	z
0	.00	.00	.30	.00	.30	.00	.58	.00	.59	.00	.90	.00	.88	.00	1.17	.00	1.18	.00	1.50	.00	1.50	.00
86	.06	.57	.30	.00	.31	.03	.58	.00	.59	.00	.90	.00	.88	.00	1.17	.00	1.18	.00	1.50	.00	1.50	.00
172	.11	1.07	.33	.51	.36	.52	.53	.06	.52	.09	.82	-.02	.80	-.01	1.14	.00	1.18	.00	1.50	.00	1.50	.00
258	.12	1.34	.32	.80	.32	.88	.59	.44	.58	.45	.64	.05	.74	.06	1.01	-.02	1.10	-.02	1.45	.00	1.50	.00
344	.12	1.56	.31	1.03	.33	1.10	.60	.66	.56	.69	.79	.33	.80	.37	.96	.03	1.02	.00	1.36	.00	1.45	.00
430	.12	1.72	.31	1.21	.33	1.23	.59	.85	.58	.84	.81	.52	.85	.56	1.02	.24	1.08	.21	1.32	.00	1.38	.00
516																						
602																						
688																						

TABLE B-I

DISPLACEMENT-TIME DATA

TEST NUMBER - 42-C

IMPACT VELOCITY - fps - 710

FELT MATERIAL - Dacron

Δr - in. - -0.05

AREAL DENSITY - oz./yd^2 - 42

TIME AFTER IMPACT	STATION																					
	0		+1		-1		+2		-2		+3		-3		+4		-4		+5		-5	
μsec	r	z	r	z	r	z	r	z	r	z	r	z	r	z	r	z	r	z	r	z	r	z
0	.00	.00	.30	.00	.31	.00	.58	.00	.60	.00	.90	.00	.91	.00	1.20	.00	1.21	.00	.150	.00	1.50	.00
86	.04	.45	.30	.05	.36	.14	.58	.00	.60	.00	.90	.00	.91	.00	1.20	.00	1.21	.00	.150	.00	1.50	.00
172	.04	.77	.36	.46	.39	.59	.55	.14	.62	.22	.79	.00	.82	.00	1.15	.00	1.14	.13	.150	.00	1.50	.00
258	.03	.94	.33	.64	.38	.77	.61	.45	.67	.56	.80	.14	.87	.20	1.05	.00	1.06	.00	.150	.00	1.49	.00
344	.03	1.03	.24	.79	.38	.88	.60	.59	.62	.69	.89	.37	.95	.48	1.13	.11	1.04	.17	.145	.00	1.39	.04
430	.02	1.08	.35	.88	.35	.95	.65	.70	.65	.78	.92	.48	.94	.59	1.23	.29	1.26	.37	.140	.00	1.48	.11
516	.00	1.11	.35	.91	.37	.98	.67	.77	.65	.83	.97	.59	.95	.66	1.26	.39	1.29	.46	1.45	.06	1.56	.28
602																						
688																						

TABLE B-I

DISPLACEMENT-TIME DATA

TEST NUMBER - 43-C

IMPACT VELOCITY - fps - 465

FELT MATERIAL - Dacron

Δr - in. - -0.10

AREAL DENSITY - oz./yd^2 - 42

TIME AFTER IMPACT	STATION																					
	0		+1		-1		+2		-2		+3		-3		+4		-4		+5		-5	
μsec	r	z	r	z	r	z	r	z	r	z	r	z	r	z	r	z	r	z	r	z	r	z
0	.00	.00	.31	.00	.32	.00	.59	.00	.60	.00	.91	.00	.89	.00	1.21	.00	1.18	.00	1.44	.00	1.48	.00
86	.03	.23	.31	.00	.32	.00	.59	.00	.60	.00	.91	.00	.89	.00	1.21	.00	1.18	.00	1.44	.00	1.46	.00
172	.03	.50	.34	.25	.40	.27	.56	.00	.59	.05	.88	.00	.83	.00	1.21	.00	1.18	.00	1.44	.00	1.48	.00
258	.03	.66	.36	.45	.37	.54	.60	.21	.65	.31	.84	.00	.85	.06	1.16	.00	1.11	.00	1.44	.00	1.48	.00
344	.03	.73	.33	.54	.37	.62	.63	.38	.67	.42	.88	.15	.91	.27	1.14	.00	1.13	.05	1.49	.00	1.43	.00
430																						
516																						
602																						
688																						

TABLE B-I

DISPLACEMENT-TIME DATA

TEST NUMBER - 44-C

IMPACT VELOCITY - fps - 400

FELT MATERIAL - Dacron

Δr - in. - 0.00

AREAL DENSITY - oz./yd^2 - 42

TIME AFTER IMPACT	STATION																					
	0		+1		−1		+2		−2		+3		−3		+4		−4		+5		−5	
μsec	r	z	r	z	r	z	r	z	r	z	r	z	r	z	r	z	r	z	r	z	r	z
0	.00	.00	.30	.00	.30	.00	.60	.00	.61	.00	.92	.00	.89	.00	1.22	.00	1.16	.00	1.50	.00	1.48	.00
86	.00	.14	.30	.00	.30	.00	.60	.00	.61	.00	.92	.00	.89	.00	1.22	.00	1.16	.00	1.50	.00	1.48	.00
172	.00	.42	.26	.22	.34	.23	.57	.00	.58	.00	.92	.00	.89	.00	1.22	.00	1.16	.00	1.50	.00	1.48	.00
258	.00	.57	.26	.44	.36	.45	.60	.21	.61	.21	.86	.00	.82	.03	1.17	.00	1.10	.00	1.50	.00	1.48	.00
344	.00	.68	.23	.53	.34	.53	.63	.36	.64	.36	.87	.13	.88	.19	1.15	.00	1.08	.03	1.50	.00	1.48	.00
430	.00	.73	.29	.61	.35	.59	.63	.45	.65	.46	.94	.28	.92	.32	1.22	.09	1.15	1.17	1.46	.00	1.43	.00
516																						
602																						
688																						

TABLE B-I

DISPLACEMENT-TIME DATA

TEST NUMBER - 45-C

IMPACT VELOCITY - fps - 505

FELT MATERIAL - Dacron

Δr - in. - 0.00

AREAL DENSITY - oz./yd^2 - 42

TIME AFTER IMPACT	STATION																					
	0		+1		−1		+2		−2		+3		−3		+4		−4		+5		−5	
μsec	r	z	r	z	r	z	r	z	r	z	r	z	r	z	r	z	r	z	r	z	r	z
0	.00	.00	.29	.09	.32	.00	.61	.00	.60	.00	.91	.00	.90	.00	1.18	.00	1.20	.00	1.50	.00	1.47	.00
86	-.03	.42	.31	.04	.36	.04	.61	.00	.60	.00	.91	.00	.90	.00	1.18	.00	1.20	.00	1.50	.00	1.47	.00
172	-.03	.63	.37	.48	.40	.47	.58	.10	.59	.13	.84	-.02	.83	-.02	1.13	-.01	1.14	-.01	1.47	-.01	1.44	.00
258	-.03	.84	.33	.67	.36	.65	.63	.40	.66	.45	.84	.11	.86	.17	1.08	.00	1.07	-.01	1.41	-.01	1.38	.00
344	-.03	.95	.31	.78	.38	.76	.61	.55	.63	.57	.92	.36	.93	.39	1.13	.16	1.12	.16	1.43	.02	1.36	.02
430	.02	1.06	.34	.85	.37	.83	.65	.65	.66	.67	.95	.46	.94	.49	1.23	.32	1.24	.33	1.47	.11	1.43	.13
516																						
602																						
688																						

TABLE B-I

DISPLACEMENT-TIME DATA

TEST NUMBER - 47-C

IMPACT VELOCITY - fps - 700

FELT MATERIAL - Dacron

Δr - in. - −0.53

AREAL DENSITY - oz./yd² - 42

TIME AFTER IMPACT μsec	STATION																					
	0		+1		−1		+2		−2		+3		−3		+4		−4		+5		−5	
	r	z	r	z	r	z	r	z	r	z	r	z	r	z	r	z	r	z	r	z	r	z
0	.00	.00	.31	.00	.29	.00	.60	.00	.60	.00	.90	.00	.89	.00	1.22	.00	1.18	.00	1.51	.00	1.48	.00
86	.06	.52	.32	.03	.37	.19	.59	-.02	.54	.00	.90	.00	.89	.00	1.22	.00	1.18	.00	—	—	1.48	.00
172	-.03	.76	.38	.48	.39	.62	.55	.14	.60	.35	.79	.00	.81	.00	1.18	-.02	1.10	.00	—	—	1.45	-.02
258	-.05	1.02	.36	.68	.38	.88	.62	.46	.62	.55	.82	.23	.90	.31	1.09	.00	1.05	.04	—	—	1.37	-.01
344	-.05	1.13	.34	.78	.38	.91	.63	.59	.62	.69	.90	.44	.95	.52	1.18	.20	1.12	.28	1.42	.00	1.33	.03
430	-.05	1.21	.37	.86	.35	.99	.69	.70	.61	.79	.95	.56	.92	.58	1.30	.38	1.18	.39	1.52	.14	1.38	.16
516																						
602																						
688																						

TABLE B-I

DISPLACEMENT-TIME DATA

TEST NUMBER - 49-C

IMPACT VELOCITY - fps - 555

FELT MATERIAL - Dacron

Δr - in. - +0.05

AREAL DENSITY - oz./yd^2 - 42

TIME AFTER IMPACT	STATION																					
	0		+1		−1		+2		−2		+3		−3		+4		−4		+5		−5	
μsec	r	z	r	z	r	z	r	z	r	z	r	z	r	z	r	z	r	z	r	z	r	z
0	.00	.00	.28	.00	.30	.00	.57	.00	.59	.00	.89	.00	.91	.00	1.18	.00	1.16	.00	1.48	.00	1.54	.00
86	-.04	.36	.33	.09	.23	.00	.57	.00	.59	.00	.89	.00	.87	.00	1.18	.00	1.16	.00	1.48	.00	1.54	.00
172	-.02	.22	.37	.46	.37	.38	.59	.13	.54	.07	.83	-.03	.85	.00	1.15	.00	1.06	.00	1.47	.00	1.53	.00
258	.00	.77	.35	.60	.34	.55	.62	.40	.57	.32	.85	.10	.83	.05	1.10	.00	1.11	.00	1.46	.00	1.48	.00
344	.02	.93	.37	.69	.30	.64	.61	.48	.58	.41	.92	.29	.87	.22	1.15	.10	1.06	.03	1.44	.00	1.44	.02
430	.02	.87	.37	.74	.39	.70	.65	.57	.58	.50	.96	.38	.92	.24	1.23	.24	1.13	.15	1.47	.05	1.47	.04
516																						
602																						
688																						

TABLE B-I

DISPLACEMENT-TIME DATA

TEST NUMBER - 53-C

IMPACT VELOCITY - fps - 525

FELT MATERIAL - Dacron

Δr - in. - −0.07

AREAL DENSITY - oz./yd^2 - 42

TIME AFTER IMPACT	STATION																					
	0		+1		−1		+2		−2		+3		−3		+4		−4		+5		−5	
μsec	r	z	r	z	r	z	r	z	r	z	r	z	r	z	r	z	r	z	r	z	r	z
0	.00	.00	.29	.00	.30	.00	.58	.00	.61	.00	.90	.00	.89	.00	1.17	.00	1.18	.00	1.48	.00	1.51	.00
86	.04	.32	.29	.03	.36	.10	.55	.00	.61	.00	.90	.00	.89	.00	1.17	.00	1.23	.00	1.48	.00	1.51	.00
172	.00	.57	.34	.39	.35	.47	.56	.01	.64	.21	.84	.00	.82	.00	1.13	.00	1.20	.00	1.45	.00	1.49	.00
258	.00	.74	.33	.52	.33	.62	.61	.33	.65	.41	.85	.09	.87	.23	1.10	.00	1.15	-.02	1.42	.00	1.45	.00
344	.00	.82	.33	.64	.35	.73	.62	.44	.68	.54	.91	.27	.93	.40	1.13	.09	1.24	.00	1.39	.00	1.47	.02
430																						
516																						
602																						
688																						

TABLE B-I

DISPLACEMENT-TIME DATA

TEST NUMBER - 54-C

IMPACT VELOCITY - fps - 460

FELT MATERIAL - Dacron

Δr - in. - -0.08

AREAL DENSITY - oz./yd^2 - 42

TIME AFTER IMPACT	STATION																					
	0		+1		−1		+2		−2		+3		−3		+4		−4		+5		−5	
μsec	r	z	r	z	r	z	r	z	r	z	r	z	r	z	r	z	r	z	r	z	r	z
0	.00	.00	.30	.00	.30	.00	.58	.00	.60	.00	.88	.00	.89	.00	1.20	.00	1.20	.00	1.48	.00	1.53	.00
86	.03	.25	.27	.00	.33	.06	.58	.00	.60	.00	.88	.00	.89	.00	1.20	.00	1.20	.00	1.48	.00	1.53	.00
172	.03	.50	.33	.32	.37	.41	.56	.04	.59	.13	.83	.00	.83	.00	1.20	.00	1.16	.00	1.48	.00	1.53	.00
258	.03	.65	.32	.47	.35	.56	.60	.29	.64	.39	.82	.06	.86	.18	1.13	.00	1.12	.02	1.48	.00	1.53	.00
344	.02	.75	.32	.58	.36	.67	.60	.40	.64	.49	.89	.26	.93	.34	1.16	.09	1.21	.18	1.44	.00	1.50	.00
430																						
516																						
602																						
688																						

TABLE B-I

DISPLACEMENT-TIME DATA

TEST NUMBER - 56-C

IMPACT VELOCITY - fps - 480

FELT MATERIAL - Dacron

Δr - in. - −0.05

AREAL DENSITY - oz./yd^2 - 42

TIME AFTER IMPACT	STATION																					
	0		+1		−1		+2		−2		+3		−3		+4		−4		+5		−5	
μsec	r	z	r	z	r	z	r	z	r	z	r	z	r	z	r	z	r	z	r	z	r	z
0	.00	.00	.33	.00	.28	.00	.64	.00	.55	.00	.92	.00	.88	.00	1.22	.00	1.15	.00	1.52	.00	1.44	.00
86	.00	.30	.38	.06	.30	.06	.64	.00	.55	.00	.92	.00	.88	.00	1.22	.00	1.15	.00	1.52	.00	—	—
172	-.01	.57	.38	.49	.34	.43	.64	.13	.56	.12	.85	.00	.82	.00	1.17	.00	—	—	1.49	.00	—	—
258	-.02	.73	.35	.65	.30	.61	.65	.42	.61	.38	.89	.16	.84	.11	1.12	.00	1.06	.00	1.43	.00	—	—
344	-.02	.82	.38	.73	.32	.71	.66	.51	.62	.49	.93	.33	.91	.30	1.16	.11	1.10	.11	1.42	.00	—	—
430																						
516																						
602																						
688																						

TABLE B-I

DISPLACEMENT-TIME DATA

TEST NUMBER - 58-C

IMPACT VELOCITY - fps - 545

FELT MATERIAL - Orlon

Δr - in. - +0.05

AREAL DENSITY - oz./yd^2 - 43

TIME AFTER IMPACT μsec	STATION																					
	0		+1		−1		+2		−2		+3		−3		+4		−4		+5		−5	
	r	z	r	z	r	z	r	z	r	z	r	z	r	z	r	z	r	z	r	z	r	z
0	.00	.00	.30	.00	.31	.00	.60	.00	.61	.00	.90	.00	.90	.00	1.22	.00	1.20	.00	1.50	.00	1.50	.00
86	.00	.27	.31	.00	.31	.00	.60	.00	.61	.00	.90	.00	.90	.00	1.22	.00	1.20	.00	1.50	.00	1.50	.00
172	+.03	.56	.40	.41	.36	.27	.57	.07	.58	.00	.87	−.02	.87	−.01	1.22	.00	1.20	.00	1.50	.00	1.50	.00
258	+.02	.77	.36	.62	.38	.55	.62	.39	.62	.27	.85	.05	.78	.05	1.15	.00	1.11	−.01	1.45	.00	1.44	.00
344	+.01	.88	.33	.77	.36	.58	.63	.56	.68	.49	.90	.32	.88	.26	1.12	.05	1.09	.04	1.40	.00	1.38	−.01
430																						
516																						
602																						
688																						

TABLE B-I

DISPLACEMENT-TIME DATA

TEST NUMBER - 59-C

IMPACT VELOCITY - fps - 700

FELT MATERIAL - Orlon

Δr - in. - 0.00

AREAL DENSITY - oz./yd^2 - 43

TIME AFTER IMPACT	STATION																					
	0		+1		−1		+2		−2		+3		−3		+4		−4		+5		−5	
μsec	r	z	r	z	r	z	r	z	r	z	r	z	r	z	r	z	r	z	r	z	r	z
0	.00	.00	.34	.00	.25	.00	.63	.00	.58	.00	.96	.00	.88	.00	1.28	.00	1.20	.00	1.60	.00	1.50	.00
86	.00	.40	.35	.00	.29	.03	.63	.00	.58	.00	.95	.00	.88	.00	1.28	.00	1.20	.00	1.60	.00	1.50	.00
172	-.02	.71	.46	.45	.30	.52	.62	.06	.59	.05	.90	-.03	.82	-.02	1.25	-.01	1.18	-.01	1.60	.00	1.50	.00
258	-.02	.95	.39	.78	.32	.81	.69	.44	.68	.45	.78	.06	.84	.10	1.17	-.02	1.06	-.01	1.51	.00	1.44	-.02
344	-.01	1.09	.30	.93	.29	.94	.70	.65	.70	.70	.97	.38	.94	.44	1.19	.07	1.10	.13	1.45	.00	1.34	-.02
430																						
516																						
602																						
688																						

TABLE B-I

DISPLACEMENT-TIME DATA

TEST NUMBER - 60-C

IMPACT VELOCITY - fps - 620

FELT MATERIAL - Orlon

Δr - in. - 0.00

AREAL DENSITY - oz./yd^2 - 43

TIME AFTER IMPACT	STATION																					
	0		+1		−1		+2		−2		+3		−3		+4		−4		+5		−5	
μsec	r	z	r	z	r	z	r	z	r	z	r	z	r	z	r	z	r	z	r	z	r	z
0	.00	.00	.27	.00	.30	.00	.60	.00	.61	.00	.94	.00	.93	.00	1.23	.00	—	—	1.51	.00	1.55	.00
86	−.10	.27	.29	.00	.30	.00	.60	.00	.61	.00	.94	.00	.93	.00	1.23	.00	—	—	1.51	.00	1.55	.00
172	−.03	.63	.41	.42	.43	.33	.60	.00	.61	.00	.94	.00	.93	.00	1.23	.00	—	—	1.51	.00	1.55	.00
258	−.05	.86	.37	.77	.40	.65	.66	.35	.65	.33	.85	.00	.85	.04	1.11	−.01	—	—	1.42	.00	1.49	−.02
344	−.08	1.00	.30	.87	.35	.80	.70	.62	.71	.60	.94	.30	.93	.32	1.11	.05	1.15	.05	1.35	.00	1.44	−.02
430	−.10	1.09	.23	1.00	.36	.89	.65	.73	.68	.71	1.24	.53	1.01	.55	1.22	.31	1.25	.30	1.41	.08	1.48	.05
516																						
602																						
688																						

TABLE B-I

DISPLACEMENT-TIME DATA

TEST NUMBER - 62-C

IMPACT VELOCITY - fps - 780

FELT MATERIAL - Orlon

Δr - in. - ±0.06

AREAL DENSITY - oz./yd^2 - 43

TIME AFTER IMPACT μsec	STATION																					
	0		+1		−1		+2		−2		+3		−3		+4		−4		+5		−5	
	r	z	r	z	r	z	r	z	r	z	r	z	r	z	r	z	r	z	r	z	r	z
0	.00	-00	—	—	—	—	.63	.00	.57	.00	.93	.00	.87	.00	1.23	.00	1.17	.00	1.52	.00	1.45	.00
86	-.05	.48	—	—	—	—	.63	.00	.57	.00	.93	.00	.87	-.02	1.23	.00	1.17	.00	1.52	.00	1.45	.00
172	.00	.83	—	—	—	—	.63	.11	.50	.09	.86	-.04	.78	.14	1.20	-.02	1.12	-.02	1.52	.00	1.45	.00
258	+.03	1.10	—	—	—	—	.71	.48	.66	.48	.89	.15	.81	.47	1.10	-.03	1.03	-.04	1.42	-.03	1.45	.00
344	-.02	1.21	—	—	—	—	.69	.69	.68	.72	.99	.47	.93	.72	1.15	.17	1.11	.18	1.35	-.01	1.35	-.01
430	-.06	1.28	—	—	—	—	.64	.80	.65	.81	1.00	.62	.98	.80	1.30	.44	1.25	.40	1.47	.16	1.45	.19
516																						
602																						
688																						

TABLE B-I

DISPLACEMENT-TIME DATA

TEST NUMBER - 65-C

IMPACT VELOCITY - fps - 465

FELT MATERIAL - Nylon

Δr - in. - 0.00

AREAL DENSITY - oz./yd^2 - 19

TIME AFTER IMPACT	STATION																					
	0		+1		−1		+2		−2		+3		−3		+4		−4		+5		−5	
μsec	r	z	r	z	r	z	r	z	r	z	r	z	r	z	r	z	r	z	r	z	r	z
0	.00	.00	.28	.00	.31	.00	.60	.00	.61	.00	.91	.00	.89	.00	1.18	.00	1.20	.00	1.50	.00	1.47	.00
86	-.02	.47	.29	.02	.35	.03	.60	.00	.61	.00	.91	.00	.89	.00	1.18	.00	1.20	.00	1.50	.00	1.47	.00
172	-.02	.81	.26	.32	.34	.39	.52	-.01	.55	.07	.87	.00	.84	.00	1.15	.00	1.17	.00	1.50	.00	1.47	.00
258	-.04	1.09	.30	.66	.34	.65	.50	.24	.56	.28	.80	.00	.79	.05	1.10	.00	1.16	.00	1.50	.00	1.47	.00
344	-.05	1.28	.24	.83	.33	.81	.57	.59	.59	.49	.80	.14	.78	.22	1.06	.00	1.02	.02	1.45	.00	1.43	.00
430	-.06	1.42	.24	.98	.34	.95	.55	.66	.59	.63	.86	.33	.86	.41	1.09	.09	1.09	.15	1.40	.00	1.40	.00
516	-.06	1.48	.24	1.04	.33	1.03	.56	.75	.62	.76	.92	.47	.91	.55	1.18	.25	1.19	.32	1.43	.05	1.44	.01
602																						
688																						

TABLE B-I

DISPLACEMENT-TIME DATA

TEST NUMBER - 66-C

IMPACT VELOCITY - fps - 630

FELT MATERIAL - Nylon

Δr - in. - +0.07

AREAL DENSITY - oz./yd^2 - 19

TIME AFTER IMPACT μsec	STATION																					
	0		+1		−1		+2		−2		+3		−3		+4		−4		+5		−5	
	r	z	r	z	r	z	r	z	r	z	r	z	r	z	r	z	r	z	r	z	r	z
0	.00	.00	.27	.00	.30	.00	.59	.00	.62	.00	.87	.00	.93	.00	1.18	.00	1.22	.00	1.47	.00	1.50	.00
86	+.02	.61	.27	.12	.33	.21	.57	.00	.62	.00	.87	.00	.93	.00	1.18	.00	1.22	.00	1.47	.00	1.50	.00
172	+.03	1.07	.26	.53	.33	.66	.51	.09	.57	−.02	.78	.00	.91	.00	1.14	−.01	1.22	.00	1.44	.00	1.48	.00
258	−.01	1.36	.26	.83	.30	.93	.52	.41	.56	.53	.71	.11	.84	.00	1.05	−.02	1.17	.00	1.39	−.02	1.46	.00
344	−.04	1.59	.27	1.07	.34	1.12	.52	.64	.55	.71	.75	.36	.86	.39	1.04	.05	1.07	−.02	1.33	−.03	1.42	−.01
430	−.05	1.72	.24	1.24	.33	1.25	.57	.81	.57	.85	.80	.54	.90	.55	1.12	.23	1.20	.30	1.37	.04	1.39	−.02
516	−.05	1.76	.30	1.30	.33	1.30	.60	.93	.60	.95	.88	.70	.95	.70	1.21	.41	1.27	.47	1.45	.26	1.51	.26
602																						
688																						

TABLE B-I

DISPLACEMENT-TIME DATA

TEST NUMBER - 68-C

IMPACT VELOCITY - fps - 545

FELT MATERIAL - Nylon

Δr - in. - 0.00

AREAL DENSITY - oz./yd^2 - 19

TIME AFTER IMPACT	STATION																					
	0		+1		−1		+2		−2		+3		−3		+4		−4		+5		−5	
μsec	r	z	r	z	r	z	r	z	r	z	r	z	r	z	r	z	r	z	r	z	r	z
0	.00	.00	.28	.00	.31	.00	.60	.00	.60	.00	.87	.00	.89	.00	1.17	.00	1.20	.00	1.50	.00	1.49	.00
86	+.03	.54	.29	.07	.31	.11	.60	.00	.57	.00	.87	.00	.89	.00	1.17	.00	1.20	.00	1.50	.02	1.49	.00
172	+.02	.94	.28	.45	.33	.54	.50	.04	.51	.13	.83	.00	.89	.00	1.17	.00	1.20	.00	1.50	.00	1.49	.00
258	.00	1.23	.30	.76	.30	.80	.54	.38	.54	.42	.74	.02	.79	.00	1.08	.00	1.16	.00	1.45	−.01	1.43	.00
344	.00	1.44	.28	.97	.31	1.01	.57	.57	.56	.65	.79	.32	.76	.34	.99	.00	1.06	.00	1.39	−.03	1.38	.00
430	.00	1.57	.30	1.11	.30	1.14	.57	.71	.55	.79	.84	.43	.85	.56	1.08	.22	1.11	.27	1.37	−.04	1.41	.05
516	.00	1.62	.29	1.16	.30	1.20	.60	.80	.58	.90	.90	.57	.88	.70	1.19	.32	1.24	.49	1.44	−.04	1.49	.20
602																						
688																						

APPENDIX - C

RESIDUAL VELOCITY DATA

TABLE C-I

RESIDUAL VELOCITY DATA

MATERIAL									
POLYPROPYLENE 40 oz./yd.^{2}		ORLON 43 oz./yd.^{2}		DACRON 42 oz./yd.^{2}		NYLON 43 oz./yd.^{2}		NYLON 53 oz./yd.^{2}	
V_0 - fps	V_r - fps	V_0 - fps	V_r - fps	V_0 - fps	V_r - fps	V_0 - fps	V_r - fps	V_0 - fps	V_r - fps
420	0	735	0	640	0	815	0	810	0
810	0	780	0	670	0	900	0	915	0
905	0	855	585	690	0	915	40	985	0
945	400	915	730	720	0	1010	390	1050	595
995	945	980	850	765	455	1110	770	1120	860
1050	610	1225	1130	820	595	1185	1015	1185	940
1115	915	1630	1520	1105	960	1320	1100	1250	1100
1180	970	1790	1710	1130	1020	1925	1900	1460	1310
1310	1160			1460	1360			1980	1870
1985	1900			1510	1450				
				2100	2015				

Unclassified

Security Classification

DOCUMENT CONTROL DATA - R&D

(Security classification of title, body of abstract and indexing annotation must be entered when the overall report is classified)

1. ORIGINATING ACTIVITY (Corporate author)	2a. REPORT SECURITY CLASSIFICATION
Denver Research Institute University of Denver Denver, Colorado	Unclassified 2b. GROUP

3. REPORT TITLE

RESPONSE OF NON-WOVEN SYNTHETIC FIBER TEXTILES TO BALLISTIC IMPACT

4. DESCRIPTIVE NOTES (Type of report and inclusive dates)

Final Report July 1963 - October 1965

5. AUTHOR(S) (Last name, first name, initial)

Ipson, Thomas W., Wittrock, Edward P.

6. REPORT DATE	7a. TOTAL NO. OF PAGES	7b. NO. OF REFS
July 1966	110	15

8a. CONTRACT OR GRANT NO.	9a. ORIGINATOR'S REPORT NUMBER(S)
DA19-129-AMC-157(N) b. PROJECT NO. 1K024401A113 c. d.	9b. OTHER REPORT NO(S) (Any other numbers that may be assigned this report) 67-8-CM TS-142

10. AVAILABILITY/LIMITATION NOTICES

Distribution of this document is unlimited. Release to CFSTI is authorized.

11. SUPPLEMENTARY NOTES	12. SPONSORING MILITARY ACTIVITY
	U. S. Army Natick Laboratories Natick, Massachusetts 01760

13 ABSTRACT When organic fiber felt materials are impacted by blunt fragments, stress waves propagating laterally into the material transfer projectile momentum to an increasing (roughly conical) volume of felt material. By applying a retarding force to the projectile, stresses in the felts can be maintained below rupture values, provided that the felts are free to move in the direction of the projectile. The objective of this program was to define the transient behavior of the felt and the force interaction between it and the projectile.

An experimental technique was developed whereby the position-time histories of eleven points (spark gaps) on the rear surface of a felt sample could be determined. The center spark station, being on the projectile trajectory, provides projectile displacement-time data. Other stations provide both radial and transverse displacements. The longitudinal radial wave gives material particles an initial radial velocity inward; later, the slower moving transverse wave imparts a transverse velocity to the felt, usually stopping or reversing radial motion. Measurement errors average less than two percent.

Six felt samples (nylon (3), orlon, dacron, polypropylene) were tested using the 17-grain fragment simulating projectile at various velocities up to and greater than the ballistic limit velocity. Graphical differentiation was used to obtain velocity-time, force-time, and force-distance relationships. Qualitative evaluations reveal that strength, elongation, and transverse wave velocity are the three predominant parameters in determining effectiveness. The energy absorbed by a felt is maximum at the ballistic limit velocity and decreases dramatically at higher (complete perforation) velocities. An analytical model based upon momentum considerations is compared to the experimental results.

DD FORM 1 JAN 64 1473

Unclassified

Security Classification

KEY WORDS	LINK A		LINK B		LINK C	
	ROLE	WT	ROLE	WT	ROLE	WT
Ballistics	8					
Perforating	8					
Resistance	8					
Nonwovens	9		7			
Felts	9		7			
Projectiles			6			
Velocity			6, 7			
Displacemt			7			

INSTRUCTIONS

1. **ORIGINATING ACTIVITY:** Enter the name and address of the contractor, subcontractor, grantee, Department of Defense activity or other organization *(corporate author)* issuing the report.

2a. **REPORT SECURITY CLASSIFICATION:** Enter the overall security classification of the report. Indicate whether "Restricted Data" is included. Marking is to be in accordance with appropriate security regulations.

2b. **GROUP:** Automatic downgrading is specified in DoD Directive 5200.10 and Armed Forces Industrial Manual. Enter the group number. Also, when applicable, show that optional markings have been used for Group 3 and Group 4 as authorized.

3. **REPORT TITLE:** Enter the complete report title in all capital letters. Titles in all cases should be unclassified. If a meaningful title cannot be selected without classification, show title classification in all capitals in parenthesis immediately following the title.

4. **DESCRIPTIVE NOTES:** If *appropriate*, enter the type of report, e.g., interim, progress, summary, annual, or final. Give the inclusive dates when a specific reporting period is covered.

5. **AUTHOR(S):** Enter the name(s) of author(s) as shown on or in the report. Enter last name, first name, middle initial. If military, show rank and branch of service. The name of the principal author is an absolute minimum requirement.

6. **REPORT DATE:** Enter the date of the report as day, month, year, or month, year. If more than one date appears on the report, use date of publication.

7a. **TOTAL NUMBER OF PAGES:** The total page count should follow normal pagination procedures, i.e., enter the number of pages containing information.

7b. **NUMBER OF REFERENCES:** Enter the total number of references cited in the report.

8a. **CONTRACT OR GRANT NUMBER:** If appropriate, enter the applicable number of the contract or grant under which the report was written.

8b, &c, & 8d. **PROJECT NUMBER:** Enter the appropriate military department identification, such as project number, subproject number, system numbers, task number, etc.

9a. **ORIGINATOR'S REPORT NUMBER(S):** Enter the official report number by which the document will be identified and controlled by the originating activity. This number must be unique to this report.

9b. **OTHER REPORT NUMBER(S):** If the report has been assigned any other report numbers *(either by the originator or by the sponsor)* also enter this number(s).

10. **AVAILABILITY/LIMITATION NOTICES:** Enter any limitations on further dissemination of the report, other than those imposed by security classification, using standard statements such as:

(1) "Qualified requesters may obtain copies of this report from DDC."

(2) "Foreign announcement and dissemination of this report by DDC is not authorized."

(3) "U. S. Government agencies may obtain copies of this report directly from DDC. Other qualified DDC users shall request through _____."

(4) "U. S. military agencies may obtain copies of this report directly from DDC. Other qualified users shall request through _____."

(5) "All distribution of this report is controlled. Qualified DDC users shall request through _____."

If the report has been furnished to the Office of Technical Services, Department of Commerce, for sale to the public, indicate this fact and enter the price, if known.

11. **SUPPLEMENTARY NOTES:** Use for additional explanatory notes.

12. **SPONSORING MILITARY ACTIVITY:** Enter the name of the departmental project office or laboratory sponsoring *(paying for)* the research and development. Include address.

13. **ABSTRACT:** Enter an abstract giving a brief and factual summary of the document indicative of the report, even though it may also appear elsewhere in the body of the technical report. If additional space is required, a continuation sheet shall be attached.

It is highly desirable that the abstract of classified reports be unclassified. Each paragraph of the abstract shall end with an indication of the military security classification of the information in the paragraph, represented as *(TS)*, *(S)*, *(C)*, or *(U)*.

There is no limitation on the length of the abstract. However, the suggested length is from 150 to 225 words.

14. **KEY WORDS:** Key words are technically meaningful terms or short phrases that characterize a report and may be used as index entries for cataloging the report. Key words must be selected so that no security classification is required. Identifiers, such as equipment model designation, trade name, military project code name, geographic location, may be used as key words but will be followed by an indication of technical context. The assignment of links, rules, and weights is optional.